6-23-2014

The Role of the Transcription Factor Ets1 in Melanocyte Development

Amy Saldana Tavares
Florida International University, asald001@fiu.edu

DOI: 10.25148/etd.FI14071121

FLORIDA INTERNATIONAL UNIVERSITY

Miami, Florida

THE ROLE OF THE TRANSCRIPTION FACTOR ETS1 IN MELANOCYTE DEVELOPMENT

A dissertation submitted in partial fulfillment of

the requirements for the degree of

DOCTOR OF PHILOSOPHY

in

BIOLOGY

by

Amy Saldana Tavares

2014

To: Interim Dean Michael R. Heithaus
College of Arts and Sciences

This dissertation, written by Amy Saldana Tavares, and entitled The Role of the Transcription Factor Ets1 in Melanocyte Development, having been approved in respect to style and intellectual content, is referred to you for judgment.

We have read this dissertation and recommend that it be approved.

_____
James Grichnik

_____
Robert Lickliter

_____
Fernando G. Noriega

_____
M. Alejandro Barbieri

_____
Lidia Kos, Major Professor

Date of Defense: June 23, 2014

The dissertation of Amy Saldana Tavares is approved.

_____
Interim Dean Michael R. Heithaus
College of Arts and Sciences

_____
Dean Lakshmi N. Reddi
University Graduate School

Florida International University, 2014

DEDICATION

To my family - for their love, encouragement, and prayers.

ACKNOWLEDGMENTS

The work presented in this dissertation would not have been possible without the support of many individuals who have in different ways contributed to my experience and my work. I am grateful to God for all the people who have in some way, whether directly or indirectly, helped me throughout these years, and for giving me the strength to persevere and the grace to finally appreciate the value of unforeseen obstacles.

I would like to thank my graduate advisor Dr. Lidia Kos, who gave me the opportunity to join her lab as an undergraduate student and inspired me to pursue a graduate degree. She challenged me to step out of my comfort zone, yet was always kind and understanding. I am certainly not fearless, but her constant nudging has given me more faith in myself.

I would also like to thank the others members of my graduate committee, Dr. Alejandro Barbieri, Dr. Robert Lickliter, Dr. James Grichnik, and Dr. Fernando Noriega for their guidance and words of encouragement. Special thanks to Dr. Noriega for allowing me to use equipment in his lab which was essential for the completion of this work. Also, thanks to all of the members from Dr. Noriega's lab for their kindness and generosity towards me. Many thanks also to Dr. Mauricio Rodriguez-Lanetty for allowing me to use the equipment in his lab, to Dr. Paul Sharp from the FIU DNA Core Facility for his assistance with DNA sequencing, and to Dr. Maureen Donnelly for her candid words of advice and reassurance. I would also like to extend my gratitude to Dr. Paulette Johnson and Dr. Jianbin Zhu from FIU Statistical Consulting for their help with data analysis.

I would like thank the members of my lab, both past and present, for their help and support. Thanks to Dr. Marcy Lowesntein and Dr. Flavia Brito for their guidance, especially during my first years as a graduate student. Many thanks to Ana Paula Benaduce, Nikeisha Chin, and Javier Pino, with whom I was lucky to share both the excitements and uncertainties of this experience, their advice and friendship throughout the years has been invaluable to me. Thanks also to Dr. Erasmo Perera, not only for his help with questions about techniques, but also for his words of encouragement. To Natasha Fernandez, Denisse Diaz and Rodrigo Garcia, for being so welcoming when I first joined the lab as an undergraduate student and for taking the time to teach me how to work with the mice, run PCRs, etc. Very special thanks to Natasha, for always being there when I needed a helping hand or someone to talk to. I would also like to thank present and former members of neighboring labs, particularly, Boris Chabeco, Maria Pulido, Dr. Marbelys Rodriguez, Dr. Adriana Galvis, and Dr. Sushmita Mustafi who were very helpful with questions regarding different techniques, thank you for taking of your time to help me with those.

I would like to thank all of my family for their love and support, especially, my mother, Rosaura Velazquez, and grandmother, Fanny Tavarez, who have taught me the value of hard work and education and who have been inspiring role models of strength and determination; thank you for your love and constant prayers for me. I also want to thank my husband, Ricky Caboverde, for listening to me talk about my research, even when he did not understand what I was saying, for celebrating my successes and being there for me through the difficult times, for allowing me to be a little obsessive about my

experiments but helping me to stay grounded, for urging me to keep going and especially for all of his prayers for me.

Lastly but certainly not least, I would like to acknowledge various sources of funding, without which the completion of this work would not have been possible. This research was supported by an R15 NIH grant to Dr. Lidia Kos. This research was also supported by funding from Biomedical Research Initiative Student Summer Research Awards. I would like to also acknowledge the Florida International University Teaching Assistantship and the MBRS-RISE program for financial support. Many thanks to Dr. Charles Bigger and the MBRS-RISE program staff, especially Aileen Landry, Thelma Robles, Charles Soto, and Esther Lopez, for their support. I would finally like to thank Helen Forlong, from our department, for her assistance with Purchase Orders and TARs, as well as for her kindness and willingness to help.

ABSTRACT OF THE DISSERTATION

THE ROLE OF THE TRANSCRIPTION FACTOR ETS1 IN MELANOCYTE DEVELOPMENT

by

Amy Saldana Tavares

Florida International University, 2014

Miami, Florida

Professor Lidia Kos, Major Professor

Melanocytes, pigment-producing cells, derive from the neural crest (NC), a population of pluripotent cells that arise from the dorsal aspect of the neural tube during embryogenesis. Many genes required for melanocyte development were identified using mouse pigmentation mutants. The deletion of the transcription factor *Ets1* in mice results in hypopigmentation; nevertheless, the function of *Ets1* in melanocyte development is unknown. The goal of the present study was to establish the temporal requirement and role of *Ets1* in murine melanocyte development. In the mouse, *Ets1* is widely expressed in developing organs and tissues, including the NC. In the chick cranial NC, *Ets1* is required for the expression of *Sox10*, a transcription factor critical for the development of melanocytes, enteric ganglia, and other NC derivatives.

Using a combination of immunofluorescence and cell survival assays *Ets1* was found to be required between embryonic days 10 and 11, when it regulates NC cell and melanocyte precursor (melanoblast) survival. Given the requirement of *Ets1* for *Sox10* expression in the chick cranial NC, a potential interaction between these genes was investigated. Using genetic crosses, a synergistic genetic interaction between *Ets1* and

Sox10 in melanocyte development was found. Since *Sox10* is essential for enteric ganglia formation, the importance of *Ets1* on gut innervation was also examined. In mice, *Ets1* deletion led to decreased gut innervation, which was exacerbated by *Sox10* heterozygosity.

At the molecular level, Ets1 was found to activate a *Sox10* enhancer critical for *Sox10* expression in melanoblasts. Furthermore, mutating *Ets1* at a site I characterized in the spontaneous variable spotting mouse pigmentation mutant, led to a 2-fold decrease in enhancer activation. Overexpression and knockdown of *Ets1* did not affect *Sox10* expression; nonetheless, *Ets1* knockdown led to a 6-fold upregulation of the transcription factor *Sox9*, a gene required for melanocyte and chondrocyte development, but which impairs melanocyte development when its expression is prolonged. Together, these results suggest that *Ets1* is required early during melanocyte development for NC cell and melanoblast survival, possibly acting upstream of *Sox10*. The transcription factor Ets1 may also act indirectly in melanocyte fate specification by repressing *Sox9* expression, and consequently cartilage fate.

TABLE OF CONTENTS

CHAPTER PAGE

I. INTRODUCTION 1
1.1 The neural crest 3
1.1.1 Neural crest induction 3
1.1.2 Specification of the neural plate border and neural crest specifier genes 6
1.1.3 Neural crest delamination and neural crest derivatives 9
1.2 Melanocyte development 11
1.3 Genetic network of melanocyte development: Lessons from pigmentation mutants 13
1.3.1 Cell intrinsic factors 13
1.3.2 Signaling molecules and receptors 24
1.4 Research Questions 29
1.5 References 38

II. TEMPORAL REQUIREMENT OF THE TRANSCRIPTION FACTOR *Ets1* IN MURINE MELANOCYTE DEVELOPMENT 49
2.1 Abstract 50
2.2 Introduction 51
2.3 Materials and methods 54
2.3.1 Animals 54
2.3.2 Genotyping 55
2.3.3 β-galactosidase and Lysotracker Red staining of whole mount embryos 57
2.3.4 Immunofluorescence 58
2.3.5 Probe preparation for in situ hybridization 59
2.3.6 In situ hybridization 60
2.3.7 Statistical analysis 63
2.4 Results 63
2.4.1 *Ets1* null embryos show reduced numbers of melanoblasts 63
2.4.2 *Ets1* deletion results in decreased melanoblast survival 64
2.4.3 *Ets1* deletion results in decreased neural crest cell survival 65
2.5 Discussion 66
2.6 References 77

III. GENETIC INTERACTION BETWEEN THE TRANSCRIPTION FACTORS *Ets1* AND *Sox10* IN THE DEVELOPMENT OF MELANOCYTES AND ENTERIC GANGLIA 81
3.1 Abstract 82
3.2 Introduction 83
3.3 Materials and methods 87
3.3.1 Animals 87

3.3.2 Genotyping....88
3.3.3 Crosses and phenotypic analysis....89
3.3.4 β-galactosidase staining of whole mount embryos....89
3.3.5 Colon dissection and Acetylcholinesterase staining....90
3.3.6 Statistical analysis....91
3.4 Results....92
3.4.1 *Ets1* and *Sox10* double heterozygosity increases hypopigmentation frequency....92
3.4.2 *Ets1* and *Sox10* double heterozygosity exacerbates hypopigmentation....93
3.4.3 *Ets1* null mutants show decreased gut innervation....93
3.4.4 *Ets1* null mutants appear to display decreased *Sox10* expression....95
3.5 Discussion....96
3.6 References....108

IV. THE TRANSCRIPTION FACTOR Ets1 ACTIVATES THE MELANOCYTE LINEAGE-SPECIFIC *Sox10*-MCS4 ENHANCER....111
4.1 Abstract....112
4.2 Introduction....113
4.3 Materials and methods....116
4.3.1 Mapping of Ets1 binding sites in the *Sox10*-MCS4 and *Sox10*-MCS7 enhancers....116
4.3.2 Cell culture....117
4.3.3 Plasmid constructs....117
4.3.4 Sequencing the variable spotting mutation....118
4.3.5 Site-directed mutagenesis....118
4.3.6 Plasmid DNA transfections and luciferase assay....119
4.3.7 Statistical analysis....120
4.4. Results....121
4.4.1 The *Sox10*-MCS4 and *Sox10*-MCS7 enhancers contain putative Ets1 binding sites....121
4.4.2 Transactivation of the *Sox10*-MCS4 enhancer by Ets1....121
4.4.3 *Ets1* is the mutated gene in the spontaneous variable spotting mouse mutant....121
4.4.4 The variable spotting mutation results in decreased *Sox10*-MCS4 activation....122
4.5 Discussion....122
4.6 References....129

V. *Ets1* KNOCKDOWN INDUCES THE UPREGULATION OF THE TRANSCRIPTION FACTOR *Sox9* IN MOUSE MELANOMA CELLS....131
5.1 Abstract....132
5.2 Introduction....133
5.3 Materials and methods....137
5.3.1 Cell culture....137

5.3.2 Plasmid constructs 137
5.3.3 Plasmid DNA transfections....138
5.3.4 siRNA transfections 138
5.3.5 RNA extraction, cDNA synthesis and semi-quantitative real-time PCR....140
5.3.6 Protein extraction and Western Blot 142
5.4 Results....143
5.4.1 *Ets1* overexpression does not affect the expression of melanoblast-specific genes in mouse melanocytes and mouse melanoma cells....143
5.4.2 Knockdown of *Ets1* leads to *Sox9* upregulation in mouse melanoma cells....144
5.5 Discussion 145
5.6 References....156

VI. CONCLUSIONS AND FUTURE DIRECTIONS 160
6.1 Conclusions....161
6.2 Future directions 166
6.3 References....170

APPENDICES 172

VITA 188

LIST OF FIGURES

FIGURE PAGE

Figure 1.1. Mouse pigmentation mutants 33

Figure 1.2. Neural crest development 34

Figure 1.3. Melanocyte development from the neural crest 36

Figure 2.1. Ventral hypopigmentation in *Ets1* mutant mice 70

Figure 2.2. *Ets1* null mutant embryos have decreased melanoblast numbers 71

Figure 2.3. Decreased melanoblast survival in E10.75 *Ets1* null mutants 72

Figure 2.4. Melanoblasts in E10.5 *Ets1* null vs. *Ets1* heterozygous mouse embryos 73

Figure 2.5. Decreased neural crest cell survival in E10.25 *Ets1* null mutants 74

Figure 2.6 *Sox10* Expression in E9.5 *Ets1* mutant embryos examined via in situ hybridization 75

Figure 2.7. *Sox10* expression in *Ets1* mutant embryos visualized via LacZ staining 76

Figure 3.1. *Ets1* and *Sox10* double heterozygosity increases hypopigmentation frequency 101

Figure 3.2. *Ets1* and *Sox10* double heterozygotes display increased ventral hypopigmentation compared to single heterozygotes 102

Figure 3.3. *Ets1* and *Sox10* double heterozygosity results in an aggravated hypopigmentation phenotype 103

Figure 3.4. Aganglionic megacolon in $Ets1^{-/-}::Sox10^{LacZ/+}$ mice. 104

Figure 3.5. *Ets1* null mutants show decreased gut innervation 105

Figure 3.6. *Ets1* deficiency results in decreased gut innervation 106

Figure 3.7. *Sox10* expression in *Ets1* mutant embryos 107

Figure 4.1. Activation of the *Sox10*-MCS4 enhancer by Ets1 126

Figure 4.2. Mutation analysis of variable spotting mice 127

Figure 4.3. The variable spotting mutation inhibits Ets1-induced *Sox10*-MCS4 enhancer activation 128

Figure 5.1. The molecular basis for melanocyte development 151

Figure 5.2. *Ets1* overexpression in melan-a cells does not substantially affect the expression of melanoblast-specific genes 152

Figure 5.3. *Ets1* overexpression in B16 cells does not considerably affect the expression of melanoblast-specific genes 153

Figure 5.4. *Ets1* knockdown in melan-a cells does not substantially affect the expression of melanoblast-specific genes 154

Figure 5.5. *Ets1* knockdown in B16 melanoma cells results in *Sox9* upregulation 155

Figure A.1 Normal Q-Q plots of raw and transformed hypopigmentation area data for generation 1 175

Figure A.2 Normal Q-Q plots of raw and transformed hypopigmentation area data for generation 2 177

Figure A.3 Normal Q-Q plots of raw and transformed hypopigmentation area data for generation 3 180

Figure A.4. Acetylcholinesterase staining on the distal portion of colons from $Ets1^{+/-}$ *::Sox10*$^{+/+}$ mice 183

Figure A.5. Acetylcholinesterase staining on the distal portion of colons from $Ets1^{+/-}$ *::Sox10*$^{LacZ/+}$ mice 184

Figure A.6. Acetylcholinesterase staining on the distal portion of colons from $Ets1^{-/-}$ *::Sox10*$^{+/+}$ mice 185

Figure A.7. Acetylcholinesterase staining on the distal portion of colons from $Ets1^{-/-}$ *::Sox10*$^{LacZ/+}$ mice 186

LIST OF TABLES

TABLE PAGE

Table 4.1. Putative Ets1 binding sites in the *Sox10*-MCS4 enhancer sequence 125

Table A.1. Descriptive statistics for Box-Cox-transformed hypopigmentation area data for generation 1. 175

Table A.2. Levene's test of Homogeneity of Variances for the areas of hypopigmentation of $Ets1^{+/-}$, $Sox10^{LacZ/+}$, and $Ets1^{+/-}::Sox10^{LacZ/+}$ mice in generation 1 176

Table A.3. One-Way ANOVA for the areas of hypopigmentation of $Ets1^{+/-}$, $Sox10^{LacZ/+}$, and $Ets1^{+/-}::Sox10^{LacZ/+}$ mice in generation 1 176

Table A.4. Contrast Coefficients assigned to $Ets1^{+/-}$, $Sox10^{LacZ/+}$, and $Ets1^{+/-}::Sox10^{LacZ/+}$ mice in generation 1.....176

Table A.5. Contrast test comparing the sum of the mean areas of hypopigmentation in $Ets1^{+/-}$ and $Sox10^{LacZ/+}$ mice to the mean area of hypopigmentation of $Ets1^{+/-}::Sox10^{LacZ/+}$ mice in generation 1.....177

Table A.6. Descriptive statistics for Box-Cox-transformed hypopigmentation area data for generation 2. 178

Table A.7. Levene's test of Homogeneity of Variances for the areas of hypopigmentation of $Ets1^{+/-}$, $Sox10^{LacZ/+}$, and $Ets1^{+/-}::Sox10^{LacZ/+}$ mice in generation 2.....178

Table A.8. One-Way ANOVA for the areas of hypopigmentation of $Ets1^{+/-}$, $Sox10^{LacZ/+}$, and $Ets1^{+/-}::Sox10^{LacZ/+}$ mice in generation 2. 178

Table A.9. Contrast Coefficients assigned to $Ets1^{+/-}$, $Sox10^{LacZ/+}$, and $Ets1^{+/-}::Sox10^{LacZ/+}$ mice in generation 2.....179

Table A.10. Contrast test comparing the sum of the mean areas of hypopigmentation in $Ets1^{+/-}$ and $Sox10^{LacZ/+}$ mice to the mean area of hypopigmentation of $Ets1^{+/-}::Sox10^{LacZ/+}$ mice in generation 2.....179

Table A.11. Descriptive statistics for Box-Cox-transformed hypopigmentation area data for generation 3. 180

Table A.12. Levene's test of Homogeneity of Variances for the areas of hypopigmentation of *Ets1*$^{+/-}$, *Sox10*$^{LacZ/+}$, and *Ets1*$^{+/-}$*::Sox10*$^{LacZ/+}$ mice in generation 3.....181

Table A.13. One-Way ANOVA for the areas of hypopigmentation of *Ets1*$^{+/-}$, *Sox10*$^{LacZ/+}$, and *Ets1*$^{+/-}$*::Sox10*$^{LacZ/+}$ mice in generation 3. 181

Table A.14. Contrast Coefficients assigned to *Ets1*$^{+/-}$, *Sox10*$^{LacZ/+}$, and *Ets1*$^{+/-}$*::Sox10*$^{LacZ/+}$ mice in generation 3. 181

Table A.15. Contrast test comparing the sum of the mean areas of hypopigmentation in *Ets1*$^{+/-}$ and *Sox10*$^{LacZ/+}$ mice to the mean area of hypopigmentation of *Ets1*$^{+/-}$*::Sox10*$^{LacZ/+}$ mice in generation 3.....182

ABBREVIATIONS AND ACCRONYMS

ACK2 ..... Anti-c-Kit antibody

AIM-1 ..... Absent in melanoma-1

AP2 ..... Activating enhancer binding protein 2 alpha

ANOVA ..... Analysis of Variance

ARF ..... Alternate Reading Frame

ba1 ..... First branchial arch

ba2 ..... Second branchial arch

Bcl2 ..... B-Cell CLL/Lymphoma 2

BCIP 5-Bromo-4-chloro-3-indolyl-phosphate

BMP ..... Bone Morphogenetic protein

bp..... base pair

BSA ..... Bovine Serum Albumin

$CaCl_2$ ..... Calcium Chloride

CBP ..... CREB-binding protein transcription factor

Cdk2 ..... Cyclin-dependent kinase 2

cDNA ..... Complimentary Deoxyribonucleic acid

cg..... Cranial ganglia

ChIP ..... Chromatin Immunoprecipitation

c-Myb ..... Myeloblastosis viral oncogene homolog

CO_2..... Carbon dioxide

Col2A1 ..... alpha-1 type-II Colagen

DAB ..... 3,3'-Diaminobenzidine

Dct ..... Dopachrome tautomerase

DEPC ..... Diethyl Pyrocarbonate

Dlx3 ..... Distal-less homeobox 3

Dlx5 ..... Distal-less homeobox 5

DMEM ..... Dubelcco's Modified Eagle's Medium

DNA ..... Deoxyribonucleic acid

Dom ..... Dominant megacolon

DRG ..... Dorsal root ganglia

E ..... Embryonic day

EDN3 or Edn3 ..... Endothelin 3

EDNRB or Ednrb ..... Endothelin receptor B

EDTA ..... Ethylenediaminetetraacetic acid

EMT ..... Epithelial-to-mesenchymal transition

ERK ..... Extracellular signal regulated kinase

Ets ..... E26 Transforming specific sequence

F1 ..... Generation 1

F2 ..... Generation 2

F3 ..... Generation 3

FBS ..... Fetal Bovine Serum

FoxD3 ..... Forkhead box D3

FGF ..... Fibroblast growth factor

Gapdh ..... Glyceraldehyde 3-phosphate dehydrogenase

HA ..... Hyaluronic acid

HGF ..... Hepatocyte growth factor

HMG ..... High mobility group

HPLC ..... High Performance Liquid Chromatography

HPRT ..... Guanine phosphoribosyltransferase

HRP ..... Horseradish Peroxidase

IACUC ..... Institutional Animal Care and Use Committee

INK ..... Inhibitor of CDK4

KCl ..... Potassium Chloride

Kitl ..... Kit ligand

LacZ ..... β-galactosidase

LB ..... Luria Broth

Lef1 ..... Lymphoid enhancer binding factor 1

LiCl ..... Lithium Chloride

MCS ..... Multiple conserved sequences

M .....Molar

MAPK ..... Mitogen activated protein kinase

MART1 ..... Melanoma antigen recognized by T-cells 1

mg .....milligram

$MgCl_2$ ..... Magnesium Chloride

MITF or Mitf ..... Microphthalmia- associated transcription factor

ml .....milliliter

mm ..... millimeter

mm^2 ..... millimeter squared

mM ..... millimolar

MMP ..... Matrix metalloprotease

mRNA ..... Messenger Ribonucleic acid

MSA ..... Migration staging area

Msx1 ..... Msh homeobox 1

Msx2 ..... Msh homeobox 2

n ..... sample size

NaCl ..... Sodium Chloride

NBT ..... 4-Nitro blue tetrazolium chloride

NC ..... Neural crest

Nf1 ..... Neurofibromin

NIH ..... National Institute of Health

NTMT Sodium-Tris-Magnesium-Tween-20

NTP ..... Nucleotide tri-phosphate

ORF ..... Open reading frame

ot ..... otocyst

$p19^{ARF}$ ..... Alternate product $p19^{ARF}$

PAX3 or Pax3 ..... Paired box 3

PBS ..... Phosphate Buffered Saline

PBT ..... PBS containing 0.1% Tween 20

PCMV ..... Human cytomegalovirus promoter

PCR ..... Polymerase Chain Reaction

PKC ..... Protein kinase C

PMEL17 or Pmel17 ..... Melanocyte protein 17 precursor

pmol ..... picomol

PMSF ..... phenylmethylsulfonyl fluoride

PNT ..... Pointed

PVDF ..... Polyvinylidene difluoride

RNA ..... Ribonucleic acid

RPE ..... Retinal pigmented epithelium

RPM ..... Revolutions per minute

s ..... seconds

SCF ..... Stem Cell Factor

SCP ..... Schwann cell precursor

SDS ..... Sodium dodecyl sulfate

SDS-PAGE ..... Sodium dodecyl sulfate polyacrylamide gel electrophoresis

SILV ..... Silver homolog

siRNA ..... Small interfering Ribonucleic acid

SNAI1 or Snai1 ..... Snail Family Zinc Finger 1 or Snail Homolog 1

SNAI2 or Snai2 ..... Snail Family Zinc Finger 1 or Snail Homolog 2

Sox8 ..... Sex determining region Y (SRY)-box 8

Sox9 ..... Sex determining region Y (SRY)-box 9

Sox10 ..... Sex determining region Y (SRY)-box 10

SSC ..... Sodium chloride, Sodium citrate, Citric acid

TBS ..... Tris Buffered Saline

TBST ..... TBS + 0.1% Tween 20

TBX2 or Tbx2 ..... T-Box transcription factor 2

TFAP2 ..... Activating enhancer binding protein 2 alpha

TPA ..... Tetradecanoyl phorbol 13-acetate

Trp1 ..... Tyrosinase-related protein 1

Trp2 ..... Tyrosinase related protein 2

tRNA ..... Transfer Ribonucleic acid

Tyr ..... Tyrosinase

Typ1 ..... Tyrosinase-related protein 1

UCSC ..... University of California at Santa Cruz

μg ..... microgram

μl ..... microliter

μm ..... micrometer

UV ..... ultraviolet

WS ..... Waardenburg Syndrome

Zic1 ..... Zinc finger protein of the cerebellum 1

CHAPTER I

INTRODUCTION

I. INTRODUCTION

Melanocytes, the pigment producing cells, are derived from neural crest (NC) cells, a population of pluripotent cells that arise from the dorsal aspect of the neural tube during vertebrate embryogenesis (Le Douarin and Kalcheim, 1999). Neural crest cells undergo an epithelial to mesenchymal transition (EMT) and migrate out of the neural tube along distinct pathways to contribute to different tissues and organs (Le Douarin et al., 2004). In addition to melanocytes, other NC-derived lineages include endocrine cells, glial cells, neurons, craniofacial bone and cartilage, and cardiac cells (Le Douarin and Kalcheim, 1999). Defects in NC cell development result in a range of human disorders known as Neurocristopathies (Bolande, 1997). These include craniofacial malformations, cardio- and neurocutaneous syndromes, Waardenburg Syndrome (WS), Hirschsprung's disease, Tietz Syndrome, and piebaldism, among others (reviewed in Hou and Pavan, 2008; Pingault et al., 2010).

Neurocristopathies are caused by mutations in genes required for proper NC cell development. Mutations in the transcription factors sex determining region Y (SRY)-box 10 (*SOX10*), paired box 3 (*PAX3*), Microphthalmia-associated transcription factor (*MITF*) and snail homolog 2 (*SNAI2*) and in the signaling molecules Endothelin 3 (*EDN3*) and Endothelin receptor b (*EDNRB*) are responsible for the four different known types of WS. Waardenburg Syndrome is characterized by pigmentation defects, congenital deafness, and heterochromia irides; however, other anomalies, such as craniofacial and limb abnormalities, aganglionosis of the distal colon (Hirschsprung's disease), and neurological defects are found in a group of WS patients and serve for the classification of the different types of WS. The study of mouse pigmentation mutants

was instrumental in the identification of the genes involved in WS (reviewed in Tachibana et al., 2003) (Figure 1.1). The first indication that *PAX3* mutations were responsible for WS type I was the identification of loss of function mutations in the murine ortholog *Pax3* gene in the *Splotch* mouse, an embryonic lethal pigmentation mutant that exhibits neural tube and NC defects (Tassabehji et al., 1992). In the same manner, the *piebald lethal* and *lethal spotting* mouse mutants, which harbor spontaneous mutations in *Ednrb* and *Edn3* respectively, were instrumental for the identification of mutations in these genes in WS type IV and in Hirschsprung's disease (Hosoda et al., 1994; Puffenberger et al., 1994). The study of mouse pigmentation mutants has also been important for the elucidation of signaling pathways required for proper melanocyte and NC cell development and for understanding other pathological conditions of NC-derived cell lineages (Barsh, 1996; Baxter et al., 2004)

1.1 The neural crest

1.1.1 Neural crest induction

The neural crest (NC) is a transient population of cells that originates during embryonic development, between the neural ectoderm and the non-neural ectoderm, which give rise to the central nervous system and the epidermis, respectively (Le Douarin and Kalcheim, 1999). Neural crest cells delaminate from the dorsal aspect of the neural tube and travel through the embryo giving rise to various cell lineages, which include neurons and glia of the sympathetic, parasympathetic, and sensory nervous systems, smooth muscle cells, facial cartilage and bone cells, medullary secretory cells, and pigment cells or melanocytes (reviewed in Dupin et al., 2006). Much of what is known about the NC has been elucidated using avian and amphibian embryos, since these

develop externally, and are easier to manipulate than mouse embryos. Additionally, NC cells arise very early in development, at a time when mouse embryos are difficult to experiment on as a result of their small size (Gammill and Bronner-Fraser, 2003).

Transplantation and in vitro culture experiments using quail and chick neural plate and prospective epidermis have demonstrated that both the neural and the non-neural ectoderm contribute to the formation of the NC. Nonetheless, older neural plates, in the absence of prospective epidermis, are able to give rise to certain NC derivatives, particularly melanocytes, under permissive culture conditions (Selleck and Broner-Fraser, 1995). The paraxial mesoderm, which gives rise to paired somites from which the axial skeleton and skeletal muscles are derived, was also found to contribute to NC cell formation (Selleck and Broner-Fraser, 1995; Bonstein et al., 1999).

Several secreted signaling molecules are required for the induction of the NC (Figure 1.2). Intermediate levels of Bone Morphogenetic Proteins (BMPs) at the neural plate border were initially thought to be required for NC induction (Marchant et al., 1998; Tribulo et al., 2003). Bone Morphogenetic Protein levels are controlled by the BMP antagonists, Noggin, Chordin and Follistatin, all of which are expressed in the paraxial mesoderm and are important for embryonic patterning (reviewed in Sauka-Spengler and Bronner-Fraser, 2008). Experiments in the avian system using the BMP inhibitor Noggin later showed that BMPs are not required for NC induction, but rather appear to be required after neural tube closure for the maintenance of the induced NC cell population (Selleck et al., 1998). Similar experiments in *Xenopus*, using the BMP inhibitor Chordin, showed that intermediate levels of BMP signaling are not essential for NC induction (LaBonne and Broner-Fraser, 1998). In frogs and birds, BMP appears to be regulated via

Notch-Delta signaling. In the avian system, Notch activation via Delta1 was found to be required for BMP4 expression in the epidermis and for inhibiting NC formation in this region (Endo et al., 2002). The requirement of Notch for both BMP4 expression and inhibition of NC cell formation in the epidermis suggests that Notch signaling is not only important for NC formation or maintenance via BMP4, but also for restricting the NC to the neural plate border (Sauka-Spengler and Bronner-Fraser, 2008). In addition to BMPs and Notch, in *Xenopus*, fibroblast growth factor (FGF) signaling proteins from the paraxial mesoderm, particularly FGF2 and FGF8, have been found to be important for NC induction (reviewed in Gammill and Bronner-Fraser, 2003; Sauka-Spengler and Bronner-Fraser, 2008).

Experiments in *Xenopus*, zebrafish, and the chick have placed the canonical Wnt signaling pathway at the center of NC induction. In *Xenopus*, β-catenin overexpression can cell autonomously induce the expression of the NC marker *Slug* in cells that normally give rise to the epidermis (LaBonne and Broner-Fraser, 1998). Furthermore, overexpression of *Wnt3a* in the neuroectoderm can expand the number of cells expressing the NC markers *Slug* and *Krox20*, even in the presence of proliferation inhibitors. Conversely, overexpression of the β-catenin inhibitor, glycogen synthase kinase 3 beta (*GSK3β*), was found to inhibit NC cell formation (Saint-Jeannet et al., 1997). Similarly, in zebrafish, early blockage of Wnt signaling results in a significant loss of expression of NC cell markers. Moreover, transplantation experiments confirmed that Wnt acts cell-autonomously to direct the formation of NC cells (Lewis et al., 2004). In the chick, blocking Wnt signaling inhibits the expression of the NC cell marker *Slug*. On the other hand, incubating naïve neural plate cells in medium containing the Drosophila Wnt

homolog wingless, can induce NC cell formation, in the absence of other factors. These experiments showed that Wnt signaling is both required and sufficient for NC induction in the chick embryo (Garcia-Castro et al., 2002).

In the mouse, the role of the canonical Wnt signaling pathway in NC induction has not been well established (Sauka-Spengler and Bronner-Fraser, 2008). Double knockout mouse embryos of *Wnt1* and *Wnt3a* have severely reduced numbers of cells expressing NC markers and decreased numbers of NC derivatives. Similarly, conditional *β-catenin* knockout mice have severe abnormalities in cranial NC cell derivatives, but the expression of NC cell markers is unaffected in these embryos. Given the normal levels of NC cell marker expression in *β-catenin* knockout mice, it is unclear whether the decrease in NC cells seen in these mutant embryos is the result of improper NC formation or of decreased survival or proliferation (reviewed in Wu et al., 2003).

1.1.2 Specification of the neural plate border and neural crest specifier genes.

The induction signals at the border between the neural and non-neural ectoderm, lead to the expression of transcription factors that serve to specify the neural plate border, which is the region from which NC cells will be derived (Figure 1.2). The transcription factors expressed in this region are known as neural plate border specifiers (Sauka-Spengler and Bronner-Fraser, 2008). The neural plate border is not a well demarcated area (Sargent, 2006). Fate mapping experiments in the chick embryo have shown that NC cells are interspersed with otic placode precursor cells, epidermal, and neural progenitor cells in this region (Streit, 2002). The neural plate border specifier genes include the zinc-finger transcription factor *Zic1*, the activating enhancer binding protein 2 alpha (*TFAP2* or *AP2*) transcription factor, members of the paired box family of transcription factors

Pax3 and *Pax7*, the homeobox transcriptional repressors *Msx1* and *Msx2*, and the homeodomain transcription factors *Dlx3* and *Dlx5* (Figure 1.2) (reviewed in Gammill and Bronner-Fraser, 2003; Sargent, 2006; Sauka-Spengler and Bronner-Fraser, 2008). The expression of these genes at the neural plate border is required for the subsequent specification of NC cells. In addition to being expressed in prospective NC cells, some of the neural plate border specifiers are expressed in the neural plate while others are expressed in the non-neural ectoderm (reviewed in Gammill and Bronner-Fraser, 2003). In the mouse, most neural plate border specifiers begin to be expressed at embryonic day (E) 7.5, around the time the neural folds form (reviewed in Stuhlmiller and Garcia-Castro, 2012).

Following neural plate border specification, a group of transcription factors required for the specification of NC cells is upregulated. Neural crest specifier transcription factors include *Snail2*, Sex determining region Y (SRY)-box 9 (*Sox9*), *Sox10* and Forkhead box D3 (*FoxD3*) (Figure 1.2). In the mouse, *Sox9*, *Sox10* and *FoxD3* are expressed in the neural folds soon after the neural plate border is specified and right before the initiation of cranial NC cell migration around E8 (reviewed in Stuhlmiller and Garcia-Castro, 2012). The expression of NC specifiers is essential for the maintenance of the NC population and for the epithelial-to-mesenchymal transition (EMT), delamination and migration that these cells must undergo in order to reach their final destinations (Sauka-Spengler and Bronner-Fraser, 2008). Members of the Snail family of transcription factors seem to play an essential role in NC specification and EMT in chick (Nieto et al., 1994; Del Barrio and Nieto, 2002; Taneyhill et al., 2007), and frog (Carl et al., 1999; LaBonne and Bronner-Fraser, 2000) embryos, however; in the mouse embryo, migrating

NC cells can be detected in double knockouts of the *Snail* and *Slug* mouse homologs *Snai1* and *Snai2*, respectively, which suggests that other transcription factors are able to compensate for the deficiency of these two (Murray and Gridley, 2006). The transcription factor *FoxD3* is also involved in NC specification. It is expressed in almost all pre-migratory and migratory NC cells, except for cells fated to become melanocyte precursors (melanoblasts) (Kos et al., 2001). In NC cells, *FoxD3* cooperates with *Snail2*, *Sox9* and *Sox10* to promote the changes required for EMT (reviewed in Theveneau and Mayor, 2012).

The transcription factors *Sox9* and *Sox10* are expressed in the pre-migratory NC in the frog and zebrafish. In the frog, *Sox9* expression is maintained in migrating NC cells (Spokony et al., 2002). In the mouse, *Sox9* is expressed in pre-migratory and migratory NC cells, while *Sox10* expression is initiated at the onset of NC cell migration. The transcription factor *Sox9* is required for the formation of NC precursor cells by driving the expression of other NC cell markers, including *Sox10* (Cheung and Briscoe, 2003; Cheung et al., 2005; Betancur et al., 2010). In addition to its importance for NC cell formation, *Sox9* is also required for NC cell survival (Yan et al., 2005; Cheung et al., 2005) and delamination (Cheung et al., 2003). Like *Sox9*, *Sox10* is also essential for NC cell survival; however, it does not appear to be required for the initial specification of the NC cells (Southard-Smith et al., 1998; Kapur, 1999). *Sox10* also appears to be required for maintaining the pluripotency of NC cells (Kim et al., 2003; McKeown et al., 2005), and in cooperation with *Sox9*, *FoxD3* and *Snail*, it is also involved in NC cell delamination (McKeown et al., 2005; reviewed in Theveneau and Mayor, 2012).

1.1.3 Neural crest delamination and neural crest derivatives

Neural crest delamination refers to the segregation of the NC into separate populations. The process of NC delamination varies according to the region along the anterior-posterior axis from which the cells delaminate. Cranial NC cell delamination occurs all at once, while trunk NC cells delaminate gradually in a cranial to caudal order. In the mouse, cranial NC cells delaminate prior to the closure of the neural tube, while trunk NC cells migrate after neural tube closure (reviewed in Theveneau and Mayor, 2012). Nevertheless, neural tube closure and NC cell delamination do not appear to be related, as NC cell delamination and NC derivatives are unaffected in *Pax3* null mouse embryos, in which failure of neural tube closure results in severe spina bifida (Estiberio et al., 1993; Franz, 1993).

Neural crest cell delamination has been mostly studied in the chick embryo; however, the general events and signaling cascades at work are common to other vertebrate species (Sauka-Spengler and Bronner-Fraser, 2008). As a result of somite maturation, BMP and Wnt signaling promote EMT via activation of the transcription factors *FoxD3*, *Snail2*, *Sox8* and *Sox9*. The combined effect of these transcription factors is a shift in the expression of calcium-dependent adhesion proteins, or Cadherins, from type I Cadherins, like E-Cadherin and N-Cadherin, which are associated with stable epithelial and neuronal cell assemblies, respectively, to type II cadherins, like Cadherin 6B, Cadherins 7 and 11, which are expressed in mesenchymal cells (Figure 1.2) (reviewed in Sauka-Spengler and Bronner-Fraser, 2008; Theveneau and Mayor, 2012). The transcription factors *FoxD3*, *Snail2*, *Sox8* and *Sox9* also activate the expression of

extracellular signaling molecules and cytoskeletal proteins and promote laminin synthesis and the degradation of the basal lamina (Theveneau and Mayor, 2012).

Neural crest cells are divided into four overlapping domains, along the anterior-posterior axis, which give rise to different cell lineages. Nonetheless, NC cells from different levels or domains contribute to both distinct and overlapping derivatives (Bronner and Le Douarin, 2012). The four NC domains are the cranial and cephalic, the vagal and sacral, the trunk, and the cardiac NC (Le Douarin, 1982). The cranial and cephalic NC includes the cells derived from the prosencephalic, mesencephalic and anterior rhomencephalic regions (Bronner and Le Douarin, 2012). Cranial NC cells migrate dorsolaterally and give rise to mesenchymal cells that contribute to cartilage, bone, cranial neurons, glia and Schwann cells, ciliary and cranial sensory ganglia, and melanocytes of the skin and inner ear (Gilbert, 2003; Dupin and Sommer, 2012; Bronner and Le Douarin, 2012). The vagal crest is composed of the posterior rhombencephalic crest at the level of somites 1 through 7, while the sacral crest refers to the NC cells caudal to somite 28. Vagal NC cells give rise to the sympathetic ganglia of the gut. Some cells from the vagal and sacral levels also give rise to melanocytes (Bronner and Le Dourain, 2012). Cardiac NC cells overlap with the anterior portion of the vagal NC. They are located in the region from the first to the third somite between the cranial and trunk NC (Gilbert, 2003). Cardiac NC cells contribute to the septum and outflow tract of the heart (Bronner and Le Douarin, 2012). They can also give rise to melanocytes, neurons, connective tissue and cartilage (Gilbert, 2003).

Trunk NC cells comprise the cells at the cervical and thoracic levels adjacent to somites 8-28 (Bronner and Le Douarin, 2012). In the mouse, trunk NC cells migrate via

two mayor pathways, the ventral and dorsolateral pathways. Cells of the ventral pathway migrate through the rostral side of the somite between the neural tube and the dermamyotome. Trunk NC cells of the ventromedial pathway migrate in two overlapping phases. The first wave of cells migrate ventrolaterally from E9 through E9.5 (Serbedzija et al., 1990); these cells migrate more ventrally than those from the second wave, and give rise to the sympathetic ganglia, the adrenal medulla, and nerves around the aorta (Gilbert, 2003). The second wave of cells migrates ventromedially, along the lateral surface of the neural tube, in the ventromedial portion of the sclerotome, from E9.5 through E10.5. The second wave of ventrally migrating trunk NC cells gives rise to the dorsal root ganglia (DRG), Schwann cells (Serbedzija et al., 1990), and a portion of the skin melanocytes that derive from Schwann cell precursor cells (Adameyko et al., 2009). Trunk NC cells of the dorsolateral pathway migrate between the dermamyotome and the epidermis (Serbedzija et al., 1990). Dorsolaterally migrating NC cells move through the epidermis to the ventral midline and give rise to skin melanocytes (Gilbert, 2003).

The NC has been referred to as the fourth germ layer because it makes contributions to almost every tissue of the body (Hall, 2000). The large diversity of cells that are derived from the neural crest contributes to numerous features that are specific to vertebrates, including craniofacial bone and sensory glia (Bronner and Le Douarin, 2012). The multipotent nature of NC cells also makes them a useful model for the field of stem cell biology (Dupin and Sommer, 2012).

1.2 Melanocyte Development

The pigment producing cells, or melanocytes, are derived from all NC domains, but most are derived from the cranial and trunk NC. In mice, the cells fated to become

melanocyte precursors (melanoblasts) develop around E8.5, when they express *Wnt1*, *Pax3* and *Sox10*. Around E10-10.5, these cells begin to express the melanoblast markers microphthalmia-associated transcription factor (*Mitf*) and *Kit*, which codes for a tyrosine kinase receptor. After a few hours, melanoblasts localize to the migration staging area (MSA), which is located in the dorsal aspect of the neural tube. At this point melanoblasts begin to express Dopachrome tautomerase (*Dct*), which codes for one of the key enzymes in the melanin synthesis pathway. Between E10 and E12.5, signaling via the Endothelin receptor b (Ednrb) and the tyrosine kinase receptor Kit are required for melanoblast survival, proliferation, and migration. At this point, melanoblasts continue to divide as they migrate through the dermis. A large portion of melanoblasts enter the epidermis between E13.5 and E14.5 and by E15.5, a subset of them populate the still developing hair follicles. At E15.5, melanoblasts begin to express other melanogenic enzymes, including Tyrosinase (*Tyr*) and Tyrosinase-related protein 1 (*Tyrp1 or Trp1*), and sometime between E15.5 and birth, these cells differentiate into mature melanocytes once they begin to produce pigment (reviewed in Silver et al., 2006) (Figure 1.3). The final steps of differentiation also require the transcription factors Mitf and Sox10 as well as Kit and Endothelin signaling for the expression of melanogenic enzymes and subsequent pigment production (Hou et al., 2004; Hou et al., 2006; Levy et al., 2006).

For many years, all trunk melanoblasts where thought to derive solely from cells traveling via the dorsolateral pathway. Recently, a second population of melanocytes was found to derive from NC cells traveling along the ventral pathway, specifically from Schwann cell precursors (SCPs) (Adameyko et al., 2009). Schwann cell precursors express *Sox10*, and associate with neuronal projections that allow them to travel long

distances along the nerves (Jessen and Mirsky, 2005). In the chick and mouse embryos, a population of Mitf-positive cells was found within nerves of the peripheral nervous system, particularly in the distal ventral ramus of the spinal nerve, which innervates the skin. These cells were associated but not in direct contact with nerve bundles, and were found, via lineage tracing experiments, to be derived from SCPs (Adameyko et al., 2009). In the mouse, a subset of cranially derived melanocytes has also been shown to arise from SCPs around cranial nerves IX-X. Similar to trunk melanoblasts of the dorsolateral pathway, cranial SCP-derived melanoblast appear to depend on Ednrb signaling for their expansion and dispersal (Adameyko et al., 2012).

1.3. Genetic network of melanocyte development: Lessons from pigmentation mutants

The development of melanocytes from the NC is dependent upon the activation of several transcription factors, including Sox10, Pax3, and Mitf, which are involved in the specification, survival and final differentiation of melanocyte precursors. In addition to these factors, environmental cues also guide the development of melanocytes. Signaling molecules such as Wnt, Kitl and Edn3 are essential for the survival, proliferation, migration and differentiation of melanocytes. Studies in various model organisms, including the chick, zebrafish, *Xenopus*, and the mouse, have been essential for understanding the various functions and interactions of these transcription factors and signaling molecules in melanocyte development (Silver et al., 2006).

1.3.1 Cell intrinsic factors

The basic-helix-loop-helix-leucine-zipper Microphthalmia-associated transcription factor (Mitf) has been described as the master regulator of melanocyte

development (McGill et al., 2002). The expression of this transcription factor is considered the key event in the specification of melanoblasts from the neural crest. In humans, *MITF* is mutated in Waardenburg syndrome type 2a (WS2a), which is characterized by a decrease in the number of melanocytes of the eye, inner ear and forelock (Levy et al., 2006). In mice, at least 25 spontaneous *Mitf* allelic mutants have been identified. The effect of these mutations range from minor pigmentation defects in some, to complete absence of mature melanocytes in others (reviewed in Hou and Pavan, 2008). In mice homozygous for a severe *Mitf* mutation in which Mitf function is completely abrogated, NC-derived cells fail to express *Dct*. In addition, a small number of *Mitf*-expressing cells arise in NC cell cultures derived from wild type and *Mitf* mutants; however, *Mitf* mutant cells fail to express *Dct* and are quickly lost (Opdecamp et al., 1997). These results suggest that *Mitf* is necessary for either the survival, proliferation, or to prevent the trans-differentiation of melanocytes into other cell lineages. Of these functions, support for the role of Mitf in survival has come from the hypomorphic $Mitf^{vit}$ mouse mutants, which initially exhibit normal coat pigmentation, but gradually lose it as a result of the depletion of melanocyte stem cells caused by reduced Mitf levels within the bulge of the hair follicles (Lerner et al., 1986; Nishimura et al., 2005).

Additional evidence supporting a role for Mitf in melanocyte survival stems from its role as a transcriptional regulator of the Bcl2 anti-apoptotic protein (McGill et al., 2002). This protein has also been shown to be required for melanocyte viability, specifically for the maintenance of melanocyte stem cells (Nishimura et al., 2005) and melanoblasts (Mak et al., 2006). Mitf also interacts with cyclin-dependent kinase 2

(Cdk2), a cell cycle regulator essential for the maintenance of melanoma cell viability and cell cycle. Phenotypes associated with deletion *Bcl2* and *Cdk2* are less severe than those that result from *Mitf* null mutations, suggesting that Mitf may be important for melanocyte survival during development through additional pathways as of yet characterized (Lin and Fisher, 2007). Another transcriptional target of Mitf, is the hepatocyte growth factor (HGF) receptor, c-Met which has been shown to be involved in melanocyte survival in vitro, where HGF treatment of NC cells results in increased melanoblast numbers, and in vivo, where restricted HGF expression in the epidermis leads to an increase in the number of melanoblasts and mature dermal melanocytes (McGill et al., 2006).

A role for Mitf in melanocyte proliferation has been suggested because many of its transcriptional targets are important regulators of cell cycle progression and proliferation. One such target is the T-Box transcription factor 2 (*TBX2*), which indirectly regulates cell cycle progression and apoptosis by repressing the p19 Alternate Reading Frame ($p19^{Arf}$) promoter and thus inducing the degradation of the pro-apoptotic p53 protein. Mitf regulation of *Cdk2* may also be important for melanocyte proliferation, as Cdk2 promotes cell cycle progression (reviewed in Hou and Pavan, 2008). Interestingly, Mitf targets also include the cell cycle inhibitors *p21* and *Ink4a* (Inhibitor of CKD4). The inhibition of cell cycle progression is essential for differentiation, an additional role of Mitf in melanocyte development. Mitf promotes early melanocyte fate specification and melanocyte differentiation through direct transcriptional regulation of Tyrosinase (*Tyr*), Tyrosinase related protein-1 (*Trp1*) and Tyrosinase-related protein-2 (*Trp2* or *Dct*), all of which code for pigment enzymes. Other genes that have been implicated in melanocyte

differentiation and are transcriptionally regulated by Mitf include absent in melanoma-1 (*AIM-1*), melanoma antigen recognized by T-cells 1 (*MART1*), and silver homolog (*SILV or PMEL17*). The latter two genes encode melanosomal structural proteins (reviewed in Levy et al., 2006).

Other transcription factors interact with Mitf to promote melanocyte development. The transcription factors Pax3 and Sox10 have been shown to activate the *Mitf* promoter both individually (Watanabe et al., 1998; Bondurand et al., 2000; Lee et al., 2000; Potterf et al., 2000; Verastegui et al., 2000) and synergistically (Bondurand et al., 2000; Potterf et al., 2000). The specific roles of Pax3 in melanocyte development are not fully understood. In humans, *PAX3* mutations are associated with Waardenburg Syndrome (WS) types 1 and 3, which are characterized, by hipopigmentation, heterochromia irides, deafness, and in type 3, skeletal abnormalities. Spontaneous *Pax3* mutations have also been described in the mouse. The spontaneous *Splotch* mouse mutant harbors a loss of function mutation in *Pax3*. Homozygous *Splotc*h mutants exhibit spina bifida and are embryonic lethal as a result. *Splotch* heterozygotes present a belly spot, suggesting a role for this transcription factor in melanocyte development (reviewed in Hou and Pavan, 2008). In homozygous *Splotch* mutants, *Dct*-positive melanoblasts can be observed traveling along the dorsolateral pathway. In these mutants melanoblast numbers are reduced but not completely absent, which suggests that *Pax3* may not be essential for the initial specification of melanoblasts, but appears to be required for their expansion (Hornyak et al., 2001).

The transcription factor Pax3 has been suggested to both promote and inhibit melanocyte fate specification (Kubic et al., 2008). By activating *Mitf*, Pax3 may influence

melanoblasts towards the melanocytic fate. At the same time Pax3 has also been shown to inhibit *Dct* activation, which is dependent on Sox10 and Mitf, by forming a repressor complex with the transcription factor Lymphoid enhancer binding factor 1 (Lef1) and the Groucho co-repressor Grg4, and by competing with Mitf for binding to *Dct* regulatory elements (Lang et al., 2005). The dual role of Pax3 in promoting *Mitf* expression while inhibiting *Dct* expression, suggests that Pax3 may be involved in the initial fate decision of melanoblasts as well as in preventing the terminal differentiation of precursors. Maintenance of melanoblasts in an undifferentiated state may be necessary to allow the sufficient expansion of melanocyte precursors before they become terminally differentiated (Lang et al., 2005). Interestingly, Pax3 may also act to promote melanocyte differentiation as it has been shown to transactivate the *Trp1* promoter (Galibert et al., 1999).

The transcription factor *Sox10* appears to be important in the specification of melanoblasts from the NC. Sox10 is a member of the SoxE family of transcription factors, which contain a high mobility group (HMG) box DNA-dependent dimerization domain (reviewed in Harris et al., 2010). Zebrafish harboring a mutant allele of the zebrafish *Sox10* homologue display an almost complete absence of NC cells on migratory pathways associated with pigment cells. In these mutants, the differentiation of certain tissues arising from NC derivatives, including craniofacial skeleton and fin mesenchyme, is unaffected, while differentiation of other NC derivatives, including melanocytes, is severely impaired and is accompanied by the lack of *Mitf* or *Kit* expression. The pigmentation phenotype of these mutants can be rescued by *Mitf* overexpression, pointing

to a role for *Sox10* in the specification of melanocytes from the NC that appears to be mediated via transcriptional activation of *Mitf* (Dutton et al., 2001).

In the mouse, the role of Sox10 in melanocyte development appears to be slightly different than in zebrafish. The spontaneous *Dominant megacolon* (*Dom*) mouse mutant harbors a mutation in *Sox10* which results in premature truncation of the Sox10 protein. Heterozygous *Dom* ($Sox10^{Dom/+}$) mutants exhibit white spotting and aganglionosis of the distal colon. Similar developmental abnormalities are observed in human cases of WS2 and WS4, a subset of which are associated with *SOX10* mutations (Bondurand et al., 2007). Homozygous *Dom* ($Sox10^{Dom/Dom}$) mutants die by E13.5 for reasons that are not fully understood. Homozygous *Dom* mutant embryos have defects in dorsal root ganglia, sympathetic ganglia, and terminal oligodendrocyte differentiation, reduced dorsal trigeminal and facial ganglia, and absence of melanoblasts and enteric neurons (Herbarth et al., 1998; Southard-Smith et al., 1998). Similar developmental defects are also observed in $Sox10^{LacZ}$ mice, in which the *Sox10* open reading frame is replaced by the *LacZ* gene (Britsch et al., 2001). The pigmentation phenotype observed in both *Sox10* mutants results from decreased melanoblast numbers. In $Sox10^{Dom/Dom}$ embryos, complete lack of *Dct* expression (Southard-Smith et al., 1998), and increased apoptosis in NC migratory pathways (Southard-Smith et al., 1998; Kapur, 1999) are observed and suggest a role for *Sox10* in NC cell survival. Overexpression of *Mitf* in NC cultures from $Sox10^{LacZ/LacZ}$ mice can partially rescue cell survival, which implies that the regulation of melanoblast survival by *Sox10* may be linked to its role in driving *Mitf* expression (Hou et al., 2006).

The role of *Sox10* in melanoblast specification appears to be both *Mitf*-dependent and *Mitf*-independent. In $Sox10^{Dom/+}$ mice, melanoblasts lack *Dct* expression between E10.5 and E12.5; nevertheless, this transient lack of *Dct* expression does not appear to affect melanocyte differentiation because adult mice are almost completely pigmented, and *Dct*-expressing melanoblasts, although in reduced numbers, can be detected after E13.5. Neural tube cultures from $Sox10^{Dom/Dom}$ mice completely lack Mitf and Kit positive cells, while those from $Sox10^{Dom/+}$ mice have Mitf and Kit positive cells, but lack *Dct* expression. The lack of *Dct* expression in Mitf positive cells from $Sox10^{Dom/+}$ mice suggests that Sox10 is required for *Dct* expression and that endogenous Mitf may not be sufficient to drive *Dct* expression when Sox10 levels are reduced. Furthermore, Sox10 was found to transactivate the *Dct* promoter in melanocyte cell lines as well as in non-melanocyte cell lines, which do not express *Mitf* (Potterf et al., 2001). The requirement of Sox10 for *Mitf* and *Dct* expression suggests a role for *Sox10* in the initial specification of melanoblasts. *Sox10* also appears to be required for the final differentiation of melanocytes via Mitf-independent transcriptional regulation of *Tyr*, the rate-limiting enzyme in melanin-synthesis (Hou et al., 2006).

Another member of the SoxE family of transcription factors that has recently been implicated in melanocyte development is Sox9. Although Sox9 appears to be involved in early melanocyte development its specific role in this process is not well characterized. In the mouse, *Sox9* is first expressed in pre-migratory NC cells around E8.5, prior to the expression of migratory NC markers, in the hindbrain region at the dorsal tip of the closing neural tube and in the dorsal folds of the neural tube in the trunk. *Sox9* remains expressed in migrating cranial NC cells (reviewed in Lee and Saint-Jeannet, 2011) but it

is downregulated in trunk NC cells soon after they become migratory (Cheung et al., 2005). The expression of *Sox9* appears to be required for the initial specification and survival of NC cells, but it is unclear whether it acts to promote melanocyte development. Loss of function experiments in the frog and zebrafish suggest that *Sox9* does not appear to be important for melanocyte development. In *Xenopus* embryos, morpholino-induced *Sox9* depletion results in decreased expression of the NC marker *Slug* (*Snail* homolog) and loss of cranial NC cell progenitors; however, melanoblasts in the trunk appear to develop normally (Spokony et al., 2002). Likewise zebrafish mutants of the *Sox9* ortholog, *Sox9b*, which is expressed in cranial and trunk NC cells, have severe craniofacial defects but only mild defects in pigment cells. These defects, which include a reduction in the number of iridophores, one of the types of pigment cells present in zebrafish, and dispersed melanosomes within melanocytes, do not seem to be associated with impaired melanocyte development because *Dct* expression is normal in *Sox9b* mutants (Yan et al., 2006).

Although loss of function experiments do not implicate *Sox9* in melanocyte development, gain of function experiments support a role for *Sox9* in the development of melanocytes from the NC. In the chick embryo, forced expression of *Sox9* in the neural tube induces neural crest-like properties at the expense of neuronal progenitors. Furthermore, *Sox9* overexpression in migrating NC cells in the trunk region seems to bias these cells to melanocyte and glial fates, at the expense of neuronal NC-derivatives (Cheung and Briscoe, 2003). In zebrafish, both *Sox9* and *Sox10* overexpression were shown to strongly favor melanocytic fate specification, as confirmed by the presence of ectopic melanoblasts, labeled via *Mitf*, *Sox10* and *Dct,* in embryos, and the presence of

greater than normal melanocyte numbers in the tadpole stage (Taylor and LaBonne, 2005). The inconsistencies observed in *Sox9* loss of function and gain of function studies suggests that other factors may be able to compensate for the absence of *Sox9* expression in melanoblast; consequently, the effects of Sox9 in melanocyte development may be more apparent when *Sox9* is overexpressed rather than when it is knocked down.

In the mouse, Sox9 appears to be important for the survival of trunk NC cells and for the formation of trunk NC cell derivatives. Homozygous embryos carrying a conditional *Sox9* null allele, exhibit reduced numbers of neurons and glia in the trunk region as a result of increased apoptosis of pre-migratory and early migrating NC cells at E9.5 and E10.5. In these embryos, *Sox10* expression is maintained in pre-migratory NC cells but is reduced along the NC cell migration route. In pre-migratory NC cells, Sox9 was also found to be required for the expression of *Snail* (Cheung et al., 2005), a transcription factor that has been implicated in early pigment cell development and differentiation (Silver et al., 2006). Although *Sox9* seems to be required for melanocyte development early on, its prolonged expression in cells fated to become melanoblast has been shown to negatively affect melanocyte development (Qin et al., 2004). The adverse effect of prolonged *Sox9* expression on melanocyte development may be an indirect result of the role of Sox9 in the development of chondrocyte precursor cells, in which Sox9 is required for the regulation of alpha-1 type-II Collagen (*Col2A1*) expression (Bell et al., 1997). Studies in the mouse, chick and *Xenopus* suggest that *Sox9* acts upstream of *Sox10* (reviewed in Silver et al., 2006). In the chick, Sox9 was recently shown to directly bind to and activate *Sox10* regulatory regions, and to be required, for *Sox10* expression in cranial NC cells (Betancur et al., 2010). The decrease in *Sox10* expression observed in

migratory trunk NC cells in *Sox9* null mutant mouse embryos also implicates Sox9 in the regulation of *Sox10* expression in the mouse. It has been suggested that the importance of Sox9 in melanocyte development may be related to its role in regulating embryonic *Sox10* expression (Harris et al., 2010).

Although in the mouse embryo, members of the *Snail* family of zinc-finger transcription factors do not seem to be required for NC formation or delamination (Murray and Gridley, 2006), the mouse *Slug* homolog gene *Snai2* appears to be involved in melanocyte development. Early in development, the expression domains of the mouse homologs of the *Snail* and *Slug* genes are reversed relative to the expression domains of these genes in the chick. Later in development the expression domains of these two transcription factors are conserved in the chicken and the mouse. In the chick, *Snail* is not expressed in pre-migratory or migratory NC cells; however, the mouse *Snail* homolog *Snai1* is expressed in both pre-migratory and migratory NC cells. In contrast, *Slug* is expressed in pre-migratory and migratory NC cells, while in the mouse the *Slug* homolog *Snai2* is expressed in migratory NC cells but not in pre-migratory NC cells (Sefton et al., 1998). *Snai2* null mutant mice exhibit pigmentation defects and display similar developmental defects as those observed in *Kit* and Kit ligand (*Kitl*) null mutant mice. The phenotypic similarities observed in *Snai2* and *Kit*/*Kitl* mutants suggests that *Snai2* may be involved in melanocyte development and that its function in this process may be associated to *Kit* expression. Kit-positive cells from wild type mice express *Snai2*, while Kit-positive cells derived from the *Kit* and *Kitl* null mutants W/W^{v} and Sl/Sl^{d} respectively, do not express *Snai2*. Furthermore, Kitl is unable to drive melanoblast migration in Kit-positive cells purified from *Snai2* null mutant mice. These results suggest that *Snai2* may

be a transcriptional target of Kit signaling, thus it is possible that at least some of the roles of Kit signaling in melanocyte development are mediated by *Snai2* (Perez-Losada et al., 2002). Mutations in the human *SNAI2* gene have been described in WS2, which is characterized by pigmentation defects and sensorineural deafness (Tachibana et al., 2003), further implicating this transcription factor in melanocyte development.

While Mitf, Pax3, Sox10, Sox9 and Slug seem to promote melanocyte development, the transcription factor FoxD3 has been found to inhibit melanocyte development. Although FoxD3 has been shown to be required for the maintenance and specification of NC cells in the chick (Kos et al., 2001), the frog (Sasai et al., 2001) and the mouse (Teng et al., 2008), it appears to negatively regulate melanoblast specification. In the chick embryo, *FoxD3* is expressed in all NC cell lineages, except for late-emigrating melanoblasts. In vitro and in vivo knockdown of *FoxD3* results in an expansion of the melanoblast lineage at the expense of neurons and glia. On the other hand, ectopic *FoxD3* expression in late-migrating NC cells prevents the entrance of these cells into the dorsolateral migration pathway. The inability of *FoxD3*-expressing NC cells to enter the dorsolateral migration pathway is assumed to be the result of FoxD3-mediated inhibition of melanoblast specification (Kos et al., 2001), because melanoblast specification has been shown to be required for dorsolateral migration (Erickson and Goins, 1995; Erickson et al., 1998; Reedy et al., 1998). In quail NC cell cultures, *FoxD3* overexpression inhibits *Mitf* expression and melanoblast specification, driving instead the expression of glial cell markers (reviewed in Thomas and Erickson, 2008). In zebrafish, FoxD3 prevents NC precursors from being specified as melanophores by inhibiting *Mitfa* expression (Curran et al., 2009). At the same time, FoxD3 works to promote the

specification of another type of pigment cell, the iridophore, by inhibiting *Mitfa* expression in a bi-potent precursor of iridophores and melanophores (Curran et al., 2010).

1.3.2. Signaling molecules and receptors

Melanocyte development begins with the induction of NC cells by cues received from the surrounding environment. In addition to its importance in NC induction, the canonical Wnt signaling pathway, which acts via the Frizzled receptor and activates the signaling molecule and transcription factor β-catenin as well as the transcription factor Lef1, is also essential for melanoblast specification. In mice, individual knockouts of *Wnt1* and *Wnt3a* do not present with defects in NC derivatives; however *Wnt1* and *Wnt3a* double knockouts have decreased numbers of melanoblasts, which appear to be result of defective melanoblast specification, rather than decreased survival or proliferation (Ikeya et al., 1997). In mice, NC-specific deletion of *β-catenin* prevents the proper formation of melanoblasts and sensory neurons (Hari et al., 2002). On the other hand, overexpression of *β-catenin* in migratory NC cells promotes the formation of pigment cells at the expense of neurons and glia in zebrafish (Dorsky et al., 1998). The transcription factor Lef1, which functions downstream of the canonical Wnt/β-catenin pathway, is also important in melanocyte development. Loss of function of *Lef1* in *Xenopus* results in the depletion of NC-derived cell lineages, including melanocytes (Roel et al., 2009). Molecular targets of the canonical Wnt signaling pathway, as it pertains to melanocyte development, include *Mitf*, *Dct*, and *Sox10*, which further supports a role for this signaling pathway in the early stages of melanoblast specification (reviewed in Larue and Delmas, 2006).

Signaling via the Endothelin receptor b is also essential for melanoblast development. In humans, mutations in *EDNRB* and its ligand Endothelin 3 (*EDN3*) are associated with WS4, which is characterized by sensorineural deafness, hypopigmentation, and aganglionosis of the distal colon (Puffenberg et al., 1994; Attie et al., 1995). Mutations or deletions of the mouse *Ednrb* and *Edn3* result in the *piebald lethal* and *lethal spotting* phenotypes, respectively, which display similar characteristics to those seen in humans. *Ednrb* and *Edn3* null homozygotes have a mostly white coat except for the head and rump, while heterozygotes usually have a belly spot. *Piebald lethal* mice also display megacolon as a result of the absence of enteric ganglia in the distal colon (Baynash et al., 1994; Hosoda et al., 1994).

Endothelin signaling plays multiple roles in melanocyte development, regulating the survival, proliferation, migration, and final differentiation of melanoblasts (reviewed in Saldana-Caboverde and Kos, 2010). In the mouse, signaling via Ednrb is required between E10 and E12.5, which corresponds to the time point when melanoblasts reach the migration stage area (MSA). Through the use of inducible mouse models, Ednrb was shown to rescue hypopigmentation in *Ednrb* mutants as late as E10 (Shin et al., 1999). Additionally, the hypopigmentation phenotype of *piebald lethal* mice was shown to be rescued by driving *Ednrb* expression via the *Dct* promoter, which does not become active until E10 (Ittah, 2005). The results of these studies suggest that Ednrb is not required for the initial specification of melanocytic fate. The presence of small numbers of melanoblasts at E10-11.5 in *Ednrb* null mutants is consistent with *Ednrb* not being required for melanoblast specification. Given that *Ednrb* is required during the time melanoblasts reach the MSA, it has been suggested that Endothelin signaling may be

required for melanoblast migration. In transgenic *Ednrb* null mice, Dct-positive cells are present and can be found at the right locations from E10.5-E11.5; however, these melanoblasts are gradually lost without apparent defects in survival, and the few melanoblasts that remain appear to accumulate in the MSA. The apparent defect in melanoblast migration observed in *Ednrb* null mice implies that Endothelin signaling may be required for these cells to enter the dorsolateral migration pathway (Lee et al., 2003).

Several in vitro studies have implicated the Ednrb signaling pathway in the survival and proliferation of melanoblasts. Endothelin 3 has been shown to promote the survival and proliferation of glia and melanocyte precursors in NC cultures (Reid et al., 1996; Lahav et al., 1998; Opdecamp et al., 1998; Dupin et al., 2000). Endothelin signaling was also shown to promote the maintenance of an undifferentiated state in vitro. Treatment of pigmented melanocytes with Edn3 can induce the expression of the NC markers *Slug*, *Sox10*, *FoxD3*, and *Pax3* in these cells and can lead to the trans-differentiation of pigmented melanocytes into cells expressing glial markers (reviewed in Saldana-Caboverde and Kos, 2010)

Although *Ednrb* does not appear to be required for the initial specification of melanoblasts and appears to favor the maintenance of undifferentiated state, in vitro and in vivo studies have implicated Endothelin signaling in melanocyte differentiation. Even though Edn3 treatment of avian NC cultures initially promotes the maintenance of undifferentiated precursors, prolonged treatment leads to the development of pigment-producing melanocytes (Lahav et al., 1996; Lahav et al., 1998). In mouse NC cultures, Dct-positive cells are found in the absence of Edn3; however, Edn3 treatment, or

activation of protein kinase C (PKC), a downstream target of Endothelin signaling, is necessary for the generation of pigmented melanocytes (Ono et al., 1998; Opdecamp et al., 1998). Similarly, Dct-positive cells from *Ednrb* null mutant embryos can express *Sox10*, *Mitf* and *Kit* but fail to express *Tyr* and do not differentiate into mature pigment-producing melanocytes (Hou et al., 2004). Together these results suggest that although Endothelin signaling does not appear to be required for the initial specification of melanoblasts, it is essential for the final differentiation of melanocytes (reviewed in Saldana-Caboverde and Kos, 2010).

Signaling via the tyrosine kinase receptor Kit has also been shown to be involved in normal melanocyte development. In the mouse, mutations in *Kit* and Kit ligand (*Kitl*) (formerly known as Stem Cell Factor) result in a phenotype characterized by a belly spot in heterozygous animals, and by anemia, lack of coat pigmentaion, and sterility in homozygotes that survive to adulthood. In humans, *KIT* and *KITL* mutations are responsible for piebaldism, which is characterized by hair and skin hypopigmentation (reviewed in Hou and Pavan, 2008). Similar to Endothelin signaling, Kit signaling does not appear to be required for the initial specification of melanoblasts, as Dct and Mitf positive cells are present in *Kit* null mutants and in mice carrying a dominant negative form of the Kit receptor (reviewed in Sommer, 2011).

Kit ligand is produced in soluble and membrane bound forms, which are differentially required in melanocyte development, with the former being required for melanoblast migration on the lateral pathway and/or their survival in the MSA, and the latter being required for melanoblast survival in the dermis (Wherler-Haller and Weston, 1995). During development, melanocyte precursors are sensitive to Kit signaling at

particular stages, specifically during migration in the dermis and after entering the epidermal layer before entering the hair follicle. Inhibition of Kit signaling with the ACK2 anti-Kit antibody during these stages results in the loss of melanocytes hinting at the importance of Kit signaling for melanocyte survival and proliferation (Yoshida et al., 1996). Additional evidence for these roles comes from the *K14-SCF* transgenic mouse, in which transgenic *Kitl* (formerly known as *SCF*) expression in the epidermis promotes the survival of melanocytes in the epidermis, where they are not normally found in the adult mouse, and leads to a large increase in melanocyte numbers (Kunisada et al., 1998).

Endothelin and Kit signaling have been found to interact in melanocyte development. In mouse NC cultures, treatment with Edn3 and Kitl significantly increases melanoblasts numbers, compared to treatment with either factor on its own. Nevertheless, Edn3 treatment of *Kitl* null NC cells cannot induce *Kit* expression or the generation of fully pigmented melanocytes in vitro. Similarly, Kitl treatment in the absence of Edn3 cannot induce the differentiation of pigment-producing melanocytes, which can only be found in culture in the presence of both factors (Ono et al., 1998). The apparent interaction between Endothelin and Kit signaling may underlie the non-cell autonomous and cell-autonomous roles of Ednrb signaling in melanocyte differentiation. Neural crest cells from *Ednrb* null mice can give rise to melanoblasts; however, these melanoblasts fail to express *Tyr*. Treatment of *Ednrb* null melanoblasts with Kitl can induce *Tyr* expression; nevertheless, pigmented melanocytes do not develop in the absence of functional Ednrb signaling. These results suggest that Ednrb functions non-cell autonomously to induce *Tyr* expression in the presence of Kitl, and cell-autonomously in

the final differentiation of melanocytes (Hou et al., 2004). These results also help explain why both factors are needed for the generation of fully pigmented melanocytes

1.4 Research Questions

Melanocytes provide pigmentation to skin and hair via the production of melanin, and confer protection against the damaging effects of ultraviolet radiation. Mutations or deletions in genes required for the development of melanocytes from the NC can result in hypopigmentation owing to the reduction or complete loss of melanocyte precursors (melanoblasts) or to the impaired migration of these precursors (reviewed in Lin and Fisher, 2007). For this reason, the study of mouse pigmentation mutants has been instrumental for the elucidation of genes and signaling pathways involved in NC and melanocyte development (Baxter et al., 2004). Nevertheless, fundamental questions regarding the transcriptional regulation of these genes as well as their interactions in NC and melanocyte development remain to be answered. In recent studies, mice having a targeted disruption of the transcription factor *Ets1* were shown to develop cardiac malformations, as a result of NC defects, and to exhibit ventral hypopigmentation (Gao et al., 2010). A specific role for *Ets1* in melanocyte development has not been established; however, the hypopigmentation phenotype observed in *Ets1* mutants suggests that this transcription factor is involved in this process. Recent studies in the chick embryo have established a requirement for Ets1 in the endogenous expression of the transcription factor *Sox10* in cranial NC cells (Betancur et al., 2010); therefore, it is possible that the role of *Ets1* in melanocyte development could be mediated via transcriptional activation of *Sox10*. Establishing the function(s) of this transcription factor in melanocyte development has important implications for understanding pathological NC and

melanocytic conditions. It can also serve to provide a more complete picture of the transcriptional network that controls melanocyte development. My central hypothesis is that *Ets1* plays a role in early melanocyte development and regulates the activity of other critical melanoblast-specific genes. To test this hypothesis I addressed the following questions:

Question 1: What is the temporal requirement of *Ets1* in murine melanocyte development?

I hypothesized that *Ets1* is required early in melanocyte development. I used *Dct-LacZ* transgenic mice in which *LacZ* expression is driven to melanoblasts under the control of the Dopachrome tautomerase (Dct) promoter (Zhao and Overbeek, 1999), to label melanoblasts via β-galactosidase activity in *Ets1* null, heterozygous, and wild type embryos in order to determine the earliest time at which differences in melanoblast numbers and/or position can be observed.

Question 2: Is *Ets1* required for melanoblast survival or proliferation in the mouse embryo?

Given the hypopigmentation phenotype observed in *Ets1* mutant mice, I hypothesized that *Ets1* regulates melanocyte survival or proliferation during embryonic development. Using a combination of in vivo and in vitro proliferation and cell survival assays I compared the extent of melanoblast survival and proliferation in *Ets1* null, heterozygous, and wild type mouse embryos.

Question 3: Does *Ets1* genetically interact with the transcription factor *Sox10* in melanocyte development?

Findings in the avian system, which implicate *Ets1* in the regulation of the transcription factor *Sox10* (Betancur et al., 2010), pointed to a potential interaction between *Ets1* and *Sox10* in melanocyte development. To establish whether *Ets1* genetically interacts with *Sox10*, *Ets1* heteroxygous ($Ets1^{+/-}$) mice were crossed to *Sox10* heterozygous ($Sox10^{LacZ/+}$) mice, in which *LacZ* is inserted into the *Sox10* locus (Britsch et al., 2001). The hypopigmentation phenotypes of the double heterozygous progeny were compared to that of single heterozygotes in 3 generations of mice, to establish whether an additive, epistatic, suppressed, or synergistic genetic interaction exists between *Ets1* and *Sox10* in melanocyte development.

Question 4: Does *Ets1* affect the development of enteric ganglia and does it interact with the transcription factor *Sox10* in enteric innervation?

In addition to being required for melanocyte development, *Sox10* is also required for the development of NC-derived enteric ganglia (Kapur, 1999) and mutations in this transcription factor have been described in both syndromic and non-syndromic aganglionosis of the distal colon or Hirschsprung's disease (Sanchez-Mejias et al., 2010). Given the importance of *Sox10* for proper gut innervation, I also analyzed the guts of *Ets1* heterozygous and null mutant mice that were either wild type or heterozygous for *Sox10*, to establish whether *Ets1* plays a role in the development of enteric ganglia, and if so, whether it genetically interacts with *Sox10* to promote proper gut innervation.

Question 5: Can Ets1 transcriptionally regulate *Sox10*?

In light of the importance of Ets1 for *Sox10* expression in cranial NC cells in the chick embryo, I hypothesized that Ets1 can activate the expression of *Sox10* by binding to cis-binding sites on *Sox10* enhancers. To address this question I tested the ability of wild type and mutated Ets1 protein to activate the *Sox10*-MCS4 enhancer, which is known to drive *Sox10* expression to melanocytes and melanoblasts in the mouse (Antonellis et al., 2008).

Question 6: Does Ets1 regulate the expression of genes required for melanoblast development?

In order to characterize the molecular basis for the hypopigmentation phenotype observed in *Ets1* mutant mice, I analyzed the effect of *Ets1* overexpression and knockdown on the expression of various genes required for melanocyte development. Using semi-quantitative real-time Polymerase Chain Reaction (PCR), I compared the expression levels of the transcription factors *Pax3*, *Mitf*, *Sox9,* and *Sox10*, and of the *Ednrb* and *Kit* receptors, in mouse melanocyte and melanoma cell lines transfected with *Ets1* and control siRNAs or with *Ets1* overexpression and control vectors.

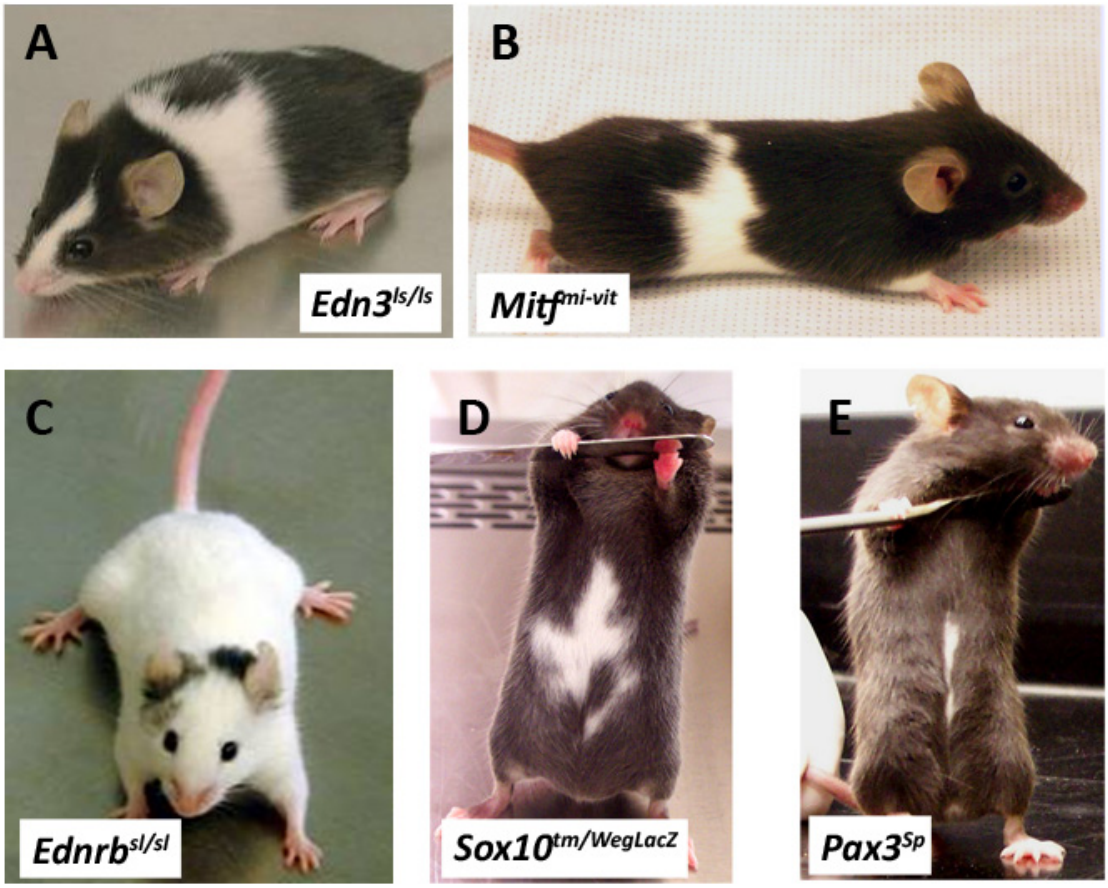

Figure 1.1. Mouse pigmentation mutants. Mutations in Endothelin 3 (*Edn3*) (A) and the Endothelin receptor b (*Ednrb*) (C) are responsible for the hypopigmentation phenotypes of the *lethal spotting* ($Edn3^{ls/ls}$) and *piebald lethal* ($Ednrb^{sl/sl}$) spontaneous mouse mutants. Mutations or deletions in the transcription factors *Mitf* (B), *Sox10* (D) and *Pax3* (E) also result in hypopigmentation in mice.

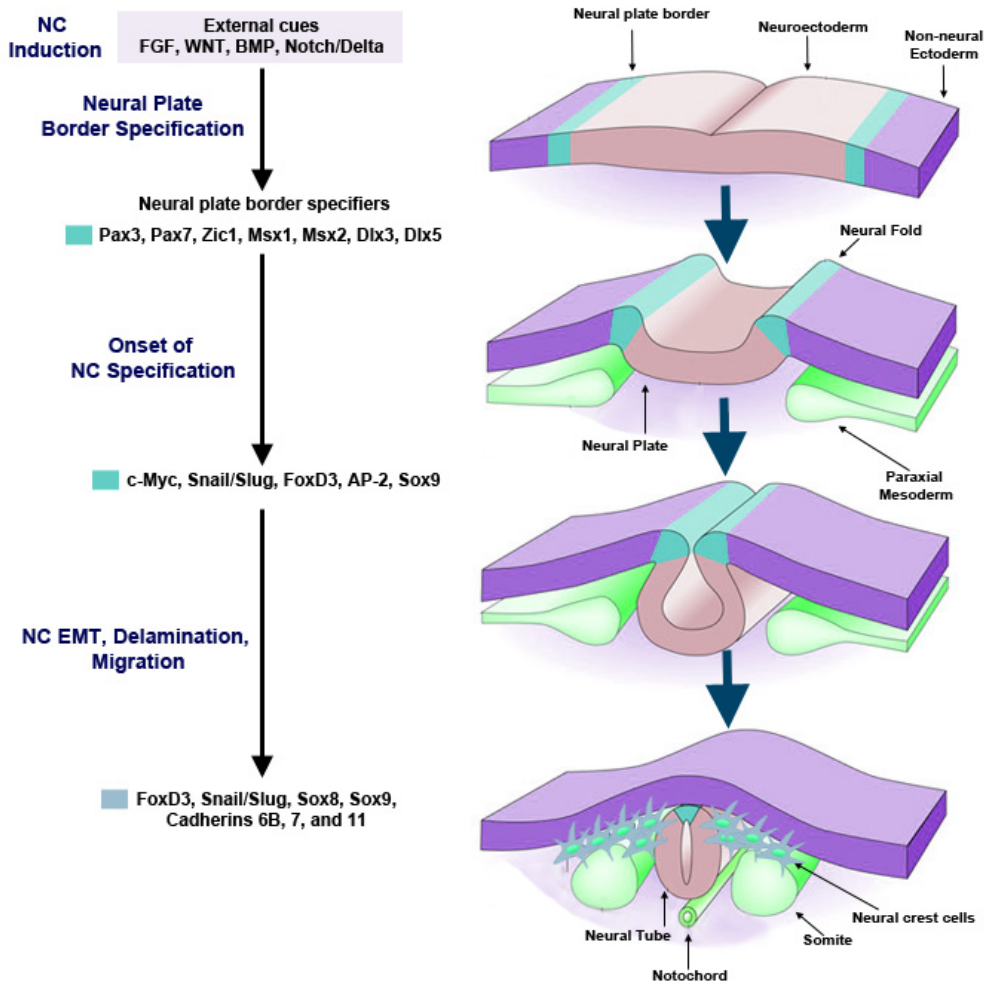

Figure 1.2. Neural crest development. Neural crest induction is mediated by Wnt, BMP, Delta and FGF signaling molecules which are released from the surrounding neuroectoderm, paraxial mesoderm and non-neural ectoderm. The induction signals at the border between the neural and non-neural ectoderm, lead to the expression of transcription factors that serve to specify the neural plate border, which is the region from which NC cells will be derived. The neural plate border specifiers include the transcription factors *Pax3*, *Pax7*, *Zic*, *Msx1*, *Msx2*, *Dlx3*, and *Dlx5*. Following neural plate border specification, a group of transcription factors required for the specification of NC cells is upregulated. These transcription factors include *Snail2*, *Sox9*, *Sox10* and *FoxD3*. In the mouse, *Sox9*, *Sox10* and *FoxD3* are expressed in the neural folds soon after the neural plate border is specified. The expression of NC specifiers is essential for the maintenance of the NC population and for the epithelial-to-mesenchymal transition (EMT), delamination and migration that these cells must undergo in order to reach their final destinations. Neural crest EMT, delamination and migration are mediated by the

transcription factors, *FoxD3*, *Snail2*, *Sox8* and *Sox9*. These transcription factors work together to induce a switch in the expression of calcium-dependent adhesion proteins (Cadherins), from type I Cadherins to type II Cadherins. They also activate the expression of extracellular signaling molecules and cytoskeletal proteins and promote laminin synthesis and the degradation of the basal lamina.

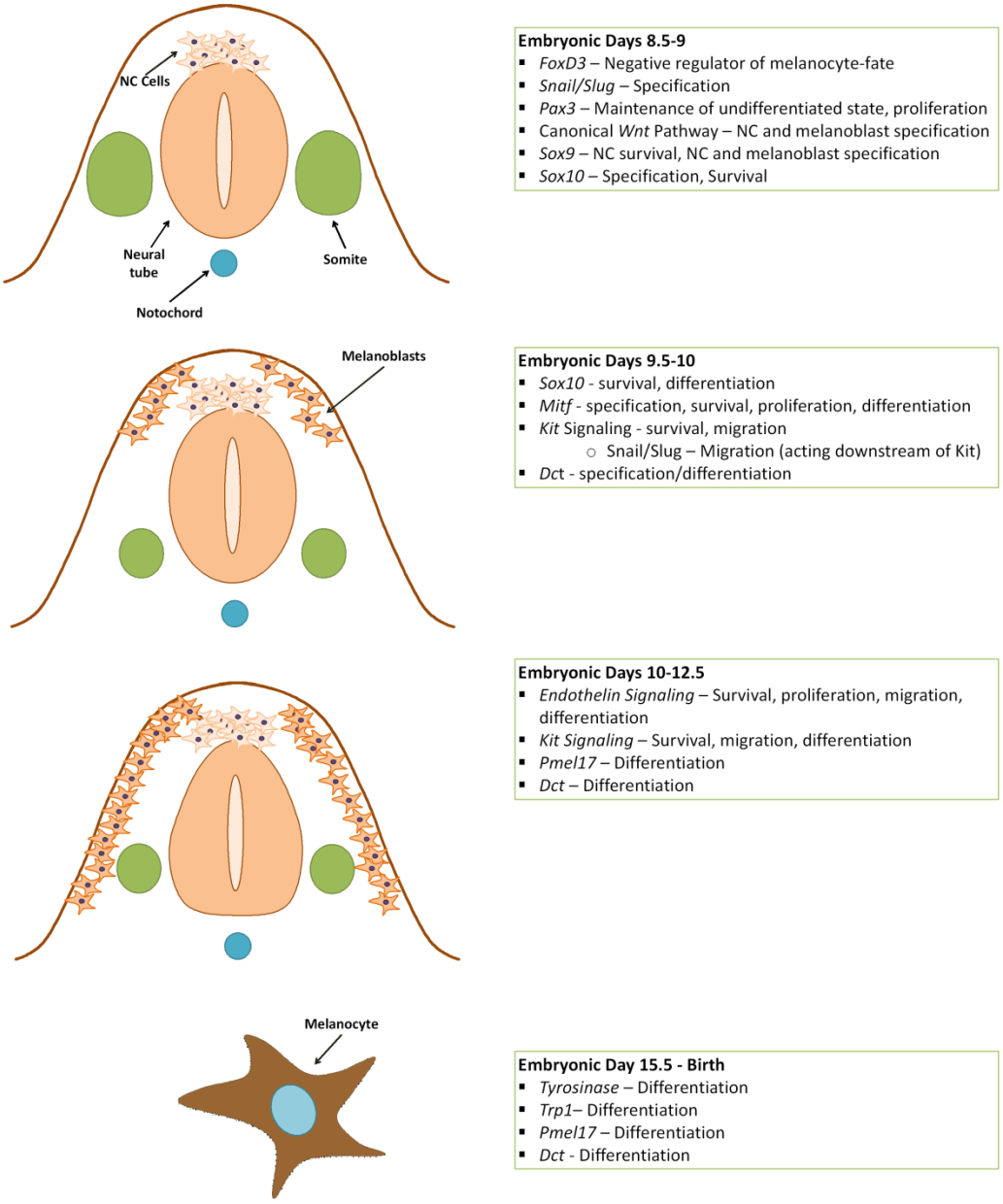

Figure 1.3. Melanocyte development from the neural crest. Cells fated to give rise to melanocyte precursors are specified by Wnt signaling and the transcription factors *Pax3* and *Sox10*, among others. Around E10-10.5, these cells begin to express the melanoblast markers *Kit* and *Mitf* and localize to the migration staging area (MSA), which is located in the dorsal aspect of the neural tube. At this point melanoblasts begin to express *Dct*, which codes for one of the key enzymes in the melanin synthesis pathway. Between E10 and E12.5, signaling via the Endothelin receptor b (Ednrb) and the tyrosine kinase receptor Kit are required for melanoblast survival, proliferation, and migration, and differentiation. Melanoblasts continue to divide as they migrate through the dermis. A

large portion of melanoblasts enter the epidermis between E13.5 and E14.5 and by E15.5, a subset of them populate the still developing hair follicles. At E15.5, melanoblasts begin to express other melanogenic enzymes, including Tyrosinase (*Tyr*) and Tyrosinase-related protein 1 (*Tyrp1 or Trp1*), which are transcriptionally regulated by Mitf and Sox10. Sometime between E15.5 and birth, these cells differentiate into mature melanocytes once they begin to produce pigment.

1.5 References

Adameyko, I., Lallemend, F., Aquino, J., Pereira, J., Topilko, P., Müller, T., Fritz, N., Beljajeva, A., Mochii, M., Liste, I., Usoskin, D., Suter, U., Birchmeier, C., Ernfors, P. (2009). Schwann cell precursors from nerve innervation are a cellular origin of melanocytes in skin. *Cell* 139, 366–379.

Adameyko, I., Lallemend, F., Furlan, A., Zinin, N., Aranda, S., Kitambi, S., Blanchart, A., Favaro, R., Nicolis, S., Lübke, M., Müller, T., Birchmeier, C., Suter, U., Zaitoun, I., Takahashi, Y. and Ernfors, P. (2011). Sox2 and Mitf cross-regulatory interactions consolidate progenitor and melanocyte lineages in the cranial neural crest. *Development* 139, 397–410.

Antonellis, A., Huynh, J., Lee-Lin, S.-Q., Vinton, R., Renaud, G., Loftus, S., Elliot, G., Wolfsberg, T., Green, E., McCallion, A. S. and Pavan, W. J. (2008). Identification of neural crest and glial enhancers at the mouse Sox10 locus through transgenesis in zebrafish. *PLoS genetics* 4, e1000174.

Attié, T., Till, M., Pelet, A., Amiel, J., Edery, P., Boutrand, L., Munnich, A. and Lyonnet, S. (1995). Mutation of the endothelin-receptor B gene in Waardenburg-Hirschsprung disease. *Human molecular genetics* 4, 2407–2409.

Barsh, G. (1996). The genetics of pigmentation: from fancy genes to complex traits. *Trends in genetics : TIG* 12, 299–305.

Baxter, L., Hou, L., Loftus, S. and Pavan, W. J. (2004). Spotlight on spotted mice: a review of white spotting mouse mutants and associated human pigmentation disorders. *Pigment cell research* 17, 215–224.

Baynash, A., Hosoda, K., Giaid, A., Richardson, J., Emoto, N., Hammer, R. and Yanagisawa, M. (1994). Interaction of endothelin-3 with endothelin-B receptor is essential for development of epidermal melanocytes and enteric neurons. *Cell* 79, 1277–1285.

Bell, D., Leung, K., Wheatley, S., Ng, L., Zhou, S., Ling, K., Sham, M., Koopman, P., Tam, P. and Cheah, K. (1997). SOX9 directly regulates the type-II collagen gene. *Nature genetics* 16, 174–178.

Betancur, P., Bronner-Fraser, M. and Sauka-Spengler, T. (2010). Genomic code for Sox10 activation reveals a key regulatory enhancer for cranial neural crest. *Proc. Natl. Acad Sci U.S.A.* 107, 3570–3575.

Bolande, R. P. (1997). Neurocristopathy: its growth and development in 20 years. *Pediatric pathology & laboratory medicine* 17, 1–25.

Bondurand, N., Pingault, V., Goerich, D., Lemort, N., Sock, E., Le Caignec, C., Wegner, M. and Goossens, M. (2000). Interaction among SOX10, PAX3 and MITF, three genes altered in Waardenburg syndrome. *Human molecular genetics* 9, 1907–1917.

Bondurand, N., Moal, F. D.-L., Stanchina, L., Collot, N., Baral, V., Marlin, S., Attie-Bitach, T., Giurgea, I., Skopinski, L., Reardon, W., Toutain, A., Sarda P., Echaieb, A., Lackmy-Port-Lis, M., Touraine, R., Amiel J., Goossens, M. and Pingault, V. (2007). Deletions at the SOX10 Gene Locus Cause Waardenburg Syndrome Types 2 and 4. *The American Journal of Human Genetics* 81, 1169-1185.

Bonstein, L., Elias, S. and Frank, D. (1998). Paraxial-fated mesoderm is required for neural crest induction in Xenopus embryos. *Developmental biology* 193, 156–168.

Britsch, S., Goerich, D., Riethmacher, D., Peirano, R., Rossner, M., Nave, K., Birchmeier, C. and Wegner, M. (2001). The transcription factor Sox10 is a key regulator of peripheral glial development. *Genes & development* 15, 66–78.

Bronner, M. E. and Le Douarin, N. M. (2012). Development and evolution of the neural crest: An overview. *Developmental Biology* 366, 2-9.

Carl, T., Dufton, C., Hanken, J. and Klymkowsky, M. (1999). Inhibition of neural crest migration in Xenopus using antisense slug RNA. *Developmental biology* 213, 101–115.

Cheung, M. and Briscoe J. (2003). Neural crest development is regulated by the transcription factor Sox9. *Development* 130, 5681-5693.

Cheung, M., Chaboissier, M.-C., Mynett, A., Hirst, E., Schedl, A. and Briscoe, J. (2005). The transcriptional control of trunk neural crest induction, survival, and delamination. *Developmental cell* 8, 179–192.

Curran, K., Raible, D. and Lister, J. (2009). Foxd3 controls melanophore specification in the zebrafish neural crest by regulation of Mitf. *Developmental biology* 332, 408–417.

Curran, K., Lister, J., Kunkel, G., Prendergast, A., Parichy, D. and Raible, D. (2010). Interplay between Foxd3 and Mitf regulates cell fate plasticity in the zebrafish neural crest. *Developmental biology* 344, 107–118.

Del Barrio, M. and Nieto, M. (2002). Overexpression of Snail family members highlights their ability to promote chick neural crest formation. *Development* 129, 1583–1593.

Dorsky, R., Moon, R. and Raible, D. (1998). Control of neural crest cell fate by the Wnt signalling pathway. *Nature* 396, 370–373.

Dupin, E., Glavieux, C., Vaigot, P. and Le Douarin, N. (2000). Endothelin 3 induces the reversion of melanocytes to glia through a neural crest-derived glial-melanocytic progenitor. *Proc. Natl. Acad Sci U.S.A.* 97, 7882–7887.

Dupin, E., Creuzet, S. and Le Douarin, N. M. (2005). The contribution of the neural crest to the vertebrate body. *Advances in experimental medicine and biology* 589, 96–119.

Dupin, E., Creuzet, S. and Le Douarin, N. M. (2006). "The contributions of the neural crest to the vertebrate body." *Neural Crest Induction and Differentiation*. Ed. Saint-Jeannet, J-.P. Georgetown: Landes Biosciences 96-113.

Dupin, E. and Sommer, L. (2012). Neural crest progenitors and stem cells: From early development to adulthood. *Developmental Biology* 366, 83-95.

Dutton, K., Pauliny, A., Lopes, S., Elworthy, S., Carney, T., Rauch, J., Geisler, R., Haffter, P. and Kelsh, R. (2001). Zebrafish colourless encodes sox10 and specifies non-ectomesenchymal neural crest fates. *Development* 128, 4113–4125.

Endo, Y., Osumi, N. and Wakamatsu, Y. (2002). Bimodal functions of Notch-mediated signaling are involved in neural crest formation during avian ectoderm development. *Development* 129, 863–873.

Erickson, C. A. and Goins, T. L. (1995). Avian neural crest cells can migrate in the dorsolateral pathway only if they are specified as melanocytes. *Development* 121, 915-924.

Erickson, C. A. and Reedy, M. (1998). Neural crest development: the interplay between morphogenesis and cell differentiation. *Current topics in developmental biology* 40, 177–209.

Estibeiro, J., Brook, F. and Copp, A. (1993). Interaction between splotch (Sp) and curly tail (ct) mouse mutants in the embryonic development of neural tube defects. *Development* 119, 113–121.

Franz, T. (1992). Neural tube defects without neural crest defects in splotch mice. *Teratology* 46, 599–604.

Galibert, M., Yavuzer, U., Dexter, T. and Goding, C. (1999). Pax3 and regulation of the melanocyte-specific tyrosinase-related protein-1 promoter. *The Journal of biological chemistry* 274, 26894–26900.

Gammill, L. and Bronner-Fraser, M. (2003). Neural crest specification: migrating into genomics. *Nature reviews. Neuroscience* 4, 795–805.

Gao, Z., Kim, G., Mackinnon, A., Flagg, A., Bassett, B., Earley, J. and Svensson, E. (2010). Ets1 is required for proper migration and differentiation of the cardiac neural crest. *Development* 137, 1543–1551.

Garcia-Castro, M., Marcelle, C. and Bronner-Fraser, M. (2002). Ectodermal Wnt function as a neural crest inducer. *Science* 297, 848–851.

Gilbert, S. (2003). Developmental Biology. Sunderland: Sinauer Associates, Inc

Hall, B. (2000). The neural crest as a fourth germ layer and vertebrates as quadroblastic not triploblastic. *Evolution & development* 2, 3–5.

Hari, L., Brault, V., Kléber, M., Lee, H.-Y., Ille, F., Leimeroth, R., Paratore, C., Suter, U., Kemler, R. and Sommer, L. (2002). Lineage-specific requirements of beta-catenin in neural crest development. *The Journal of cell biology* 159, 867–880.

Harris, M. L., Baxter, L. L., Loftus, S. K. and Pavan, W. J. (2010). Sox proteins in melanocyte development and melanoma. *Pigment Cell & Melanoma Research* 23, 456-513.

Herbarth, B., Pingault, V., Bondurand, N., Kuhlbrodt, K., Hermans-Borgmeyer, I., Puliti, A., Lemort, N., Goossens, M. and Wegner, M. (1998). Mutation of the Sry-related Sox10 gene in Dominant megacolon, a mouse model for human Hirschsprung disease. *Proc. Natl. Acad Sci U.S.A.* 95, 5161–5165.

Hornyak, T., Hayes, D., Chiu, L. and Ziff, E. (2001). Transcription factors in melanocyte development: distinct roles for Pax-3 and Mitf. *Mechanisms of development* 101, 47–59.

Hosoda, K., Hammer, R., Richardson, J., Baynash, A., Cheung, J., Giaid, A. and Yanagisawa, M. (1994). Targeted and natural (piebald-lethal) mutations of endothelin-B receptor gene produce megacolon associated with spotted coat color in mice. *Cell* 79, 1267–1276.

Hou, L., Pavan, W., Shin, M. and Arnheiter, H. (2004). Cell-autonomous and cell non-autonomous signaling through endothelin receptor B during melanocyte development. *Development* 131, 3239–3247.

Hou, L., Arnheiter, H. and Pavan, W. (2006). Interspecies difference in the regulation of melanocyte development by SOX10 and MITF. *Proc. Natl. Acad Sci U.S.A.* 103, 9081–9085.

Hou, L. and Pavan, W. (2008). Transcriptional and signaling regulation in neural crest stem cell-derived melanocyte development: do all roads lead to Mitf? *Cell research* 18, 1163–1176.

Ikeya, M., Lee, S., Johnson, J., McMahon, A. and Takada, S. (1997). Wnt signalling required for expansion of neural crest and CNS progenitors. *Nature* 389, 966–970.

Ittah, A. (2005). Endothelin receptor B and neural crest derived melanocyte development. FIU Electronic Theses and Dissertations. Paper AAI3217573. http://digitalcommons.fiu.edu/dissertations/AAI3217573

Jessen, K. and Mirsky, R. (2005). The origin and development of glial cells in peripheral nerves. *Nature reviews. Neuroscience* 6, 671–682.

Kapur, R. P. (1999). Early death of neural crest cells is responsible for total enteric aganglionosis in Sox10(Dom)/Sox10(Dom) mouse embryos. *Pediatric and developmental pathology* 2, 559–569.

Kim, J., Lo, L., Dormand, E. and Anderson, D. (2003). SOX10 maintains multipotency and inhibits neuronal differentiation of neural crest stem cells. *Neuron* 38, 17–31.

Kos, R., Reedy, M., Johnson, R. and Erickson, C. (2001). The winged-helix transcription factor FoxD3 is important for establishing the neural crest lineage and repressing melanogenesis in avian embryos. *Development* 128, 1467-1479.

Kubic, J., Young, K., Plummer, R., Ludvik, A. and Lang, D. (2008). Pigmentation PAX-ways: the role of Pax3 in melanogenesis, melanocyte stem cell maintenance, and disease. *Pigment cell & melanoma research* 21, 627–645.

Kunisada, T., Lu, S. Z., Yoshida, H., Nishikawa, S., Mizoguchi, M., Hayashi, S., Tyrrell, L., Williams, D. A., Wang, X. and Longley, B. J. (1998). Murine cutaneous mastocytosis and epidermal melanocytosis induced by keratinocyte expression of transgenic stem cell factor. *Journal of Experimental Medicine* 187, 1565-1573.

LaBonne, C. and Bronner-Fraser, M. (1998). Neural crest induction in Xenopus: evidence for a two-signal model. *Development* 125, 2403-2414.

LaBonne, C. and Bronner-Fraser, M. (2000). Snail-related transcriptional repressors are required in Xenopus for both the induction of the neural crest and its subsequent migration. *Developmental biology* 221, 195–205.

Lahav, R., Ziller, C., Dupin, E. and Le Douarin, N. (1996). Endothelin 3 promotes neural crest cell proliferation and mediates a vast increase in melanocyte number in culture. *Proc. Natl. Acad Sci U.S.A.* 93, 3892–3897.

Lahav, R., Dupin, E., Lecoin, L., Glavieux, C., Champeval, D., Ziller, C. and Le Douarin, N. (1998). Endothelin 3 selectively promotes survival and proliferation of neural crest-derived glial and melanocytic precursors in vitro. *Proc. Natl. Acad Sci U.S.A.* 95, 14214–14219

Lang, D., Lu, M., Huang, L., Engleka, K., Zhang, M., Chu, E., Lipner, S., Skoultchi, A., Millar, S. and Epstein, J. (2005). Pax3 functions at a nodal point in melanocyte stem cell differentiation. *Nature* 433, 884–887.

Larue, L. and Delmas, V. (2006). The WNT/Beta-catenin pathway in melanoma. *Frontiers in Bioscience* 11, 733-742.

Le Douarin, N. and Kalcheim, C. (1982). The neural crest. Cambridge: Cambridge University Press.

Le Douarin, N. and Kalcheim, C. (1999). The neural crest, 2nd ed. Cambridge: Cambridge University Press.

Le Douarin, N., Creuzet, S., Couly, G. and Dupin, E. (2004). Neural crest cell plasticity and its limits. *Development* 131, 4637–4650.

Lee, M., Goodall, J., Verastegui, C., Ballotti, R. and Goding, C. (2000). Direct regulation of the Microphthalmia promoter by Sox10 links Waardenburg-Shah syndrome (WS4)-associated hypopigmentation and deafness to WS2. *The Journal of biological chemistry* 275, 37978–37983.

Lee, H.-O., Levorse, J. and Shin, M. (2003). The endothelin receptor-B is required for the migration of neural crest-derived melanocyte and enteric neuron precursors. *Developmental biology* 259, 162–175.

Lee, Y.-H. and Saint-Jeannet, J.-P. (2011). Sox9 function in craniofacial development and disease. *Genesis* 49, 200-208.

Lerner, A., Shiohara, T., Boissy, R., Jacobson, K., Lamoreux, M. and Moellmann, G. (1986). A mouse model for vitiligo. *The Journal of investigative dermatology* 87, 299–304.

Levy C., Khaled M. and Fisher D.E. (2006). MITF: master regulator of melanocyte development and melanoma oncogene. *Trends in Molecular Medicine* 2, 408-414.

Lewis, J., Bonner, J., Modrell, M., Ragland, J., Moon, R., Dorsky, R. and Raible, D. (2004). Reiterated Wnt signaling during zebrafish neural crest development. *Development* 131, 1299–1308.

Lin, J. and Fisher, D. (2007). Melanocyte biology and skin pigmentation. *Nature* 445, 843–850.

Mak, S.-S., Moriyama, M., Nishioka, E., Osawa, M. and Nishikawa, S.-I. (2006). Indispensable role of Bcl2 in the development of the melanocyte stem cell. *Developmental biology* 291, 144–53.

Marchant, L., Linker, C., Ruiz, P., Guerrero, N. and Mayor, R. (1998). The inductive properties of mesoderm suggest that the neural crest cells are specified by a BMP gradient. *Developmental biology* 198, 319–329.

McGill, G. G., Horstmann, M., Widlund, H. R., Du, J., Motyckova, G., Nishimura, E. K., Lin, Y.-L., Ramaswamy, S., Avery, W. and Ding, H.-F. (2002). Bcl2 Regulation by the Melanocyte Master Regulator Mitf Modulates Lineage Survival and Melanoma Cell Viability. *Cell* 109, 707-718.

McGill, G., Haq, R., Nishimura, E. and Fisher, D. (2006). c-Met expression is regulated by Mitf in the melanocyte lineage. *The Journal of biological chemistry* 281, 10365–10373.

McKeown, S., Lee, V., Bronner-Fraser, M., Newgreen, D. and Farlie, P. (2005). Sox10 overexpression induces neural crest-like cells from all dorsoventral levels of the neural tube but inhibits differentiation. *Developmental dynamics* 233, 430–444.

Murray, S. and Gridley, T. (2006). Snail family genes are required for left-right asymmetry determination, but not neural crest formation, in mice. *Proc. Natl. Acad Sci U.S.A.* 103, 10300–10304.

Nieto, M., Sargent, M., Wilkinson, D. and Cooke, J. (1994). Control of cell behavior during vertebrate development by Slug, a zinc finger gene. *Science* 264, 835-839.

Nishimura, E. K., Granter, S. E. and Fisher, D. E. (2005). Mechanisms of hair graying: incomplete melanocyte stem cell maintenance in the niche. *Science* 307, 720-724.

Ono, H., Kawa, Y., Asano, M., Ito, M., Takano, A., Kubota, Y., Matsumoto, J. and Mizoguchi, M. (1998). Development of melanocyte progenitors in murine Steel mutant neural crest explants cultured with stem cell factor, endothelin-3, or TPA. *Pigment cell research* 11, 291–298.

Opdecamp, K., Nakayama, A., Nguyen, M., Hodgkinson, C., Pavan, W. and Arnheiter, H. (1997). Melanocyte development in vivo and in neural crest cell cultures: crucial dependence on the Mitf basic-helix-loop-helix-zipper transcription factor. *Development* 124, 2377–2386.

Pérez-Losada, J., Sánchez-Martín, M., Rodríguez-García, A., Sánchez, M., Orfao, A., Flores, T. and Sánchez-García, I. (2002). Zinc-finger transcription factor Slug contributes to the function of the stem cell factor c-kit signaling pathway. *Blood* 100, 1274–1286.

Pingault, V., Ente, D., Dastot-Le Moal, F., Goossens, M., Marlin, S. and Bondurand, N. (2010). Review and update of mutations causing Waardenburg syndrome. *Human mutation* 31, 391–406.

Potterf, S., Furumura, M., Dunn, K., Arnheiter, H. and Pavan, W. (2000). Transcription factor hierarchy in Waardenburg syndrome: regulation of MITF expression by SOX10 and PAX3. *Human genetics* 107, 1–6.

Potterf, S., Mollaaghababa, R., Hou, L., Southard-Smith, E., Hornyak, T., Arnheiter, H. and Pavan, W. (2001). Analysis of SOX10 function in neural crest-derived melanocyte development: SOX10-dependent transcriptional control of dopachrome tautomerase. *Developmental Biology* 237, 245–257.

Puffenberger, E., Hosoda, K., Washington, S., Nakao, K., deWit, D., Yanagisawa, M. and Chakravart, A. (1994). A missense mutation of the endothelin-B receptor gene in multigenic Hirschsprung's disease. *Cell* 79, 1257–1266.

Qin, Y., Kong, L., Poirier, C., Truong, C., Overbeek, P. and Bishop, C. (2004). Long-range activation of Sox9 in Odd Sex (Ods) mice. *Human molecular genetics* 13, 1213–1218.

Reedy, M., Faraco, C. and Erickson, C. (1998). The delayed entry of thoracic neural crest cells into the dorsolateral path is a consequence of the late emigration of melanogenic neural crest cells from the neural tube. *Developmental biology* 200, 234–246.

Reid, K., Turnley, A., Maxwell, G., Kurihara, Y., Kurihara, H., Bartlett, P. and Murphy, M. (1996). Multiple roles for endothelin in melanocyte development: regulation of progenitor number and stimulation of differentiation. *Development* 122, 3911–3919.

Roël, G., Gent, Y., Peterson-Maduro, J., Verbeek, F. and Destrée, O. (2008). Lef1 plays a role in patterning the mesoderm and ectoderm in Xenopus tropicalis. *The International journal of developmental biology* 53, 81–89.

Saint-Jeannet, J., He, X., Varmus, H. and Dawid, I. (1997). Regulation of dorsal fate in the neuraxis by Wnt-1 and Wnt-3a. *Proc. Natl. Acad Sci U.S.A.* 94, 13713–13718.

Saldana-Caboverde, A. and Kos, L. (2010). Roles of endothelin signaling in melanocyte development and melanoma. *Pigment cell & melanoma research* 23, 160–170.

Sánchez-Mejías, A., Watanabe, Y., Fernández, R. M., López-Alonso, M., Antiñolo, G., Bondurand, N. and Borrego, S. (2010). Involvement of SOX10 in the pathogenesis of Hirschsprung disease: report of a truncating mutation in an isolated patient. *Journal of Molecular Medicine* 88, 507-514.

Sargent, T. (2005). Transcriptional regulation at the neural plate border. *Advances in experimental medicine and biology* 589, 32–44.

Sasai, N., Mizuseki, K. and Sasai, Y. (2001). Requirement of FoxD3-class signaling for neural crest determination in Xenopus. *Development* 128, 2525–2536.

Sauka-Spengler, T. and Bronner-Fraser, M. (2008). A gene regulatory network orchestrates neural crest formation. *Nature reviews. Molecular cell biology* 9, 557–68.

Sefton, M., Sánchez, S. and Nieto, M. (1998). Conserved and divergent roles for members of the Snail family of transcription factors in the chick and mouse embryo. *Development* 125, 3111-3121.

Selleck, M. and Bronner-Fraser, M. (1995). Origins of the avian neural crest: the role of neural plate-epidermal interactions. *Development* 121, 525–538.

Selleck, M., García-Castro, M. and Artinger, K.B. and Bronner-Fraser, M. (1998). Effects of Shh and Noggin on neural crest formation demonstrate that BMP is required in the neural tube but not ectoderm. *Development* 125, 4919-4930.

Serbedzija, G., Fraser, S. and Bronner-Fraser, M. (1990). Pathways of trunk neural crest cell migration in the mouse embryo as revealed by vital dye labelling. *Development* 108, 605-612.

Shin, M., Levorse, J., Ingram, R. and Tilghman, S. (1999). The temporal requirement for endothelin receptor-B signalling during neural crest development. *Nature* 402, 496–501.

Silver, D., Hou, L. and Pavan, W. (2006). The genetic regulation of pigment cell development. Georgetown: Landes Biosciences, 155-169.

Sommer, L. (2011). Generation of melanocytes from neural crest cells. *Pigment cell & melanoma research* 24, 411–421.

Southard-Smith, E., Kos, L. and Pavan, W. (1998). Sox10 mutation disrupts neural crest development in Dom Hirschsprung mouse model. *Nature Genetics* 18, 60–64.

Spokony, R., Aoki, Y., Saint-Germain, N., Magner-Fink, E., and Saint-Jeannet, J.-P. (2002). The transcription factor Sox9 is required for cranial neural crest development in Xenopus. *Development* 129, 421-432.

Streit, A. (2002). Extensive Cell Movements Accompany Formation of the Otic Placode. *Developmental Biology* 249, 237-254.

Stuhlmiller, T. and García-Castro, M. (2012). Current perspectives of the signaling pathways directing neural crest induction. *Cellular and molecular life sciences : CMLS* 69, 3715–3737.

Tachibana, M., Kobayashi, Y. and Matsushima, Y. (2003). Mouse models for four types of Waardenburg syndrome. *Pigment cell research* 16, 448–454.

Taneyhill, L. A., Coles, E. G. and Bronner-Fraser, M. (2007). Snail2 directly represses cadherin 6B during epithelial-to-mesenchymal transitions of the neural crest. *Development* 134, 1481-1490.

Tassabehji, M., Read, A., Newton, V., Harris, R., Balling, R., Gruss, P. and Strachan, T. (1992). Waardenburg's syndrome patients have mutations in the human homologue of the Pax-3 paired box gene. *Nature* 355, 635–636.

Taylor, K. and Labonne, C. (2005). SoxE factors function equivalently during neural crest and inner ear development and their activity is regulated by SUMOylation. *Developmental cell* 9, 593–603.

Teng, L., Mundell, N., Frist, A., Wang, Q. and Labosky, P. (2008). Requirement for Foxd3 in the maintenance of neural crest progenitors. *Development* 135, 1615–1624.

Theveneau, E. and Mayor, R. (2012). Neural crest delamination and migration: from epithelium-to-mesenchyme transition to collective cell migration. *Developmental biology* 366, 34–54.

Thomas, A. and Erickson, C. (2008). The making of a melanocyte: the specification of melanoblasts from the neural crest. *Pigment cell & melanoma research* 21, 598–610.

Tribulo, C., Aybar, M., Nguyen, V., Mullins, M. and Mayor, R. (2003). Regulation of Msx genes by a Bmp gradient is essential for neural crest specification. *Development* 130, 6441–6452.

Verastegui, C., Bille, K., Ortonne, J. and Ballotti, R. (2000). Regulation of the microphthalmia-associated transcription factor gene by the Waardenburg syndrome type 4 gene, SOX10. *The Journal of biological chemistry* 275, 30757–30760.

Watanabe, A., Takeda, K., Ploplis, B. and Tachibana, M. (1998). Epistatic relationship between Waardenburg syndrome genes MITF and PAX3. *Nature genetics* 18, 283–286.

Wehrle-Haller, B. and Weston, J. (1995). Soluble and cell-bound forms of steel factor activity play distinct roles in melanocyte precursor dispersal and survival on the lateral neural crest migration pathway. *Development* 121, 731–742.

Wu, J., Saint-Jeannet, J.-P. and Klein, P. (2003). Wnt-frizzled signaling in neural crest formation. *Trends in neurosciences* 26, 40–45.

Yan, Y.-L., Willoughby, J., Liu, D., Crump, J., Wilson, C., Miller, C., Singer, A., Kimmel, C., Westerfield, M. and Postlethwait, J. (2006). A pair of Sox: distinct and overlapping functions of zebrafish sox9 co-orthologs in craniofacial and pectoral fin development. *Development* 132, 1069–1083.

Yoshida, H., Kunisada, T., Kusakabe, M., Nishikawa, S. and Nishikawa, S.-I. (1996). Distinct stages of melanocyte differentiation revealed by anlaysis of nonuniform pigmentation patterns. *Development* 122, 1207-1214.

Zhao, S. and Overbeek, P. (1999). Tyrosinase-related protein 2 promoter targets transgene expression to ocular and neural crest-derived tissues. *Developmental Biology* 216, 154–163.

CHAPTER II

TEMPORAL REQUIREMENT OF THE TRANSCRIPTION FACTOR *Ets1* IN MURINE MELANOCYTE DEVELOPMENT

II. TEMPORAL REQUIREMENT OF THE TRANSCRIPTION FACTOR *Ets1* IN MURINE MELANOCYTE DEVELOPMENT

2.1 Abstract

Melanocytes are derived from neural crest (NC) cells, which arise from the dorsal aspect of the neural tube. Several genes required for the specification of melanocytes were identified via the study of mouse pigmentation mutants. Recently, the deletion of the transcription factor *Ets1* was shown to cause hypopigmentation in mice; however, the role of *Ets1* in melanocyte development is unknown. The *Ets1* gene codes for a helix-turn-helix transcription factor that is expressed in various developing organs and tissues, including the NC, in the mouse embryo. It is required for the expression of the melanocyte-specific transcription factor *Sox10* in the chick cranial NC. The goal of the present study is to determine the temporal requirement and mechanism of action of *Ets1* in melanocyte development. Embryos from crosses between *Ets1* heterozygous ($Ets1^{+/-}$) and *Dct-LacZ* transgenic mice, in which *LacZ* expression is driven to melanocyte precursors (melanoblasts) under the control of the Dopachrome tautomerase (*Dct*) promoter, were harvested between embryonic days (E) 10.75-15.5 and LacZ staining was performed. $Ets1^{-/-}$ embryos have fewer melanoblasts compared to $Ets1^{+/-}$ and wild type littermates. Cell survival assays showed increased melanoblast cell death in E10.75 $Ets1^{-/-}$ embryos. Similarly, double-label immunofluorescence staining against Sox10 and cleaved Caspase-3 showed increased NC cell death in E10.25 $Ets1^{-/-}$ embryos. The increased numbers of dying NC cells and melanoblasts in *Ets1* null mutants suggest that *Ets1* acts early during melanocyte development and regulates melanoblasts and NC cell survival.

2.2 Introduction

The transcription factor Ets1 is a member of a large family of helix-turn-helix transcription factors that are characterized by the presence of the E26 transforming specific sequence (Ets) domain, which was first identified in the avian erythroblastosis virus, E26. The Ets domain recognizes the core nucleotide sequence GGAA/T (Dittmer, 2003). Human homologs of the viral Ets were later discovered on chromosomes 11 and 21, and designated *Ets1* and *Ets2* respectively (Watson et al., 1985). Homologs of *Ets1* from a wide variety of species, which include birds, amphibians, fish and mammals, share high sequence similarity. In fact, the mouse and human Ets1 protein sequences are highly homologous, sharing 97% amino acid identity (Garrett-Sinha, 2013).

The transcription factor *Ets1* is widely expressed during embryonic development. In the chick embryo, *Ets1* is expressed in the mesoderm, the blood-forming system endothelial cells (Vandenbunder et al., 1989), in mesenchymal cells, lymphocytes, erithrocytes (Queva et al., 1993), and NC cells (Fafeur et al., 1997; Theveneau et al., 2007). In the mouse embryo, *Ets1* is expressed early in the developing hindbrain, the neural tube, the second and third brachial arches (Maroulakou et al., 1994), and the NC (Kola et al., 1993; Maroulakou et al., 1994; Dittmer et al., 2003; Gao et al., 2010; Ye et al., 2010). It is later expressed in the blood-forming system, lymphoid organs, lung, gut, and skin (Maroulakou et al., 1994) and becomes expressed in all organs by embryonic day (E) 15 (Kola et al., 1993). In later stages of fetal development and after birth, *Ets1* expression becomes primarily restricted to lymphoid organs and the brain (Kola et al., 1993). Expression of *Ets1* has also been correlated with pathological invasive processes. It has been found to be upregulated in various tumor types, including melanoma (Keehn

et al., 2003; Rothhammer et al., 2004; Rothhammer et al., 2005; reviewed in Garrett-Sinha, 2013), and its expression in certain tumors has been correlated with the expression of matrix metalloproteases (MMPs), particularly MMP1, MMP2 and MMP9 (reviewed in Dittmer, 2003; Rothhammer et al., 2004; Okuducu et al., 2006). The Ets1-induced upregulation of MMPs has also been reported in several in vitro and in vivo *Ets1* overexpression studies (Oda et al., 1999; Park et al., 2008; Nagarajan et al., 2009).

Several studies implicate *Ets1* in the proper development of NC cell derivatives. In the mouse, *Ets1* is expressed by cardiac NC cells and *Ets1* deletion was found to produce cardiac malformations (Gao et al., 2010; Ye et al., 2010). Some of these cardiac malformations were found to arise as a result of the lack of NC-derived cells in the proximal aspects of the outflow tract endocardial cushions and the presence of an abnormal nodule of NC-derived cartilage within the heart. The cardiac defects seen in *Ets1* null mice have been attributed to a role of *Ets1* in proper NC cell migration and differentiation (Gao et al., 2010). During chick embryonic development, *Ets1* expression is correlated with epithelial-to-mesenchymal transition (EMT). It is expressed in migrating NC cells and in dispersing somites but is not detected in tissues where EMT does not occur (Fafeur et al., 1997). Additionally, *Ets1* is required for the initiation of cranial NC cell delamination by promoting cell mobilization, and can induce cranial-like delamination when misexpressed in trunk NC cells. Although *Ets1* is not required for cranial NC cell EMT per se, it cooperates with the transcription factor Snail homolog 2 (*Snail2*) to promote EMT in NC cells (Theveneau et al., 2007).

In addition to being involved in NC cell migration, Ets1 is also required for the survival of various cell lineages. Murine thymocytes and T cells derived from *Ets1* null

mutant mice display higher apoptotic rates compared to those derived from wild type mice (Muthusamy et al., 1995). In cooperation with Ets2, Ets1 is also required for the survival of endothelial cells in the developing mouse embryo. Although, *Ets1*$^{-/-}$ mice and mice carrying a mutation in an important threonine target of ERK (extracellular signal regulated kinase) phosphorylation in *Ets2* (*Ets2*$^{A72/A72}$) are viable, *Ets1*$^{-/-}$;*Ets2*$^{A72/A72}$ double homozygous mutants are embryonic lethal. The embryonic lethality observed in these double mutant mice is caused by impaired angiogenesis as a result of decreased endothelial cell survival (Wei et al., 2009).

Recently, the deletion of the transcription factor *Ets1* in particular murine genetic backgrounds (i.e., C57BL/6J), was shown to produce ventral hypopigmentation (Gao et al., 2010) (Figure 2.1), hinting to the involvement of this transcription factor in melanocyte development from the NC. The exact mechanism by which *Ets1* deficiency during embryonic development results in hypopigmentation is currently unknown. In the chick embryo, Ets1 is required for the activation of the transcription factor sex determining region Y (SRY)-box 10 (*Sox10*) (Betancur et al., 2010), a gene required for the development of various NC cell derivatives, including melanocytes (Herbarth et al., 1998; Southard-Smith et al., 1998; Kapur, 1999; Potterf et al., 2001). The importance of *Sox10* for melanocyte survival is evidenced by the hypopigmentation phenotype that results when it is mutated or deleted. The targeted deletion of *Sox10* in the mouse results in almost a complete absence of trunk melanoblasts (Hou et al., 2006). Although *Ets1* has not been linked to *Sox10* expression in the mouse embryo, its requirement for proper *Sox10* expression in the chick embryo and the hypopigmentation phenotype of *Ets1* null mutants, suggests that *Ets1* could also play an important role in the regulation of this and other melanocyte-specific

genes in the mouse. Furthermore, the involvement of Ets1 in normal and pathological invasive processes (Fafeur et al., 1997; Theveneau et al., 2007; Garrett-Sinha, 2013), and its requirement for the survival of certain cell lineages (Muthusamy et al., 1995; Wei et al., 2009) suggest that this transcription factor may be an important regulator of NC cell and/or melanoblast survival, proliferation, migration, and/or differentiation.

2.3 Materials and methods

2.3.1 Animals

Mice heterozygous for *Ets1* were obtained from Dr. Eric Svensson (Universtiy of Chicago, Chicago, IL) and generated as previously described to harbor a targeted deletion of exons 3 and 4 of the *Ets1* gene (Barton et., al. 1998). Mice heterozygous for *Ets1* were re-derived by outcrossing to C57BL/6J mice for eight generations (Gao et., al. 2010). They have been maintained on C57BL/6J genetic background by intercrossing and by outcrossing to C57BL/6J mice (Jackson Laboratories). Mice carrying the *Dct-LacZ* transgene were obtained from Dr. Paul Overbeek (Baylor College of Medicine, Houston, TX). The *Dct-LacZ* transgenic mice were generated on an FVB/N genetic background as previously described (Zhao and Overbeek, 1999) by embryonic microinjection of a transgene composed of the mouse Dopachrome tautomerase (*Dct*) promoter upstream of the *LacZ* gene. $Sox10^{tm1WegLacZ}$ mice (hereafter referred to as $Sox10^{LacZ/+}$) were obtained from Dr. Michael Wegner (Institut für Biochemie, Universität Erlangen-Nürnberg, Germany). $Sox10^{LacZ/+}$ mice were generated as previously described (Britsch et al., 2001) via insertion of the *LacZ* gene into the *Sox10* coding sequence. $Sox10^{LacZ/+}$ mice have been maintained on their original C3H mixed background by backcrossing.

Timed matings were set for the generation of embryos. Animals were mated overnight, and females were examined for vaginal plugs after approximately 16 hours. Noon of the day a vaginal plug was observed, was considered embryonic day (E) 0.5. Pregnant females were euthanized by exposure to Isoflurane (Vedco, Inc.) followed by cervical dislocation, and an abdominal incision was made to expose the uterus. As soon as embryos were recovered from the euthanized mother, they were dissected out of the uterine sacs and placed in Phosphate Buffered Saline (PBS) (pH7.2 or 7.4, depending on the procedure for which the embryos were used). For all embryos, yolk sacs were isolated for genotyping. Embryos that were used for Lysotracker Red staining were stained immediately after dissection and fixed in 2% paraformaldehyde prior to β-galactosidase staining. Embryos that were used for immunofluorescence staining of tissue sections were fixed with 4% paraformaldehyde immediately after dissection. Embryos that were used for in situ hybridization were dehydrated via incubation in methanol solutions of increasing concentrations (25%, 50%, 75% methanol in PBT (PBS containing 0.1% Tween 20 (Fisher Scientific)), and 100% methanol, 5 minutes each at room temperature) and stored at -20˚C. All animal work was performed according to institutional guidelines established by the National Institutes of Health (NIH) (Guide for the Care and Use of Laboratory Animals, 2011; Institutional Animal Care and Use Committee (IACUC) Protocol No. 13-064).

2.3.2 Genotyping

Genomic DNA was isolated from tail biopsies for adult mice or yolk sacs for embryos, and used for PCR genotyping. Genotyping for *Ets1*was performed using the primers 5’-GTCTTCTTCTCTAGTTTCTGAGTGCTC, 5’-

GTCCTGCTTACAACACTCTGAATCCTG and 5'-GCCTGCTCTTTACTGAAGGCTCTTT (Gao et al., 2010), under standard PCR conditions (35 cycles of 94˚C for 60 s, 60˚C for 60 s, and 72˚C for 60 s). Products were visualized in a 2% agarose gel containing 0.5µg/ml Ethidium Bromide (Fisher Scientific). The wild type *Ets1* allele produced a 438bp product while the mutant allele produced a 350bp product (Gao et al., 2010). Heterozygous animals were identified by the presence of both PCR products. For *Sox10*, genotyping of adult mice and embryos was performed using the primers 5'-CAGGTGGGCGTTGGGCTC, 5'-CAGAGCTTGCCTAGTGTCT, and 5'-TAAAAATGCGCTCAGGTCAA, under standard PCR conditions (35 cycles of 94˚C for 30 s, 55˚C for 30 s, and 72˚C for 30 s). Products were visualized in a 2% agarose gel containing 0.5µg/ml Ethidium Bromide (Fisher Scientific). The wild type *Sox10* allele produced a 500bp product while the mutant allele produced a 600bp product (Britsch et al., 2001). Heterozygous animals were identified by the presence of both PCR products.

The *Dct-LacZ* mice were genotype via β-galactosidase staining. Briefly, ear tip biopsies were fixed with 2% paraformaldehyde for 50 minutes at room temperature. Samples were briefly washed in PBS (pH 7.2) and incubated overnight at 30.9˚C in X-gal solution consisting of 2mM $MgCl_2$, 0.01% Sodium Deoxycholate, 5mM Potassium Ferricyanide, 5mM Postassium Ferrocyanide (Fisher Scientific), 0.02% Nonidet P40 (Roche Diagnostics), and 1mg/ml X-gal (Life Technologies) (Nagy, 2003). The staining was visualized under a dissecting scope (Leica Model MZ6). Mice carrying the *Dct-LacZ* transgene were identified by positive X-gal staining.

2.3.3 β-galactosidase and Lysotracker Red staining of whole mount embryos

Embryos from intercrosses between *Ets1*$^{+/-}$*::Dct-LacZ*$^{+}$ mice were harvested between E11.5 and E15.5, while those from intercrosses between *Ets1*$^{+/-}$*::Sox10*$^{LacZ/+}$ mice were harvested at E9.5. β-galactosidase (LacZ) staining was performed using standard protocols (Nagy, 2003). Whole embryos were dissected in cold 0.05M PBS (pH7.2) and fixed with 2% paraformaldehyde for 50 minutes at room temperature. Embryos were briefly washed in PBS (pH 7.2) and incubated 3 to12 hours (the incubation time was directly proportional to the embryonic age), protected from light, at 30.9˚C in X-gal solution consisting of 2mM $MgCl_2$, 0.01% Sodium Deoxycholate, 5mM Potassium Ferricyanide, 5mM Postassium Ferrocyanide (Fisher Scientific), 0.02% Nonidet P40 (Roche Diagnostics), and 1mg/ml X-gal (Life Technologies). Embryos were washed twice in PBS to stop the reaction. The staining was visualized under a dissecting scope (Leica, Model MZ6). Whole embryos were photographed using a Leica DC500 camera. For each stage, at least 3 embryos of each genotype (*Ets1*$^{+/+}$, *Ets1*$^{+/-}$, and *Ets1*$^{-/-}$) were stained and photographed.

Embryos from crosses between *Ets1*$^{+/-}$::*Dct-LacZ*$^{+}$ mice were harvested at E10.75. Lysotracker Red (Zucker et al., 1998) and LacZ staining (Nagy, 2003) were performed after dissection to identify melanoblasts (LacZ positive cells), dying cells (Lysotracker Red positive cells), and dying melanoblasts (double-labeled cells). To perform Lysotracker Red staining, embryos were incubated in 5μM Lysotracker Red DND-99 (Life Technologies) in PBS, protected from light, at 37˚C for 30 minutes. Still protected from light, embryos were washed twice with PBS (pH7.2) and β-galactosidase staining was performed, visualized, and photographed as described above. Still protected

from light, embryos were then post-fixed in 4% paraformaldehyde, 20 minutes at room temperature, incubated in 10% sucrose 4-6 hours at 4˚C with light rocking, and in 20% sucrose, overnight at 4˚C with light rocking. Embryos were embedded in Tissue-Tek Tissue Freezing Medium (Sakura), frozen at -80˚C, and sectioned at 10μm. Sections were then stained against phospho-Histone H3 (Millipore) via immunofluorescence (as described in 2.3.4).

2.3.4 Immunofluorescence

Cryosections of 10μm thickness from E10.75 embryos previously stained with LacZ and Lysotracker Red were dried for 2 hours at 37˚C. Sections were washed with PBS and blocked with 1% Bovine Serum Albumin (BSA) (Amresco), 0.1% Triton X-100 (Sigma) in PBS 45 minutes at room temperature. Sections were incubated in rabbit anti-phospho-Histone H3 antibody (Ser10) (06-570, Millipore), (1:100 in 1% BSA, 0.1% Triton X-100 in PBS), 1 hour at room temperature, to label proliferating cells. After washing, sections were incubated in a secondary antibody against rabbit, tagged with Alexa Fluor 488 (A11008, Invitrogen) (1:200 in 1% BSA, 0.1% Triton X-100 in PBS), 1 hour at room temperature, to label proliferating cells with green fluorescence. Cell nuclei were counterstained using 1μg/ml Hoechst Dye (BioRad). Using a compound fluorescence microscope (Leica, Model DMRB), melanoblasts (LacZ positive cells), dying melanoblasts (LacZ and Lysotracker Red positive cells), and proliferating melanoblasts (LacZ and p-Histone H3 positive cells) were counted over 80 sections spanning the trunk region for E10.75 $Ets1^{-/-}$*::Dct-LacZ*$^{+}$ (n=3) and $Ets1^{+/-}$*::Dct-LacZ*$^{+}$ (n=3) embryos.

In order to label dying NC cells parallel cryosections from E10.25 embryos were stained with antibodies against Sox10, to label NC cells, and Cleaved caspase-3, to label

dying cells. Specifically, embryos were harvested in PBS and fixed in 4% paraformaldehyde, 3 hours at 4˚C with light rocking. After washing with PBS, embryos were incubated in 10% sucrose 4-6 hours at 4˚C with light rocking, and in 20% sucrose, overnight at 4˚C with light rocking. Embryos were embedded in Tissue-Tek Tissue Freezing Medium (Sakura) and frozen at -80˚C. Cryosections of 10μm thickness were prepared and dried, 2 hours at 37˚C as previously described. Sections were incubated with goat polyclonal anti-Sox10 (N20) (sc-17342, Santa Cruz Biotechnology) (1:100) antibody and rabbit anti Cleaved Caspase-3 (9664S, Cell Signaling) (1:100) antibody. After washing extensively with PBS, sections were incubated in donkey anti-goat Alexa Fluor 594 (A11058, Invitrogen) (1:200). Sections were once again washed extensively with PBS and subsequently incubated in goat anti-rabbit Alexa Fluor 488 (A11008, Invitrogen), followed by extensive PBS washes. All antibodies were diluted in 1% BSA, 0.1% Triton X-100 in PBS. All antibody incubations were carried out for 1 hour at room temperature. Cell nuclei were counterstained using 1μg/ml Hoechst Dye (BioRad). Neural crest cells (Sox10 positive cells) and dying neural crest cells (double-labeled cells) were counted over 35 sections spanning the anterior half of the trunk region for E10.25 *Ets1*$^{-/-}$ (n=3) and *Ets1*$^{+/-}$ (n=3) embryos.

2.3.5 Probe preparation for in situ hybridization

In situ hybridization probes were prepared from plasmids containing the full length *Pmel17* cDNA (Baxter and Pavan, 2003) or a 1.5kb cDNA fragment of the *Sox10* cDNA (Southard-Smith et al., 1998). The plasmids used for cloning the *Pmel17* and *Sox10* constructs contained the promoters for T3 and T7 RNA Polymerase, respectively. In these plasmids, the cDNAs are oriented such that an antisense probe can be generated from in vitro transcription. In order to have a sufficient amount of plasmid for probe

synthesis, plasmids were transformed into *Escherichia coli* Dh5α competent cells (Life Technologies) and glycerol stocks were prepared (Appendix I). Plasmids were purified from overnight cultures using the Promega Wizard Plus SV Minipreps DNA Purification System (Promega). Plasmids were linearized via restriction enzyme digestion, using KpnI (Promega) for *Pmel17* and PvuII (New England Biolabs) for *Sox10*. Digestions were carried out following manufacturer's instructions, 2 hours at 37˚C. Digestion products were visualized in a 1% agarose gel containing 0.5µg/ml Ethidium Bromide (Fisher Scientific). Linearized templates were purified via phenol-chloroform extraction, followed by ethanol precipitation. Template DNA was resuspended in Diethyl Pyrocarbonate (DEPC) (Sigma-Aldrich) treated water at an approximate concentration of 1µg/ml.

Riboprobe synthesis was carried out by incubating 5µl of linearized template with 4µl of 5x transcription buffer (Promega), 2µl of nucleotide tri-phosphate (NTP) labeling mix (Roche Diagnostics), 2µl of T3 or T7 RNA Polymerase (Promega), 1µl of RNasin RNase inhibitor (Promega) and 6µl of DEPC-treated water, 2 hours at 37˚C. Transcription efficiency was assayed by visualizing the resulting probes in a 1% agarose gel containing 0.5µg/ml Ethidium Bromide (Fisher Scientific). Probes were purified via Ethanol precipitation with 0.02M EDTA and 0.5M LiCl, and resuspended in 20µl of DEPC-treated water.

2.3.6 In situ hybridization

In situ hybridization using *Pmel17* and *Sox10* probes were performed on E10.5 and E9.5 embryos, respectively, according to standard protocols (Wilkinson and Nieto, 1993; Wilkinson, 1998). Embryos that had been previously dehydrated with methanol,

were re-hydrated by incubation in methanol solutions of decreasing concentration (75%, 50% and 25% methanol in PBT (PBS containing 0.1% Tween 20 (Fisher Scientific)), 5 minutes each at room temperature), and washed with PBT. Embryos were then bleached with 6% Hydrogen Peroxide (Fisher) in PBT, 1 hour at room temperature with light rocking. Permeabilization of the tissue was achieved by incubation in 10µg/ml Proteinase K (Fisher Scientific) in PBT (8 minutes for E9.5 and 12 minutes for E10.5). Permeabilization was stopped by incubation in 2mg/ml Glycine (Fisher Scientific) in PBT, 10 minutes at room temperature. Embryos were post-fixed in 4% paraformaldehyde, 20 minutes at room temperature and pre-hybridized by incubation in Hybridization Solution (50% Formamide (Fisher Scientific), 5XSSC, pH4.5 (0.75M NaCl, 0.075M Sodium Citrate), 50µg/ml yeast tRNA (Sigma Aldrich), 1% SDS (Fisher Scientific), 50µg/ml Heparin (Sigma-Aldrich)), 1 hour at 70˚C. Embryos were then incubated in fresh, pre-warmed (70˚C) Hybridization Solution containing hybridization probe (2µl per ml of Hybridization Solution), overnight at 70˚C.

The second day of in situ hybridization consisted of washes and antibody incubation. Embryos were first washed with Solution 1 (50% Formamide, 5XSSC, 1% SDS), 3 times at 70˚C, for 30 minutes each time. Embryos were then washed with Solution 2 (50% Formamide, 2XSSC) 3 times at 65˚C, for 30 minutes each time. Embryos were washed in TBST (Tris Buffered Saline (TBS): 137mM NaCl, 2.7mM KCl, 25mM Tris-Base (Fisher Scientific), pH8.0 + 0.1% Tween 20 (Fisher Scientific)) 3 times, 5 minutes each time at room temperature. Blocking was achieved by incubating the embryos in 10% goat serum (Gibco) in TBST, 2 hours at room temperature with rocking. During this time, the anti-Digoxigenin antibody (Roche Diagnostics) was pre-absorbed as

follows. For each embryo, a pinch of embryo powder (Appendix II) was added to 0.5ml of TBST in a 1.5ml sterile microcentrifuge tube. The embryo powder in TBST was heated at 70˚C, for 30 minutes, briefly vortexed and incubated in ice for 10 minutes. Subsequently, 5µl of heat inactivated 100% goat serum and 1µl of anti-Digoxigenin antibody were added to each tube. Tubes were rocked for 1 hour at 4˚C and centrifuged for 10 minutes at 12,000 RPM, at 4˚C. The supernatant was then collected and placed in a sterile 2ml microcentrifuge tube containing 1.5ml of 1% goat serum in TBST. Embryos were incubated in pre-absorbed anti-Digoxigenin antibody solution, overnight at 4˚C with light rocking.

On the third day of in situ hybridization, embryos were washed with TBST, 3 times, 5 minutes each time at room temperature, followed by 5 washes of at least 1 hour each, at room temperature. Embryos were incubated overnight in 2mM Levamisole (Sigma-Aldrich) in TBST. The purpose of the prolonged washes was the removal of excess antibody to prevent background staining. On the fourth and final day, embryos were washed with NTMT (100mM NaCl, 100mM Tris pH9.5, 50mM $MgCl_2$, 0.1% Tween 20 (Fisher Scientific) 2mM Levamisole (Sigma-Aldrich)), 3 times, 10 minutes each time at room temperature. Each embryo was then protected from light and incubated in a color substrate solution consisting of 4.5µl of 4-Nitro blue tetrazolium chloride (NBT) (Roche Diagnostics) and 3.5µl of 5-Bromo-4-chloro-3-indolyl-phosphate (BCIP) (Roche Diagnostics) in 1ml of NTMT for a period of 45 minutes to 2 hours, depending on the amount of time it took for the staining to develop. Embryos were monitored periodically (approximately every 20 minutes) under a dissecting scope, for color development. The staining was stopped by washing the embryos 2 times with PBT, 5

minutes each time at room temperature. Embryos were photographed in 50% Glycerol in PBT under a dissecting scope (Leica, Model MZ6) using a Leica DC500 camera. Pictures were taken at a total magnification of 40X. For each stage, at least 3 embryos of each genotype (*Ets1*$^{+/-}$ and *Ets1*$^{-/-}$) were stained and photographed.

2.3.7 Statistical analysis

The Student's t-test was used to compare the mean number of melanoblasts, as well as the mean numbers of dying and proliferating melanoblasts in E10.75 *Ets1*$^{-/-}$ and *Ets1*$^{+/-}$ embryos. The same statistical test was used to compare the mean number of NC cells and the mean number of dying NC cells in E10.25 *Ets1*$^{-/-}$ and *Ets1*$^{+/-}$ embryos. Data were considered statistically significant at $p<0.05$. All analyses were carried out using PASW Statistics 18 (IBM). Graphical representations of the data were generated using GraphPad Prism 6 (GraphPad Software, Inc).

2.4 Results

2.4.1 Ets1 null embryos show reduced numbers of melanoblasts

In order to establish the earliest time point at which *Ets1* deficiency results in impaired melanocyte development, embryos from intercrosses between *Ets1*$^{+/-}$*::Dct-LacZ*$^{+}$ mice were harvested between embryonic days (E) 10.75 and E15.5 and subjected to LacZ staining. A gross decrease in the number of trunk melanoblasts is visibly apparent in E11.5-E15.5 *Ets1*$^{-/-}$ embryos compared to *Ets1*$^{+/-}$ littermates (Figure 2.2). Melanoblasts were counted in 80 sections spanning the trunk region in E10.75 embryos (Figure 2.3). These counts revealed a significant decrease in the number of trunk melanoblasts in *Ets1*$^{-/-}$ embryos compared to *Ets1*$^{+/-}$ littermates ($p=0.018$, Figure 2.3 E).

2.4.2 Ets1 deletion results in decreased melanoblast survival

To establish the mechanism of action of *Ets1* in murine melanocyte development, the total numbers of trunk melanoblasts, as well as the numbers of dying and proliferating melanoblasts, were quantified at E10.75. The earliest time point at which *Dct* is expressed in melanoblasts is E10.5; however, at this stage most melanoblasts are restricted to the head and cervical region and the number of trunk melanoblasts is very small (Baxter et al., 2004). For this reason, trunk melanoblasts, labeled via LacZ staining, were quantified at E10.75. Embryos from crosses between $Ets1^{+/-}$*::Dct-LacZ*$^{+}$ mice were harvested at E10.75 and subjected to Lysotracker Red staining, LacZ staining, and phospho-Histone H3 immunofluorescence staining. LacZ positive cells, as well as double-labeled cells (LacZ and Lysotracker Red positive, and LacZ and phospho-Histone H3 positive) were counted in 80 sections spanning the trunk region of each embryo. As previously stated, a significant decrease in the number of trunk melanoblasts was observed in $Ets1^{-/-}$ embryos compared to $Ets1^{+/-}$ littermates ($p=0.018$, Figure 2.3 E). At this stage, the percent of proliferating melanoblasts, which are identified by LacZ and phospho-Histone H3 double-labeling, did not differ significantly between $Ets1^{+/-}$ and $Ets1^{-/-}$ littermates ($p=0.852$, Figure 2.3 G). These results indicate that *Ets1* deficiency does not result in impaired melanoblast proliferation at E10.75. A significant increase in the percent of dying melanoblasts, labeled by Lysotracker Red and LacZ staining, was observed in $Ets1^{-/-}$ embryos compared to $Ets1^{+/-}$ littermates ($p=0.023$, Figure 2.3 F). The increase in melanoblast cell death observed in E10.75 $Ets1^{-/-}$ embryos indicates that *Ets1* is required for melanoblast survival at this stage.

Melanoblasts were also labeled via *Pmel17* in situ hybridization in E10.5 embryos (Figure 2.4). The *Pmel17* gene encodes a melanocyte-specific transmembrane protein, which has been shown to label melanoblast and cells of the retinal pigmented epithelium (RPE) beginning at E9.5. At E9.5, *Pmel17* expression is restricted to the otic vesicle and presumptive RPE. At E10.5, *Pmel17* has been shown to be expressed in the RPE as well as in melanoblasts mostly in the head and neck, although a few melanoblasts are also labeled along the trunk (Baxter and Pavan, 2003). Although no gross differences in the number of melanoblasts between $Ets1^{-/-}$ and $Ets1^{+/-}$ littermates were observed at E10.5, only a few melanoblasts located in the cervical region were labeled by *Pmel17* in situ hybridization at this stage (Figure 2.4). The absence of *Pmel17*-positive cells along the trunk region did not allow for the quantification of trunk melanoblasts at this stage.

2.4.3 Ets1 deletion results in decreased neural crest cell survival

Given the increase in cell death observed in $Ets1^{-/-}$ mutant embryos at E10.75, a potential role for *Ets1* prior to melanocyte cell specification was investigated. Embryos from intercrosses between $Ets1^{+/-}$ mice were harvested at E10.25. Embryos were fixed, embedded in tissue freezing media and sectioned at 10µm. Neural crest cells were labeled via Sox10 antibody staining, while dying cells were labeled via cleaved Caspase-3 antibody staining (Figure 2.5). The transcription factor *Sox10* was chosen as a NC cell marker because it is expressed in various migrating NC cell derivatives, including the dorsal root, cranial, enteric and sympathetic ganglia (Southard-Smith et al., 1998). *Sox10* is initially expressed in NC cells as they begin to delaminate from the neural tube and persists in cells that will give rise to peripheral nervous system components (Kuhlbrodt et al., 1997) and melanocytes (Southard-Smith et al., 1998). Neural crest cells as well as

dying NC cells were counted in 35 sections spanning the anterior portion of the trunk region for 3 embryos of each genotype (*Ets1*$^{-/-}$ and *Ets1*$^{+/-}$). The total number of NC cells (Sox10 positive cells) did not differ significantly between *Ets1*$^{-/-}$ and *Ets1*$^{+/-}$ embryos (p=0.848, Figure 2.5 C). Nonetheless, the percent of dying NC cells (Sox10 and cleaved Caspase-3 positive cells) was significantly higher in *Ets1*$^{-/-}$ embryos compared to *Ets1*$^{+/-}$ littermates (p=0.033, Figure 2.5 D).

Embryos at E9.5 were also assessed for *Sox10* expression via in situ hybridization (Figure 2.6) and LacZ staining (Figure 2.7) of whole embryos from crosses between *Ets1*$^{+/-}$*::Sox10*$^{LacZ/+}$ mice. At this stage, the pattern and levels of *Sox10* expression as well as the numbers of *Sox10* positive cells do not appear to differ much between *Ets1* null embryos and *Ets1* wild type or heterozygous littermates. Nevertheless, *Sox10* in situ hybridization revealed ectopic *Sox10* expression in the frontal aspect of the head in *Ets1* null embryos.

2.5 Discussion

While coat color variations in mice are the result of changes in melanin production and distribution, white spotting is caused by impaired melanoblast development, or from defects in melanocyte stem cell survival. Specifically, defects in melanoblast survival, proliferation, migration, hair follicle and integument invasion, and stem cell renewal in the hair follicles will result in various spotting phenotypes, which include head and belly spots, white belts that extend to the caudal trunk region, piebald spotting and peppering (Baxter et al., 2004). The hypopigmentation phenotype observed in *Ets1* mutant mice pointed to a potential role for *Ets1* in melanocyte development, particularly in survival, proliferation or migration.

In vivo analysis of *Ets1* mutant embryos via labeling of melanoblasts using *Dct-LacZ* transgenic mice, revealed an apparent gross decrease in melanoblast numbers in embryos ranging from E15.5 through E10.75 (Figure 2.2). Quantification of trunk melanoblasts at E10.75 revealed a large and significant reduction in melanoblast numbers, as a result of increased apoptosis, in *Ets1* null mutants compared to heterozygous littermates (Figure 2.3). The increased melanoblast cell death observed in *Ets1* null mutants indicates that *Ets1* acts early during melanocyte development and appears to be required for the survival of melanocyte precursors. The presence of viable melanocytes in *Ets1* null mutant mice implies that *Ets1* may not be required for melanocyte differentiation. We also failed to detect significant differences in the numbers of proliferating melanoblasts between *Ets1* null and heterozygous embryos at this stage. The early defect observed in the melanoblast population in *Ets1* null mutant mice suggests that *Ets1* may be involved in the regulation of one or more early melanocyte-specific genes. Although the presence of viable melanocytes in *Ets1* null mutants suggests that *Ets1* is not required for proper melanocyte differentiation, it is possible that the large decrease in melanoblast cell numbers observed in these mice could in part arise as a consequence of altered NC cell fate decisions. The presence of ectopic NC cell-derived cartilage nodules in the hearts of *Ets1* null mutant mice suggests that *Ets1* may act as a negative regulator of cartilage fate in NC cells (Gao et al., 2010). Consequently, in spite of the melanoblast survival defect observed in *Ets1* null mutants, we cannot discard the possibility that, in addition to being required for melanoblast survival, *Ets1* may also be involved in NC cell lineage specification.

Given the increase in melanoblast cell death observed in *Ets1* null mutant mice at E10.75, it was plausible that *Ets1* may regulate the survival of NC cells prior to their specification into the melanocyte lineage. Labeling of NC cells via Sox10 antibody staining revealed similar numbers of trunk NC cells in $Ets1^{-/-}$ and $Ets1^{+/-}$ littermates. In spite of this, double-labeling with cleaved Caspase-3 antibody revealed a significant increase in the percent of dying NC cells from 4.2% in *Ets1* heterozygotes to 6.5% in *Ets1* null littermates (Figure 2.5). These results point to a role for *Ets1* as a survival factor for NC cells prior to their differentiation into the melanocytic lineage. The lack of a significant difference in the numbers of Sox10-positive NC cells at this stage, implies that *Ets1* appears to act precisely at this time point so that the effects of *Ets1* deficiency would become apparent soon after. The sharp and significant decrease observed in melanoblast numbers at E10.75 supports this possibility. Furthermore, *Sox10* expression did not appear to be affected in *Ets1* null mutant mice at E9.5, suggesting that the critical time point at which *Ets1* regulates NC cell and melanoblast survival is somewhere between E10 and E11.

Other pigmentation mutants in which melanoblast survival defects are observed as early as E10.5-E11.5 include mutants of the transcription factors *Sox10*, paired box 3 (*Pax3*), and Microphthalmia-associated transcription factor (*Mitf*) as well as mutants of the G-coupled Endothelin receptor b (*Ednrb*) and the tyrosine kinase receptor *Kit*. Mutations in these genes not only affect melanoblast survival, but also proliferation, migration and final differentiation (Baxter et al., 2004; Silver et al., 2006). The transcription factors *Pax3* and *Sox10* are initially expressed in NC cells at E8.5 prior to their commitment into the melanocytic fate. *Mitf*, *Kit*, and *Ednrb*, on the other hand are

first expressed at E10-E10.5, around the time of melanoblast specification from the NC (reviewed in Silver et al., 2006). All of these genes are required for melanoblast survival and it is possible that the Ets1-induced effect on melanoblast survival is mediated via one or more of these essential melanocytic genes. In the chick embryo, Ets1 drives *Sox10* expression in cranial NC cells via the Sox10E2 enhancer, which is critical for the initiation of *Sox10* expression in cranial NC cells. Ets1 was found to directly bind to and activate this enhancer (Betancur et al., 2010). Although the hypopigmentation phenotype observed in *Ets1* null mutant mice is the result of improper development of NC cells emerging from the trunk region, it is possible that in the mouse, *Ets1* may be an important regulator of *Sox10* in the trunk NC. The early defects in melanoblast and NC cell survival observed in *Ets1* null mutants point to *Sox10* as a probable target of Ets1, particularly in light of the essential role of *Sox10* in NC cell, melanocyte and glial cell survival (Britsch et al., 2001). In an attempt to examine whether *Ets1* acts upstream of *Sox10*, phenotypic analysis of *Ets1* and *Sox10* double heterozygous mutants will be carried in order to determine whether a synergistic genetic interaction exists between these genes in melanocyte development.

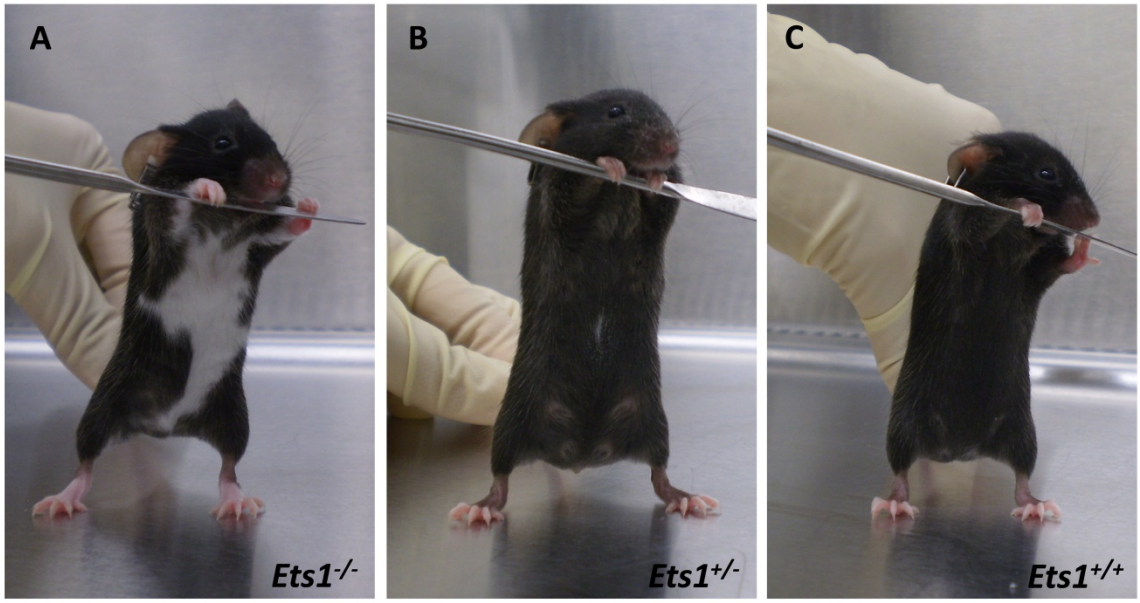

Figure 2.1. Ventral hypopigmentation in *Ets1* mutant mice. *Ets1* null (*Ets1*$^{-/-}$) and heterozygous (*Ets1*$^{+/-}$) mice (A and B, respectively) exhibit ventral hypopigmentation compared to *Ets1* wild type (*Ets1*$^{+/+}$) (C) littermates.

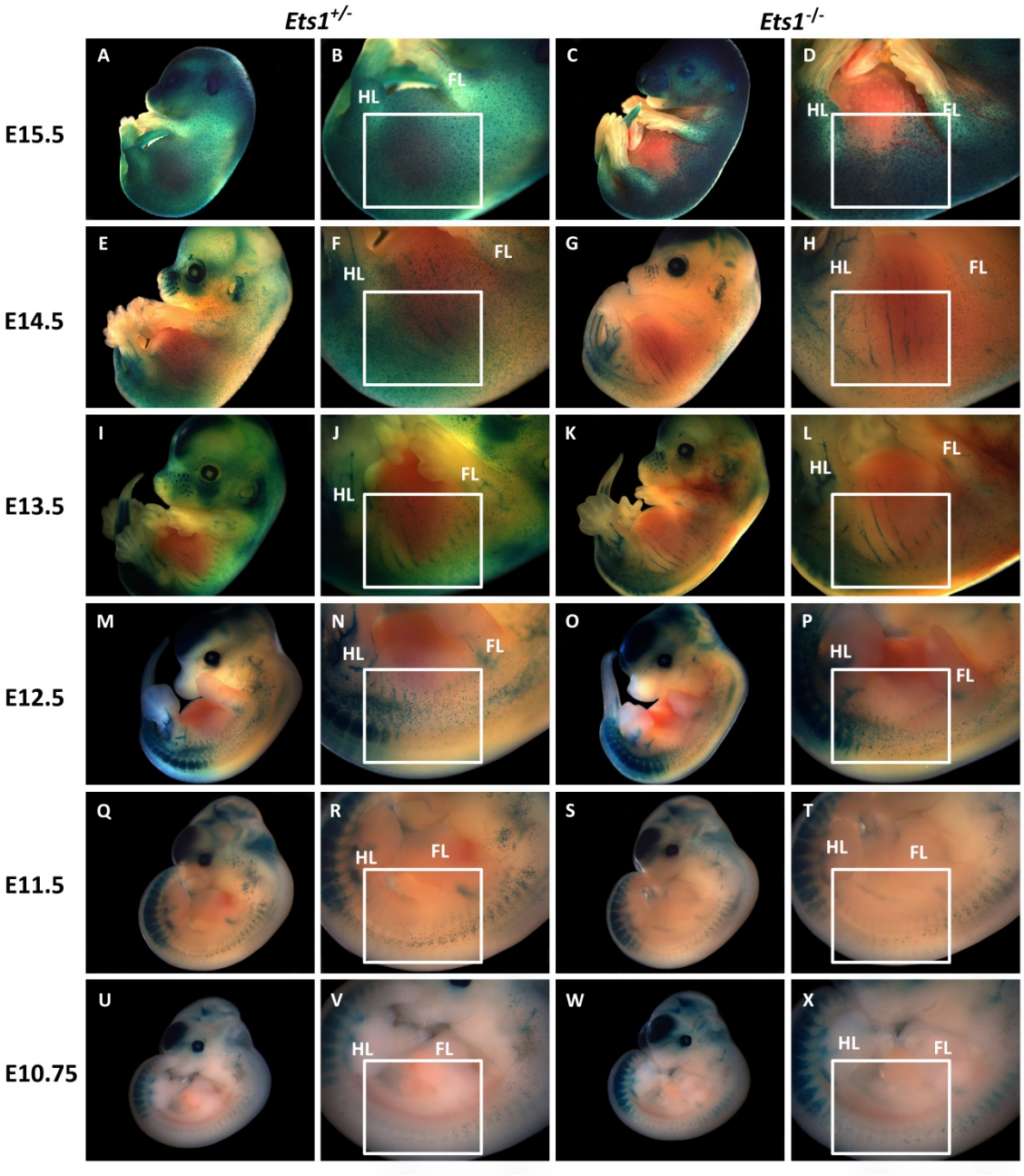

Figure 2.2. *Ets1* null mutant embryos have decreased melanoblast numbers. *Dct-LacZ* transgenic mice, in which *LacZ* expression is driven by the Dopachrome tautomerase *(Dct)* promoter that drives expression to melanoblasts, were crossed to $Ets1^{+/-}$ mice to produce $Ets1^{+/-}$::$Dct\text{-}LacZ^{+}$ mice. Embryos from intercrosses between $Ets1^{+/-}$::$Dct\text{-}LacZ^{+}$ mice were harvested at embryonic days (E)10.75-15.5, subjected to LacZ staining and analyzed for the amount and position of melanoblasts (blue dots) in the trunk region. At all these ages, $Ets1^{-/-}$ embryos have reduced numbers of melanoblasts (D, H, L, P, T, X) compared to $Ets1^{+/-}$ (B, F, J, N, R, V) and wild type (not shown) littermates (HL: Hindlimb, FL: Forelimb).

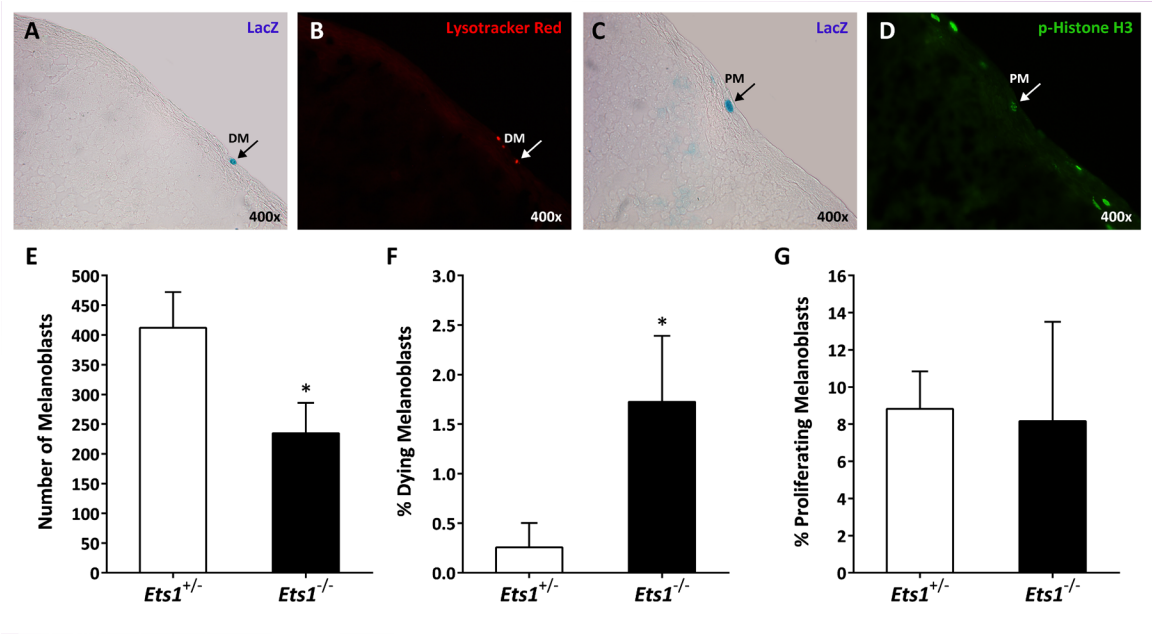

Figure 2.3. Decreased melanoblast survival in E10.75 *Ets1* null mutants. LacZ staining, Lysotracker Red staining, and phospho-Histone H3 (p-Histone H3) immunofluorescence of E10.75 mouse embryos. (A & C) Melanoblasts traveling along the surface of the embryo are marked via LacZ staining (black arrows). (B) Lysotracker Red marks lysosomes in dying cells (red fluorescence). (D) Proliferating cells are positive for the p-Histone H3 antibody (green fluorescence). (A & B) Dying melanoblasts (DM, arrows) are LacZ and Lysotracker Red positive. (C & D) Proliferating melanoblasts (PM, arrows) are LacZ and p-Histone H3 positive. (E) Melanoblasts (LacZ positive cells), (F) dying melanoblasts (LacZ and Lysotracker Red positive cells) and (G) proliferating melanoblasts (LacZ and p-Histone H3 positive cells) were counted in 80 sections for E10.75 $Ets1^{+/-}$ (n=3) and $Ets1^{-/-}$ (n=3) embryos. (E) $Ets1^{-/-}$ embryos have significantly reduced numbers of melanoblasts compared to $Ets1^{+/-}$ littermates (*$p<0.05$). (F) The percent of dying melanoblasts was significantly higher (*$p<0.05$) in $Ets1^{-/-}$ embryos compared to $Ets1^{+/-}$ littermates, (G) while the percent of proliferating melanoblasts did not differ significantly between these.

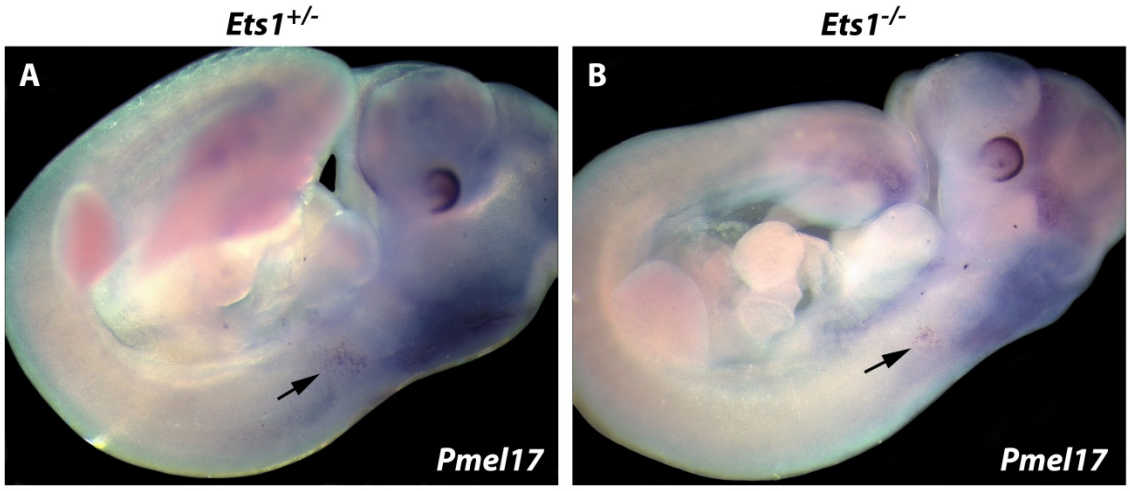

Figure 2.4. Melanoblasts in E10.5 *Ets1* null vs. *Ets1* heterozygous mouse embryos. In situ hybridization using a *Pmel17* probe was carried out to label developing melanoblasts at E10.5. No gross differences in the position and numbers of melanoblasts are apparent between *Ets1*$^{+/-}$ and *Ets1*$^{-/-}$ littermates (black arrows) (Magnification = 40x).

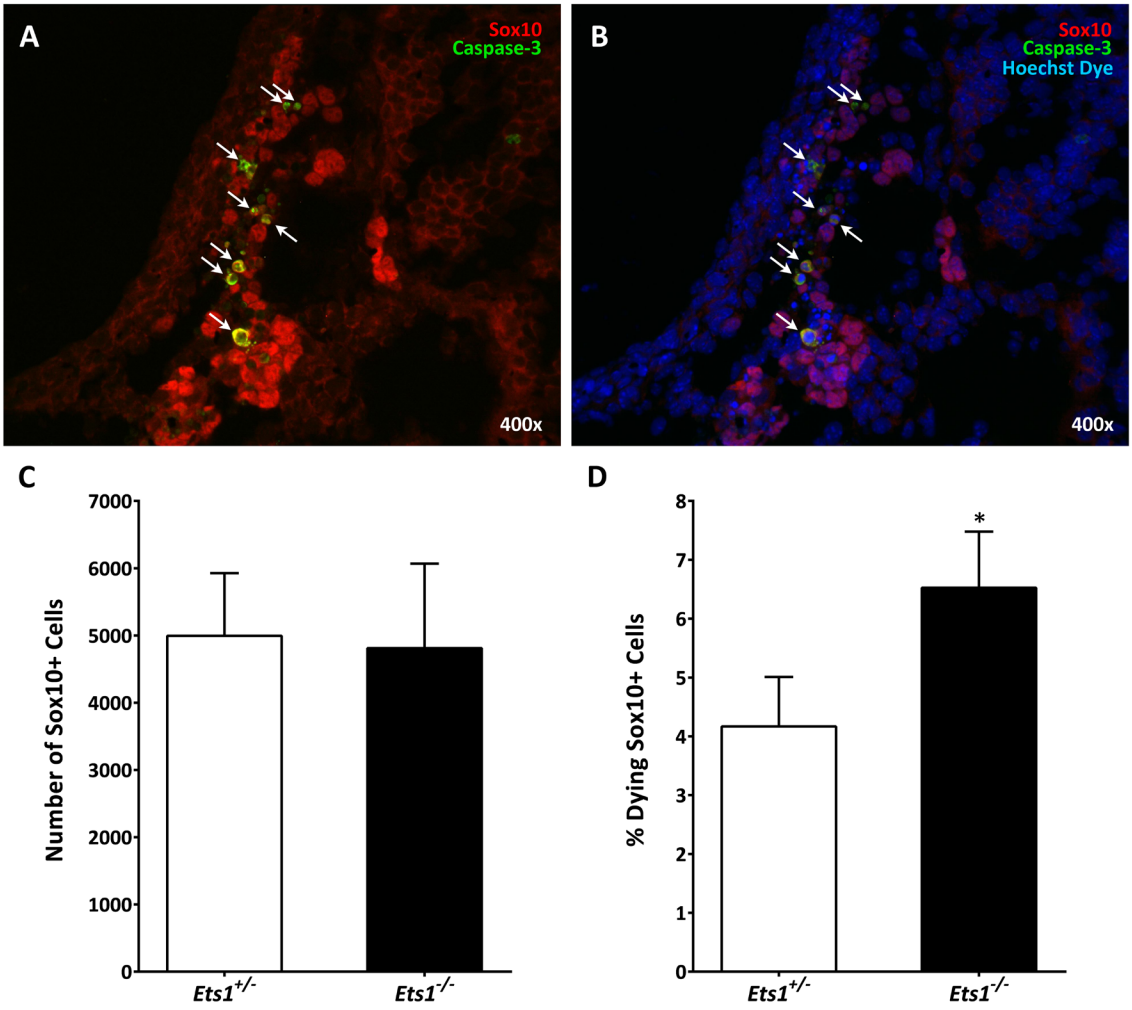

Figure 2.5. Decreased neural crest cell survival in E10.25 *Ets1* null mutants. Sox10 and cleaved Caspase-3 double-label immunofluorescence of E10.25 mouse embryos. (A & B) Neural crest (NC) cells traveling along the surface of the embryo were labeled with Sox10 antibody (red fluorescence). Dying cells were labeled using a cleaved Caspase-3 antibody (green fluorescence). Dying NC cells are positive for Sox10 and cleaved Caspase-3 (white arrows). (C) NC cells and (D) dying NC cells were counted in 35 sections spanning the anterior half of the trunk region for E10.25 $Ets1^{+/-}$ (n=3) and $Ets1^{-/-}$ (n=3) embryos. (C) The number of NC cells in $Ets1^{-/-}$ embryos is not significantly different from that of $Ets1^{+/-}$ littermates (p=0.848). (D) The percent of dying NC cells is significantly higher (*p<0.05) in $Ets1^{-/-}$ embryos compared to $Ets1^{+/-}$ littermates.

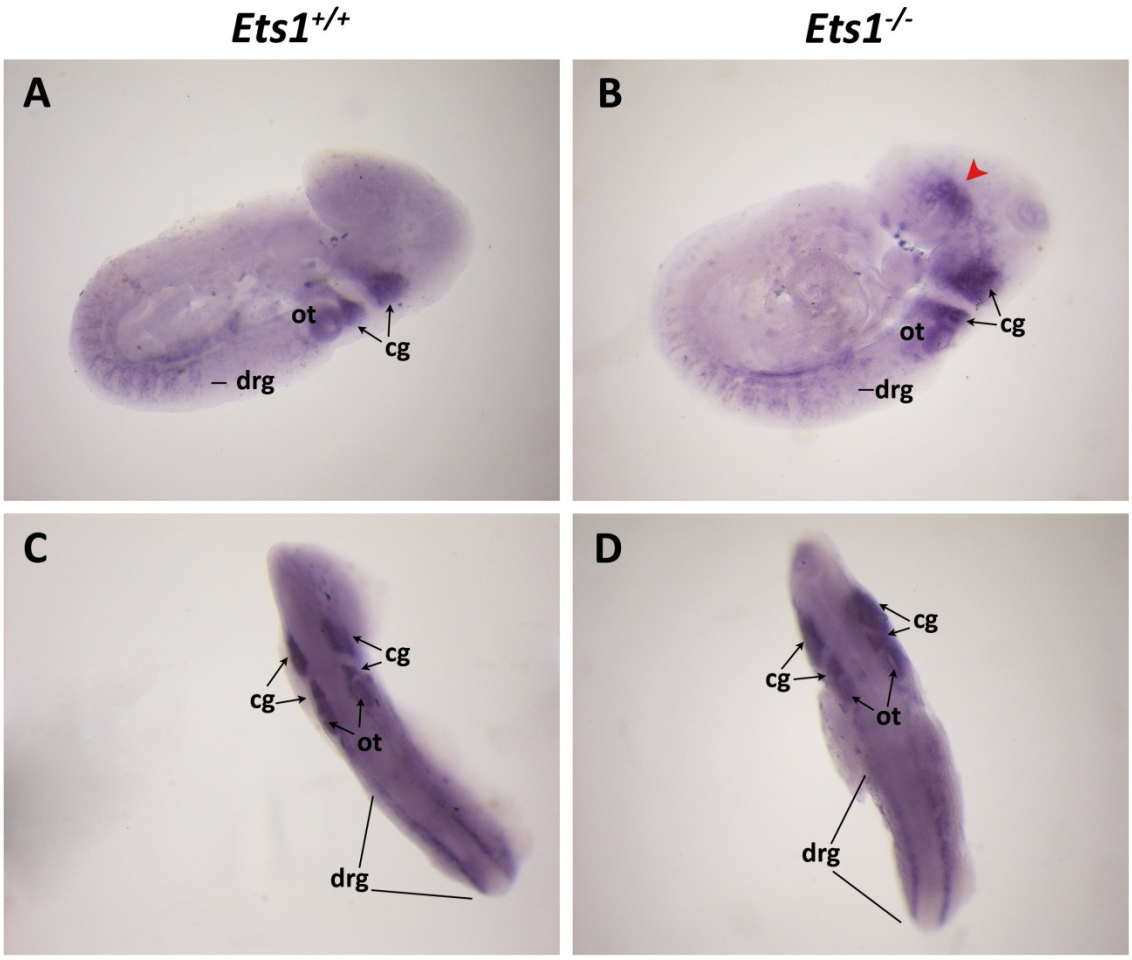

Figure 2.6. *Sox10* expression in E9.5 *Ets1* mutant embryos examined via in situ hybridization. Whole mount in situ hybridization of E9.5 embryos using a *Sox10* riboprobe. *Sox10* expression can be seen in the cranial ganglia (cg), otocyst (ot) and dorsal root ganglia (drg). Ectopic *Sox10* expression was also detected on the frontal aspect of the head in *Ets1*$^{-/-}$ embryos (red arrowhead) (Magnification = 40x).

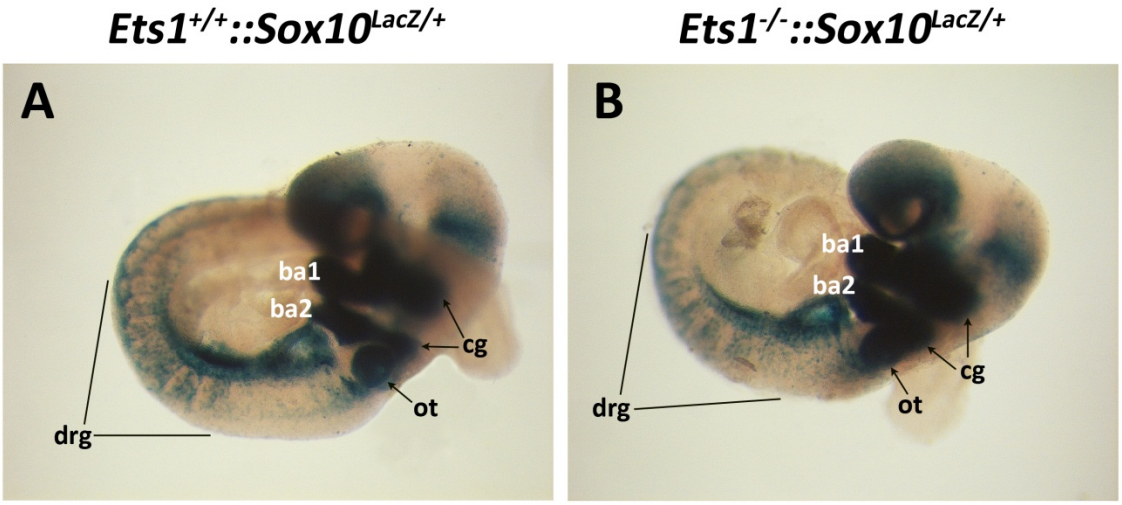

Figure 2.7. *Sox10* expression in *Ets1* mutant embryos visualized via LacZ staining. *Sox10* expression was visualized via LacZ staining in E9.5 embryos from intercrosses between $Ets1^{+/-}$::$Sox10^{LacZ/+}$ mice. *Sox10* expression can be seen in the cranial ganglia (cg), the otocyst (ot), the dorsal root ganglia (drg) and the first and second branchial arches (ba1 and ba2, respectively). Overall, no gross differences were observed in *Sox10* expression between $Ets1^{-/-}$ and $Ets1^{+/+}$ or $Ets1^{+/-}$ (not shown) littermates (Magnification: 40x).

2.6 References

Barton, K., Muthusamy, N., Fischer, C., Ting, C., Walunas, T., Lanier, L. and Leiden, J. (1998). The Ets-1 transcription factor is required for the development of natural killer cells in mice. *Immunity* 9, 555–563.

Baxter, L., Hou, L., Loftus, S. and Pavan, W. (2004). Spotlight on spotted mice: a review of white spotting mouse mutants and associated human pigmentation disorders. *Pigment Cell & Melanoma Research* 17, 215–224.

Baxter, L. and Pavan, W. (2003). Pmel17 expression is Mitf-dependent and reveals cranial melanoblast migration during murine development. *Gene expression patterns : GEP* 3, 703–707.

Betancur, P., Bronner-Fraser, M. and Sauka-Spengler, T. (2010). Genomic code for Sox10 activation reveals a key regulatory enhancer for cranial neural crest. *Proc. Natl. Acad Sci U.S.A.* 107, 3570–3575.

Britsch, S., Goerich, D., Riethmacher, D., Peirano, R., Rossner, M., Nave, K., Birchmeier, C. and Wegner, M. (2001). The transcription factor Sox10 is a key regulator of peripheral glial development. *Genes & development* 15, 66–78.

Dittmer, J. (2003). The biology of the Ets1 proto-oncogene. *Molecular Cancer* 2, 29.

Fafeur V., Tulasne D., Queva C., Vercamer C., Dimster V., Mattot V., Stehelin D., Desbiens X., Vandenbunder B. (1997). The Ets1 transcription factor is expressed during epithelial-mesenchymal transitions in the chick embryo and is activated in scatter factor-stimulated MDCK epithelial cells. *Cell Growth Differ* 8, 655-665.

Gao, Z., Kim, G., Mackinnon, A., Flagg, A., Bassett, B., Earley, J. and Svensson, E. (2010). Ets1 is required for proper migration and differentiation of the cardiac neural crest. *Development* 137, 1543–1551.

Garrett-Sinha, L. A. (2013). Review of Ets1 structure, function, and roles in immunity. *Cellular and Molecular Life Sciences* 70, 3375-3390.

Hahne J.C., Okuducu A.F., Kaminski A., Florin A., Soncin F., Wernert N. (2005). Ets-1 expression promotes epithelial cell transformation by inducing migration, invasion and anchorage-independent growth. *Oncogene* 24, 5384-5388.

Herbarth, B., Pingault, V., Bondurand, N., Kuhlbrodt, K., Hermans-Borgmeyer, I., Puliti, A., Lemort, N., Goossens, M. and Wegner, M. (1998). Mutation of the Sry-related Sox10 gene in Dominant megacolon, a mouse model for human Hirschsprung disease. *Proc. Natl. Acad Sci U.S.A.* 95, 5161–5165.

Hou, L., Arnheiter, H. and Pavan, W. (2006). Interspecies difference in the regulation of melanocyte development by SOX10 and MITF. *Proc. Natl. Acad Sci U.S.A.* 103, 9081–9085.

Le Douarin, N. M. and Kalcheim, C. (1999). The Neural Crest. New York: Cambridge University Press.

Kapur, R. P. (1999). Early death of neural crest cells is responsible for total enteric aganglionosis in Sox10(Dom)/Sox10(Dom) mouse embryos. *Pediatric and developmental pathology* 2, 559–569.

Keehn, C., Smoller, B. and Morgan, M. (2003). Expression of the ets-1 proto-oncogene in melanocytic lesions. *Modern Pathology* 16, 772–777.

Kola I., Brookes S., Green A.R., Garber R., Tymms M., Papas T.S., Seth A. (1993). The Ets1 transcription factor is widely expressed during murine embryo development and is associated with mesodermal cells involved in morphogenetic processes such as organ formation. *Proc. Natl. Acad Sci U.S.A.* 90, 7588-7592.

Kuhlbrodt, K., Herbarth, B., Sock, E., Hermans-Borgmeyer, I. and Wegner, M. (1997). Sox10, a novel transcriptional modulator in glial cells. *The Journal of Neuroscience* 18, 237–250.

Maroulakou I.G., Papas T.S., Green J.E. (1994). Differential expression of ets-1 and ets-2 proto-oncogenes during murine embryogenesis. *Oncogene* 9, 1551-1565.

Muthusamy, N., Barton, K. and Leiden, J. (1995). Defective activation and survival of T cells lacking the Ets-1 transcription factor. *Nature* 377, 639–642.

Nagarajan, P., Parikh, N., Garrett-Sinha, L. and Sinha, S. (2009). Ets1 induces dysplastic changes when expressed in terminally-differentiating squamous epidermal cells. *PloS One* 4, e4179.

Nagy, A., Gertsenstein, M., Vintersten, K., Behringer, R. (Eds.). (2003). Manipulating the Mouse Embryo. Cold Spring Harbor Laboratory Press, New York.

Oda, N., Abe, M. and Sato, Y. (1999). ETS-1 converts endothelial cells to the angiogenic phenotype by inducing the expression of matrix metalloproteinases and integrin beta3. *Journal of Cellular Physiology* 178, 121–132.

Okuducu, A., Zils, U., Michaelis, S., Mawrin, C. and von Deimling, A. (2006). Increased expression of avian erythroblastosis virus E26 oncogene homolog 1 in World Health Organization grade 1 meningiomas is associated with an elevated risk of recurrence and is correlated with the expression of its target genes matrix metalloproteinase-2 and MMP-9. *Cancer* 107, 1365–1372.

Park, Y. H., Jung, H. H., Ahn, J. S. and Im, Y.-H. (2008). Ets-1 upregulates HER2-induced MMP-1 expression in breast cancer cells. *Biochemical and Biophysical Research Communications* 377, 389-394.

Potterf, S., Mollaaghababa, R., Hou, L., Southard-Smith, E., Hornyak, T., Arnheiter, H. and Pavan, W. (2001). Analysis of SOX10 function in neural crest-derived melanocyte development: SOX10-dependent transcriptional control of dopachrome tautomerase. *Developmental Biology* 237, 245–257.

Queva C., Leprince D., Stehelin D., Vandenbunder B. (1993). $P54^{c\text{-}ets\text{-}1}$ and $P68^{c\text{-}ets\text{-}1}$, the two transcription factors encoded by the *c-ets-1* locus, are differentially expressed during the development of the chick embryo. *Oncogene* 8, 2511-2520.

Rothhammer, T., Hahne, J., Florin, A., Poser, I., Soncin, F., Wernert, N. and Bosserhoff, A.-K. (2004). The Ets-1 transcription factor is involved in the development and invasion of malignant melanoma. *Cellular and Molecular Life Sciences : CMLS* 61, 118–128.

Rothhammer, T., Poser, I., Soncin, F., Bataille, F., Moser, M. and Bosserhoff, A.-K. (2005). Bone morphogenic proteins are overexpressed in malignant melanoma and promote cell invasion and migration. *Cancer Research* 65, 448–456.

Silver, D., Hou, L. and Pavan, W. (2006). The genetic regulation of pigment cell development. Georgetown: Landes Biosciences, 155-169.

Sommer, L. (2011). Generation of melanocytes from neural crest cells. *Pigment Cell & Melanoma Research* 24, 411–421.

Southard-Smith, E., Kos, L. and Pavan, W. (1998). Sox10 mutation disrupts neural crest development in Dom Hirschsprung mouse model. *Nature Genetics* 18, 60–64.

Tahtakran, S. and Selleck, M. (2003). Ets-1 expression is associated with cranial neural crest migration and vasculogenesis in the chick embryo. *Gene Expression Patterns* 3, 455-458.

Théveneau, E., Duband, J.-L. and Altabef, M. (2007). Ets-1 confers cranial features on neural crest delamination. *PloS One* 2, e1142.

Thomas, A. and Erickson, C. (2008). The making of a melanocyte: the specification of melanoblasts from the neural crest. *Pigment Cell & Melanoma Research* 21, 598–610.

Vandenbunder, B., Pardanaud, L. and Jaffredo, T., Mirabel M.A., Stehelin D. (1989). Complementary patterns of expression of c-ets 1, c-myb and c-myc in the blood-forming system of the chick embryo. *Development* 106, 265-274.

Watson, D., McWilliams-Smith, M.J., Nunn M.F., Duesberg P.H., O'Brien S.J. and Papas T.S. (1985). The ets sequence from the transforming gene of avian erythroblastosis virus, E26, has unique domains on human chromosomes 11 and 21: both loci are transcriptionally active. *Proc. Natl. Acad Sci U.S.A.*82, 7294-7298.

Wei, G., Srinivasan, R., Cantemir-Stone, C., Sharma, S., Santhanam, R., Weinstein, M., Muthusamy, N., Man, A., Oshima, R., Leone, G., et al. (2009). Ets1 and Ets2 are required for endothelial cell survival during embryonic angiogenesis. *Blood* 114, 1123–1130.

Wilkinson, D.G. and Nieto, M.A. (1993). Detection of messenger RNA by in situ hybridization to tissue sections and whole mounts. *Methods Enzymol*. 225, 361-373.

Wilkinson, D. (1998). In Situ *Hybridization:* A Practical Approach, 2nd ed. IRL Press, Oxford.

Ye, M., Coldren, C., Liang, X., Mattina, T., Goldmuntz, E., Benson, D., Ivy, D., Perryman, M., Garrett-Sinha, L. and Grossfeld, P. (2010). Deletion of ETS-1, a gene in the Jacobsen syndrome critical region, causes ventricular septal defects and abnormal ventricular morphology in mice. *Human Molecular Genetics* 19, 648–656.

Zhao, S. and Overbeek, P. (1999). Tyrosinase-related protein 2 promoter targets transgene expression to ocular and neural crest-derived tissues. *Developmental Biology* 216, 154–163.

Zucker, R.M., Hunter, S., Rogers, J.M. (1998). Confocal laser scanning microscopy of apoptosis in organogenesis-stage mouse embryos. *Cytometry* 33, 348-354.

CHAPTER III

GENETIC INTERACTION BETWEEN THE TRANSCRIPTION FACTORS *Ets1* AND *Sox10* IN THE DEVELOPMENT OF MELANOCYTES AND ENTERIC GANGLIA

III. GENETIC INTERACTION BETWEEN THE TRANSCRIPTION FACTORS *Ets1* AND *Sox10* IN THE DEVELOPMENT OF MELANOCYTES AND ENTERIC GANGLIA

3.1 Abstract

The study of synergistic genetic interactions through the use of double heterozygous pigmentation mutants has been instrumental to the elucidation of the transcriptional networks at play in the development of melanocytes from the neural crest (NC). We previously established a role for *Ets1* in the survival of early melanocyte precursors (melanoblasts). This observation, along with findings in the avian system, which implicate *Ets1* in the regulation of the transcription factor *Sox10*, a factor critical for melanoblast survival, pointed to a potential genetic interaction between *Ets1* and *Sox10* in melanocyte development. To establish whether *Ets1* interacts with *Sox10*, $Ets1^{+/-}$ mice were crossed to $Sox10^{LacZ/+}$ mice, in which *LacZ* is inserted into the *Sox10* locus, and the hypopigmentation phenotypes of the progeny were compared. The incidence of hypopigmentation in $Ets1^{+/-}::Sox10^{LacZ/+}$ mice was significantly higher than that of $Ets1^{+/-}$ and $Sox10^{LacZ/+}$ mice. Additionally, the areas of hypopigmentation of $Ets1^{+/-}::Sox10^{LacZ/+}$ mice were significantly greater than the sum of the areas of hypopigmentation of $Ets1^{+/-}$ and $Sox10^{LacZ/+}$ mice, suggesting that a synergistic genetic interaction exists between *Ets1* and *Sox10* in melanocyte development. The transcription factor *Sox10* is also required for the development of NC-derived enteric ganglia, and mutations in this transcription factor have been described in both syndromic and non-syndromic aganglionosis of the distal colon or Hirschsprung's disease. Given the importance of *Sox10* for proper gut innervation, the enteric innervation in the distal

portion of the colon from *Ets1* heterozygous and null mutant mice, that were either wild type or heterozygous for *Sox10*, were also analyzed. Colons from $Ets1^{-/-}::Sox10^{+/+}$ mice had significantly larger nerve-free areas compared to $Ets1^{+/-}::Sox10^{+/+}$ and $Ets1^{+/-}::Sox10^{LacZ/+}$ mice. *Sox10* heterozygosity was found to exacerbate the decrease in gut innervation observed in *Ets1* null mutants. Finally, analysis of *Sox10* expression, via LacZ staining in E11.5 and E12.5 $Ets1^{-/-}::Sox10^{LacZ/+}$ and $Ets1^{+/-}::Sox10^{LacZ/+}$ littermates revealed an apparent decrease in *Sox10* expression in approximately 50% of the embryos analyzed. Together, these results suggest that *Ets1* interacts synergistically with *Sox10* in melanocyte and enteric ganglia development. Furthermore, the nature of this synergistic interaction may underlie a functional interaction, with *Ets1* acting in the regulation of *Sox10* expression during embryonic development.

3.2 Introduction

The study of genetic interactions has been widely used as a means of revealing functional interactions among genes (Mani et al., 2008). A genetic interaction is the interaction of two genetic alterations in the specification of a given phenotype (Drees et al., 2005). Genetic interactions can be additive, epistatic, suppressed, or synergistic in nature. A genetic interaction is considered additive when the phenotype of the double mutant is a combination of the phenotypes observed in the single mutants. An epistatic interaction refers to interactions in which the phenotype of the double mutant is similar to that of one of the single mutants but not the other. Suppressed genetic interactions are those in which the phenotype of the double mutant more closely resembles the wild type phenotype than the phenotype of the single mutants. A synergistic genetic interaction, on the other hand, exists when the presence of both mutations results in a more extreme or

exacerbated phenotype than would be expected from the addition of the phenotypes of the single mutants (Mani et al., 2008; Perez-Perez et al., 2009). Epistatic and suppressive genetic interactions are considered as evidence of an underlying functional relationship, while additive interactions indicate the absence of a functional relationship (Perez-Perez et al., 2009).

Instances of suppressed genetic interactions have been described in mouse pigmentation mutants. One such instance revealed a functional interaction between *Nf1*, the gene encoding the Ras-GTPase activating protein Neurofibromin, with two critical melanocytic genes, the tryrosine kinase receptor *Kit* and the Microphthalmia-associated transcription factor (*Mitf*). When mice heterozygous for *Nf1* were crossed to $Kit^{W/+}$ or $Mitf^{wh/+}$ mutant mice a reduction in the sizes of the belly spots normally present in these mutants was observed in progeny that were also heterozygous for *Nf1*. In triple heterozygotes for *Kit*, *Mitf,* and *Nf1*, *Nf1* heterozygosity was also able to partially rescue the exacerbated hypopigmentation phenotype that is normally observed in mice that are double heterozygous for $Kit^{W/+}$ and $Mitf^{Wh/+}$ ($Kit^{W/+};Mitf^{Wh/+}$). These results not only suggested a functional interaction between *Nf1* and *Kit,* and between *Nf1* and *Mitf*, but also suggested that this interaction occurs via a pathway that links *Mitf* and *Kit* rather than through independent downstream and upstream regulators of *Kit* and *Mitf*, respectively. At the cellular level, *Nf1* heterozygosity was found to induce an increase in the expression of melanogenic enzymes. Additionally, higher levels of phosphorylated ERK (extracellular signal regulated kinase), a component of the mitogen activated protein kinase (MAPK) pathway, which acts downstream of *Kit* to activate *Mitf*, were observed in $Nf1^{+/-}$ melanocytes prior to and after stimulation with Kit ligand (Diwakar et al., 2008).

Whether synergistic genetic interactions can serve as evidence of an underlying functional relationship remains controversial (Perez-Perez et al., 2009). A synergistic interaction may result if the genes in question are involved in the same genetic pathway, but act at different nodes, so that the process is more severely impaired when both genes are mutated compared to when either gene is mutated (Hekimi et al., 2001). An apparent synergistic interaction can also result if a mutation increases the sensitivity of an organism to the effects of another mutation (Perez-Perez et al., 2009).

Synergistic genetic interactions identified through the study of double heterozygous mice were the first indication of an underlying functional interaction between *Kit* and *Mitf*. Mice heterozygous for a semi-dominant *Mitf* mutation ($Mitf^{mi\text{-}wh/+}$) have a uniform ventral spot and a lighter coat color. Crossing $Mitf^{mi\text{-}wh/+}$ mice to mice heterozygous for a semi-dominant mutation in *Kit* ($Kit^{W\text{-}36H}$), which only have ventral spots and occasionally white feet and tail, resulted in an exacerbated pigmentation phenotype, which was more severe than expected if the hypopigmented areas of the single heterozygotes were added (Beechey et al., 1994). Similar results were obtained when $Mitf^{mi\text{-}wh/+}$ mice were crossed to heterozygous mice in which the *LacZ* gene was inserted into the *Kit* locus ($Kit^{W\text{-}LacZ/+}$). Additional experiments demonstrated that signaling via the *Kit* receptor modulates *Mitf* and is required for Mitf-dependent induction of Tyrosinase (*Tyr*), a rate limiting enzyme in melanin production (Hou et al., 2000). Evaluation of other *Mitf* mutant alleles, demonstrated that not all *Mitf* alleles produce a similar effect when present in a *Kit*-deficient background, even if the alleles have equivalent mutations or produce similar alterations in mRNA levels (Hou et al., 2010).

The study of double heterozygous pigmentation mutants also revealed a synergistic interaction between *Mitf* and the anti-apoptotic factor *Bcl2*. Mice homozygous for a recessive *Bcl2* null allele or for the recessive $Mitf^{vit}$ allele, exhibit gradual pigment loss over time, whereas heterozygous mice do not show pigmentation defects. Similar to the homozygous mice for either allele, double heterozygotes display a gradual loss of pigmentation as a result of melanocyte stem cell death. The synergistic genetic interaction between *Mitf* and *Bcl2* was found to be the result of a direct functional interaction between these genes, with Mitf directly binding to and activating the *Bcl2* promoter (McGill et al., 2002).

A synergistic genetic interaction has likewise been described between *Kit* and the transcription factor paired box 3 (*Pax3*). Double heterozygous mice for semi-dominant mutations in *Pax3* ($wbs^{+/-}$) and *Kit* ($wps^{+/-}$) exhibit significantly more severe dorsal and ventral hypopigmentation compared to single heterozygous littermates. At the cellular level, luciferase assays revealed the ability of Pax3 to transactivate the *Kit* promoter. Furthermore, a form of Pax3 carrying the same mutation present in the *wps* mice abrogated *Kit* promoter activation, further validating a role for *Pax3* in *Kit* regulation. Nonetheless, Pax3 was not found to directly bind the *Kit* promoter, which suggests that the functional interaction between these genes is most likely indirect (Guo et al., 2010).

Given the hypopigmentation phenotype observed in *Ets1* mutant mice and the increased melanocyte and NC cell death observed in *Ets1* null mutant embryos, it is likely that Ets1 plays a role in the regulation of melanocyte or NC-specific genes. In order to dissect potential functional interactions between *Ets1* and other melanocyte-specific genes, a genetic interactions approach was chosen because the pigmentation

phenotypes of single and double mutant progenies can be easily assessed and compared. In light of the fact that, in the chick embryo, Ets1 is required for the activation of the transcription factor sex determining region Y (SRY)-box 10 (*Sox10*) (Betancur et al., 2010), a gene required for the development of various NC cell derivatives, including melanocytes and enteric ganglia (Herbarth et al., 1998; Southard-Smith et al., 1998; Kapur, 1999; Potterf et al., 2001), *Sox10* was the best candidate for this study. A potential synergistic genetic interaction between *Ets1* and *Sox10* was studied by comparing the areas of hypopigmentation in single and double heterozygous progenies. Additionally, because *Sox10* is also required for the development of enteric ganglia, the innervation of colons from *Ets1* heterozygous and null mutant mice, that were either wild type or heterozygous for *Sox10*, was also examined.

3.3 Materials and methods

3.3.1 Animals

Mice heterozygous for *Ets1* were obtained from Dr. Eric Svensson (Universtiy of Chicago, Chicago, IL) and generated as previously described to harbor a targeted deletion of exons 3 and 4 of the *Ets1* gene (Barton et., al. 1998). Mice heterozygous for *Ets1* were re-derived by outcrossing to C57BL/6J mice for eight generations (Gao et., al. 2010). They have been maintained on C57BL/6J genetic background by intercrossing and by outcrossing to C57BL/6J mice (Jackson Laboratories). $Sox10^{tm1WegLacZ}$ mice (hereafter referred to as $Sox10^{LacZ/+}$) were obtained from Dr. Michael Wegner (Institut für Biochemie, Universität Erlangen-Nürnberg, Germany). $Sox10^{LacZ/+}$ mice were generated as previously described (Britsch et al., 2001) via insertion of the *LacZ* gene into the

Sox10 coding sequence. *Sox10*$^{LacZ/+}$ mice have been maintained on their original C3H mixed genetic background by backcrossing.

Timed matings were set for the generation of embryos. Animals were mated overnight, and females were examined for vaginal plugs after approximately 16 hours. Noon of the day a vaginal plug was observed, was considered embryonic day (E) 0.5. Pregnant females were euthanized by exposure to Isoflurane (Vedco, Inc.) followed by cervical dislocation, and an abdominal incision was made to expose the uterus. As soon as embryos were recovered from the euthanized mother, they were placed in Phosphate Buffered Saline (PBS) (pH7.2) and dissected out of the uterine sacs. For all embryos, yolk sacs were isolated for genotyping. Embryos were fixed in 2% paraformaldehyde immediately after dissection, just prior to β-galactosidase staining. All animal work was performed according to institutional guidelines established by the National Institutes of Health (NIH) (Guide for the Care and Use of Laboratory Animals, 2011; Institutional Animal Care and Use Committee (IACUC) Protocol No. 13-064).

3.3.2 Genotyping

Genomic DNA was isolated from tail biopsies from adult mice, or yolk sacs from embryos, and used for PCR genotyping. For *Ets1*, genotyping of adult mice and embryos was performed using the primers 5'-GTCTTCTTCTCTAGTTTCTGAGTGCTC, 5'-GTCCTGCTTACAACACTCTGAATCCTG and 5'-GCCTGCTCTTTACTGAAGGCTCTTT (Gao et al., 2010), under standard PCR conditions (35 cycles of 94˚C for 60 s, 60˚C for 60 s, and 72˚C for 60 s). Products were visualized in a 2% agarose gel containing 0.5µg/ml Ethidium Bromide (Fisher Scientific). The wild type *Ets1* allele produced a 438bp product while the mutant allele produced a

350bp product (Gao et al., 2010). For *Sox10*, genotyping of adult mice and embryos was performed using the primers 5'-CAGGTGGGCGTTGGGCTC, 5'-CAGAGCTTGCCTAGTGTCT, and 5'-TAAAAATGCGCTCAGGTCAA under standard PCR conditions (35 cycles of 94˚C for 30 s, 55˚C for 30 s, and 72˚C for 30 s). Products were visualized in a 2% agarose gel containing 0.5µg/ml Ethidium Bromide (Fisher Scientific). The wild type *Sox10* allele produced a 500bp product while the mutant allele produced a 600bp product (Britsch et al., 2001). Heterozygous animals were identified by the presence of both PCR products.

3.3.3 Crosses and phenotypic analysis

Heterozygous *Ets1* mutant ($Ets1^{+/-}$) mice were crossed to *Sox10* heterozygous mutants ($Sox10^{LacZ/+}$) to generate progeny that were either heterozygous for *Ets1,* heterozygous for *Sox10*, or heterozygous for both genes ($Ets1^{+/-}::Sox10^{LacZ/+}$). The single heterozygous progeny of the first generation (F_1) were intercrossed to generate the second generation (F_2) animals of the genotypes noted above. Third generation animals (F_3) were generated by intercrossing single heterozygous as well as double heterozygous F_2 mice. For each generation, the ventral aspects of each mouse were photographed at 6 weeks of age. The areas of hypopigmentation were measured using the Image J 1.44p program (NIH).

3.3.4 β-galactosidase staining of whole mount embryos

Embryos from intercrosses between $Ets1^{+/-}::Sox10^{LacZ/+}$ mice were harvested at E11.5 and E12.5. β-galactosidase (LacZ) staining was performed using standard protocols (Nagy, 2003). Whole embryos were dissected in 0.05M PBS (pH7.2) and fixed with 2% paraformaldehyde for 50 minutes at room temperature. Embryos were briefly

washed in PBS (pH 7.2) and incubated 3-5 hours (the incubation time was directly proportional to the embryonic age), protected from light, at 30.9˚C in X-gal solution consisting of 2mM $MgCl_2$, 0.01% Sodium Deoxycholate, 5mM Potassium Ferricyanide, 5mM Postassium Ferrocyanide (Fisher Scientific), 0.02% Nonidet P40 (Roche Diagnostics), and 1mg/ml X-gal (Life Technologies). Embryos were washed twice in PBS to stop the reaction. The staining was visualized under a dissecting scope (Leica, Model MZ6). Whole Embryos were photographed using a Leica DC500 camera. For each stage, at least 3 embryos of each genotype ($Ets1^{+/+}$, $Ets1^{+/-}$ and $Ets1^{-/-}$) were stained and photographed.

3.3.5 Colon dissection and Acetylcholinesterase staining

Mice heterozygous for *Ets1* ($Ets1^{+/-}$), *Sox10* ($Sox10^{LacZ/+}$) or both genes ($Ets1^{+/-}::Sox10^{LacZ/+}$) were crossed to generate progeny of the following genotypes: $Ets1^{+/-}::Sox10^{+/+}$, $Ets1^{+/-}::Sox10^{LacZ/+}$, $Ets1^{-/-}::Sox10^{+/+}$, and $Ets1^{-/-}::Sox10^{LacZ/+}$. Littermates of the genotypes listed above, ranging from 4 to 7 months of age, were euthanized and their colons dissected. Euthanasia was carried out by exposure to Isoflurane in a closed chamber, and was followed by cervical dislocation. Once euthanized, approximately 30mm of the distal aspect of the colons of each animal were removed and pinned down to 4% agar plates, with the serosa aspect of each colon facing up. Colons were fixed in 4% paraformaldehyde, containing 10mM $CaCl_2$, overnight at 4˚C. Subsequently, colons were washed twice with PBS (pH7.4), 5 minutes each time, and incubated overnight in 5% sucrose. On the third and last day, colons were washed twice with PBS (pH7.4), 5 minutes each time, and subjected to Acetylcholinesterase staining to visualize gut innervation. Briefly, colons were transferred to 3ml glass vials, and incubated in a

solution consisting of 15mM Sodium Citrate, 3mM Copper Sulfate, 64mM Sodium Acetate (Fisher Scientific), 1% Triton X-100 (Sigma-Aldrich), 0.5mM Potassium Ferricyanide (Fisher Scientific), 0.05% Acetylcholine Iodide, and 5mM Tetraisopropyl Pyrophosphoramide (Sigma-Aldrich), 3 hours at 37˚C, rocking at 75 revolutions per minute (RPM). Colons were then washed twice with PBS (pH7.4), 5 minutes each time, and incubated for 5 minutes at room temperature in a color substrate solution prepared with the SIGMA*FAST*™ Diamonobenzidine Peroxidase tablet set (Sigma-Aldrich). The solution consisted of 0.7mg/ml 3,3'-Diaminobenzidine (DAB), 2.0mg/ml Urea Hydrogen Peroxide, and 60mM Tris Buffer (Sigma-Aldrich). Finally colons were rinsed with 10mM Tris Base (pH 8.0) and pinned in 4% agar plates, with the serosa aspect of each colon facing up (Gariepy et al., 1998). The staining was visualized under a dissecting scope (Leica, Model MZ6). Colons were photographed using a Leica DC500 camera. Colons from at least 5 animals of each genotype were stained and photographed. The extent of innervation of each colon was quantified using the images captured, by measuring the white (nerve-free) area in 8 squares of 0.25mm^2 each (for a total of 2mm^2), within a region located 15mm anterior to the anus (Appendix IV). The ImageJ 1.44p program (NIH) was used for measuring the white areas in each segment of colon.

3.3.6 Statistical analysis

Statistical analyses were carried out using the PASW Statistics 18 Software (IBM). The frequency of belly spot appearance was analyzed using the Chi-square test. In order to compare the mean areas of hypopigmentation among the different genotypes, a Box-Cox transformation was applied to the belly spot area data (measured in mm^2). This transformation was used to approximate a normal distribution and to achieve equal or

near equal variances, in order to enable the use of parametric tests (Appendix III). The lambda value used for the Box-Cox transformations was 0.35 for generations 1 and 3 (F_1 and F_3) and 0.3 for generation 2 (F_2). For each generation, the transformed areas of hypopigmentation of $Ets1^{+/-}::Sox10^{LacZ/+}$ mice were compared to the sum of the transformed areas of hypopigmentation of $Ets1^{+/-}$ and $Sox10^{LacZ/+}$ mice using a One-Way ANOVA with a contrast, where $Ets1^{+/-} = 1$, $Sox10^{LacZ/+} = 1$, and $Ets1^{+/-}::Sox10^{LacZ/+} = -2$. Scatter plots of the hypopigmentation areas showing the mean and standard deviations for each group were created using GraphPad Prism 6 (GraphPad Software, Inc).

To compare the nerve-free areas in colons from $Ets1^{+/-}::Sox10^{+/+}$, $Ets1^{+/-}::Sox10^{LacZ/+}$, and $Ets1^{-/-}::Sox10^{+/+}$ mice a One-Way ANOVA with Tukey's and Bonferroni's Post-Hoc Multiple Comparisons was carried out. An independent samples t-test was carried out to compare the nerve-free area of colons from $Ets1^{-/-}::Sox10^{+/+}$ and $Ets1^{-/-}::Sox10^{LacZ/+}$ mice. All data were confirmed to follow a normal distribution and to have variances that did not differ significantly within the genotypes being tested. Scatter plots of the nerve-free areas in $2mm^2$ of colon for each genotype, showing the mean and standard deviations were created using GraphPad Prism 6 (GraphPad Software, Inc).

3.4. Results

3.4.1 Ets1 and Sox10 double heterozygosity increases hypopigmentation frequency

In order to determine whether a genetic interaction exists between *Ets1* and *Sox10*, $Ets1^{+/-}$ mice were crossed to $Sox10^{LacZ/+}$ mice and the hypopigmentation phenotypes of the progeny were examined for three generations. For all generations, the frequency of belly spot appearance in double heterozygotes ($Ets1^{+/-}::Sox10^{LacZ/+}$) was significantly higher than in $Ets1^{+/-}$ and $Sox10^{LacZ/+}$ mice (Figure 3.1, $p<0.001$ for all

generations). In the three generations examined, almost all *Ets1*$^{+/-}$*::Sox10*$^{LacZ/+}$ mice had belly spots (F_1: 97%, F_2: 96%, F_3: 100%), compared to approximately 40% for *Ets1*$^{+/-}$ mice and 48% of *Sox10*$^{LacZ/+}$ mice. The increased frequency of belly spot appearance observed in double heterozygotes suggests that a genetic interaction exists between *Ets1* and *Sox10.*

3.4.2 Ets1 and Sox10 double heterozygosity exacerbates hypopigmentation

To further characterize the nature of the genetic interaction between *Ets1* and *Sox10* the areas of the belly spots of the *Ets1* heterozygous and *Sox10* heterozygous mice were compared to the areas of the belly spots of double heterozygous mice. Mice heterozygous for *Ets1* mice usually display a normal coat color. Small belly spots are observed in approximately 40% of *Ets1*$^{+/-}$ mice. *Sox10*$^{LacZ/+}$ mice have belly spots approximately 50% of the time. The belly spots in *Sox10*$^{LacZ/+}$ mice vary in size but also tend to be small. If a synergistic interaction exists between *Ets1* and *Sox10*, the areas of the belly spots of *Ets1*$^{+/-}$*::Sox10*$^{LacZ/+}$ should be greater than the sum of the areas of the belly spots of *Ets1*$^{+/-}$ and *Sox10*$^{LacZ/+}$ mice. For all three generations examined, double heterozygotes were found to have belly spots that were significantly larger than expected from the addition of the areas of the belly spots in the single heterozygotes ($p<0.001$ for all generations, Figures 3.2 and 3.3, Apprendix III), indicating that a synergistic genetic interaction exists between *Ets1* and *Sox10* in melanocyte development.

3.4.3 Ets1 null mutants show decreased gut innervation.

Mutations in the transcription factor *Sox10* are responsible for Waardenburg syndrome type IV (WS4), which is characterized by pigmentation defects and aganglionosis of the distal colon (Hirschsprung's disease) (Pingault et al., 1998).

Mutations in *Sox10* have also been associated with non-syndromic Hirschsprung's disease (Sanchez-Mejias et al., 2010). Given the importance of *Sox10* for proper gut innervation, and the synergistic genetic interaction between *Ets1* and *Sox10* in melanocyte development, it was possible that *Ets1* deficiency would negatively affect gut innervation. Megacolon was observed in two *Ets1* null mice, both of which were heterozygous for *Sox10* ($Ets1^{-/-}::Sox10^{LacZ/+}$) (Figure 3.4). In both instances, the megacolon manifested early (3.5 weeks of age and 12 weeks of age) and was found to be the result of severe hypoganglionosis of the distal colon (Figure 3.4). Nevertheless, since megacolon was only observed in 2 animals (of the 7 animals that were obtained for this genotype), a more detailed analysis was required to determine whether or not *Ets1* deficiency results in impaired gut innervation and, if a defect was observed, whether *Sox10* heterozygosity would exacerbate this phenotype.

To analyze the effect of *Ets1* deficiency on gut innervation, colons from animals from crosses between $Ets1^{+/-}$, $Sox10^{LacZ/+}$ and $Ets1^{+/-}::Sox10^{LacZ/+}$ mice were dissected and the innervation of the gut labeled via Acetylcholinesterase staining. For each colon, the nerve-free (white) area in 8 squares of 0.25mm^2 each, within a region located 15mm anterior to the anus, was measured using the ImageJ program (Appendix IV). The mean nerve-free area in colons from $Ets1^{+/-}::Sox10^{+/+}$ mice (n=6, mean=1.260±0.048mm^2) did not differ significantly (p=1.000) from that of colons from $Ets1^{+/-}::Sox10^{LacZ/+}$ mice (n=5, mean=1.291±0.075mm^2) (Figures 3.5 and 3.6). The mean nerve-free area of colons from $Ets1^{-/-}::Sox10^{+/+}$ mice (n=8, mean=1.402±0.048mm^2) was significantly larger than the mean nerve-free areas of colons from $Ets1^{+/-}::Sox10^{+/+}$ (p=0.001) and $Ets1^{+/-}::$

Sox10$^{LacZ/+}$ (p=0.010) mice (Figures 3.5 and 3.6). These results suggest that *Ets1* deficiency results in impaired gut innervation.

Since no significant difference in gut innervation was observed between *Ets1*$^{+/-}$*::Sox10*$^{+/+}$ and *Ets1*$^{+/-}$*::Sox10*$^{LacZ/+}$ mice, in order to further explore whether a synergistic genetic interaction exists between *Ets1* and *Sox10* in gut innervation, the nerve free areas of *Ets1*$^{-/-}$, *Sox10*$^{LacZ/LacZ}$ and *Ets1*$^{-/-}$*::Sox10*$^{LacZ/LacZ}$ mice would have to be compared. Unfortunately, this comparison could not be carried out because *Sox10*$^{LacZ/LacZ}$ mutants are embryonic lethal. Nonetheless, a comparison of the mean nerve-free areas in colons from *Ets1*$^{-/-}$*::Sox10*$^{LacZ/+}$ mice (n=5, mean=1.501±0.081mm^2) and *Ets1*$^{-/-}$*::Sox10*$^{+/+}$ mice revealed a significant difference between these two groups (p=0.017) (Figures 3.5 and 3.6, Appendix IV), with colons from *Ets1*$^{-/-}$*::Sox10*$^{LacZ/+}$ having a greater nerve-free area. These results support a potential genetic interaction between *Ets1* and *Sox10* in the development of enteric ganglia. The colons from the two *Ets1*$^{-/-}$*::Sox10*$^{LacZ/+}$ animals in which megacolon was detected were not included in this analysis because these were considered extreme cases.

3.4.4 Ets1 null mutants appear to display decreased Sox10 expression

The synergistic genetic interaction observed between *Ets1* and *Sox10* in double heterozygous mutants pointed to a potential functional interaction between these transcription factors in melanocyte development. Given that *Ets1* is required for *Sox10* expression in the chick cranial NC (Betancur et al., 2010), it is possible that it could also be an important regulator of *Sox10* expression in the mouse embryo. In order to visualize gross changes in *Sox10* expression in *Ets1* null mutants, embryos from intercrosses between *Ets1*$^{+/-}$*::Sox10*$^{LacZ/+}$ mice were harvested between E11.5 and E12.5 and *Sox10*

expression was analyzed via LacZ staining. At E11.5, *Sox10* expression appeared to be reduced in 75% of the *Ets1*$^{-/-}$ (n=4) embryos examined compared to *Ets1*$^{+/-}$ (n=3) (Figure 3.7) and *Ets1*$^{+/+}$ (n=3) (not shown) littermates. At E12.5, *Sox10* expression appeared to be reduced in 50% of *Ets1*$^{-/-}$ (n=6) embryos compared to heterozygous (n=9) (Figure 3.7) and wild type (n=3) (not shown) littermates. The apparent decrease in *Sox10* expression observed in *Ets1* null mutant embryos suggests that *Ets1* may regulate *Sox10* expression during embryonic development.

3.5 Discussion

The study of the transcriptional networks underlying the development of NC cell derivatives, and particularly of melanocytes, has been largely aided by the use of double heterozygous mouse mutants (Beechey et al., 1994, Cantrell et al., 2004, Stanchina et al., 2006, Diawakar et al., 2008, Guo et al., 2010, Hou et al., 2010). In the case of melanocytes, the use of double heterozygous pigmentation mutants is well suited for the study of genetic interactions because of the ease with which these interactions can be analyzed by comparing the pigmentation phenotypes of double and single heterozygotes. The presence of a pigmentation defect in *Ets1* mutant mice points to the requirement of this transcription factor for proper melanocyte development; however, the mechanism via which *Ets1* acts to promote melanocyte development is currently unknown. We previously showed that the marked decrease in melanoblast numbers in *Ets1* null mutant embryos is caused, at least in part, by an increase in apoptosis, which suggests that *Ets1* is required for early melanoblast survival. Other genes required for melanoblast survival, include those that code for the transcription factors *Mitf*, *Sox10*, and *Pax3*, and for the signaling molecules *Edn3* and *Kitl*, and their receptors *Ednrb* and *Kit* (Silver et al., 2006).

Evidence from studies in the chick embryo pointed to a potential interaction between *Ets1* and *Sox10*. In the chick embryo, Ets1, along with Sox9 and c-Myb, directly binds to and activates a *Sox10* enhancer element that drives *Sox10* expression to cranial but not trunk or vagal NC cells (Betancur et al., 2010). Melanocytes are mostly derived from trunk NC cells, and currently there are no studies linking *Ets1* to *Sox10* expression in trunk NC cells; Nonetheless, the pigmentation defect observed in *Ets1* mutant mice, the importance of *Ets1* for melanoblast survival, and its role in the regulation of *Sox10* expression in the chick embryo, hinted to a potential genetic interaction between these two transcription factors in murine melanocyte development.

The study of genetic interactions can be influenced by the presence of genetic background modifiers, which can affect the penetrance of the phenotype in question (Cantrell et al., 2004). For this reason, genetic interactions should be studied across more than a single generation, particularly if different genetic strains are being used. The potential effect that background modifiers can exert upon a given phenotype is illustrated by studies describing both the absence and presence of a genetic interaction between *Sox10* and the Endothelin receptor b (*Ednrb*) in melanocyte development. In one study, mice heterozygous for both *Ednrb* and *Sox10* ($Ednrb^{s\text{-}l/+}$;$Sox10^{Dom/+}$), were found to exhibit belly spots that were not significantly larger than the belly spots of the single heterozygotes. In this study, progeny from a single generation of mice were analyzed and a lack of a synergistic interaction between *Sox10* and *Ednrb* was reported (Hakami et al., 2006). In a subsequent study, progeny from crosses between $Ednrb^{s\text{-}l/+}$ and $Sox10^{LacZ/+}$ mice were analyzed for three generations. In the first generation, a genetic interaction was not observed between *Sox10* and *Ednrb*; however, a synergistic genetic interaction

became apparent in the second and third generations, in which double heterozygous mice had belly spots that were significantly larger than would be expected from the sum of the areas of the belly spots present in the single heterozygous mice (Lowenstein, 2009). It is likely that in the first study, which reported a lack of a genetic interaction between *Ednrb* and *Sox10*, strain-specific loci decreased the penetrance of the hypopigmentation phenotype that results from combined *Ednrb* and *Sox10* heterozygosity, masking the existence of an interaction between these genes.

To begin dissecting a potential interaction between *Ets1* and *Sox10*, the pigmentation phenotypes of single heterozygotes were compared to those of double heterozygotes. Three generations of mice were examined in order to take into account the potential effect of background modifiers, since the $Ets1^{+/-}$ and $Sox10^{LacZ/+}$ mice were generated in different genetic backgrounds. A significant increase in the frequency of belly spot appearance was observed in $Ets1^{+/-}$*::*$Sox10^{LacZ/+}$ mice compared to single heterozygotes. These results were consistent throughout the 3 generations examined, with almost all double heterozygous mice having belly spots, compared to 40-50% of single heterozygotes. Analysis of the hypopigmentation areas of $Ets1^{+/-}$, $Sox10^{LacZ/+}$ and $Ets1^{+/-}$*::*$Sox10^{LacZ/+}$ mice revealed that the mean areas of hypopigmentation in double heterozygous mice were significantly larger than the sum of the areas of hypopigmentation in the single heterozygous progeny. These results were consistent and significant across all generations and indicate that a synergistic genetic interaction exists between *Ets1* and *Sox10*. The fact that the results were consistent across all generations suggests that the presence of strain-specific alleles did not seem to significantly affect the penetrance of the phenotype in these mice.

In addition for being required for proper melanocyte development, *Sox10* is also required for the development of enteric ganglia (Southard-Smith et al., 1998). In the spontaneous embryonic lethal $Sox10^{Dom/Dom}$ mutant mouse, NC cells fail to colonize the gut as a result of increased apoptosis (Kapur, 1999). This may be the result, at least in part, of decreased activation of the tyrosine kinase receptor c-Ret, which is also required for the development of enteric ganglia, and has been shown to be activated by Pax3 and Sox10 (Lang et al., 2000). The requirement of *Sox10* for the survival of enteric ganglia precursors prompted the examination of the guts of *Ets1* null mutant mice to determine whether *Ets1* deficiency would negatively affect gut innervation. Close examination of the guts of $Ets1^{-/-}$::$Sox10^{+/+}$ and $Ets1^{+/-}$::$Sox10^{+/+}$ mice revealed a significantly larger nerve-free area in $Ets1^{-/-}$::$Sox10^{+/+}$ mutant mice compared to $Ets1^{+/-}$::$Sox10^{+/+}$, suggesting that *Ets1* may play a role in the development of enteric ganglia during development. Given the role of *Ets1* in NC cell survival (Figure 2.5), it is possible that the decreased innervation observed in *Ets1* null mutant mice may be the result of a reduction in the number of NC cells available to colonize the distal colon.

Throughout the course of the present study, two instances of hypoganglionic megacolon were observed in *Ets1* null mutant mice, which were also heterozygous for *Sox10* ($Ets1^{-/-}$::$Sox10^{LacZ/+}$). Although no significant difference in the extent of gut innervation was observed between $Ets1^{+/-}$::$Sox10^{+/+}$ and $Ets1^{+/-}$::$Sox10^{LacZ/+}$ mice, $Ets1^{-/-}$::$Sox10^{LacZ/+}$ mice were found to have colons with greater nerve-free areas compared to $Ets1^{-/-}$ mice carrying both copies of the wild type *Sox10* allele. The significant decrease in gut innervation observed in $Ets1^{-/-}$::$Sox10^{LacZ/+}$ mice compared to $Ets1^{-/-}$::$Sox10^{+/+}$ may be the result of a synergistic interaction between *Ets1* and *Sox10*. In light of the absence

of a significant difference in gut innervation between *Ets1*$^{+/-}$*::Sox10*$^{+/+}$ and *Ets1*$^{+/-}$*::Sox10*$^{LacZ/+}$ mice and the embryonic lethality of *Sox10*$^{LacZ/LacZ}$ mutants, it was not possible to directly test the presence of a synergistic interaction by using double null mutant mice. Nevertheless, the decrease in gut innervation observed in *Ets1*$^{-/-}$*::Sox10*$^{LacZ/+}$ mice compared to *Ets1*$^{-/-}$*::Sox10*$^{+/+}$ mice and the presence of hypoganglionic megacolon in 2 of 7 *Ets1*$^{-/-}$*::Sox10*$^{LacZ/+}$ mice examined suggests that *Ets1* and *Sox10* may interact in the development of enteric ganglia. Our previous finding that *Ets1* plays a role in promoting the survival of melanoblasts and NC cells is also consistent with this hypothesis (Figure 2.3 and Figure 2.5).

A decrease in enteric progenitor cell survival has been described in *Sox10* heterozygous mice that are also homozygous for the mutant *Ednrb*$^{sl/sl}$ (*piebald*) or *Edn3*$^{ls/ls}$ (*lethal spotting*) alleles. Compared to single mutants, these animals show a dramatic decrease in the number of enteric neuronal progenitor cells in the gut, which results from increased apoptosis in vagal neural crest cells prior to the time when they begin to invade the gut at E9.5-10 (Stanchina et al., 2006). In *Sox10* homozygous mutants increased apoptosis of enteric ganglia precursor cells, also results in the failure of these cells to colonize the gut (Kapur, 1999). Additional cell survival assays to compare the numbers of dying enteric ganglia precursor cells in *Ets1*$^{-/-}$*::Sox10*$^{+/+}$ and *Ets1*$^{-/-}$*::Sox10*$^{LacZ/+}$embryos are needed to determine whether *Ets1* and *Sox10* work together to promote the survival of these cells.

Synergistic genetic interactions may or may not indicate the presence of a functional interaction between the genes in question. The apparent decrease in *Sox10* expression observed in about half of all E11.5 and E12.5 *Ets1*$^{-/-}$ embryos compared to

Ets1$^{+/-}$ and wild type littermates suggests that *Ets1* may play a role in the regulation of *Sox10* expression. However, this apparent decrease in expression may also be the result of a decrease in the number of NC cell derivatives, thus further studies are needed to determine whether *Ets1* regulates embryonic *Sox10* expression. In order to gain a better understanding of the underlying functional interaction that may exist between *Ets1* and *Sox10*, the ability of wild type and mutated Ets1 protein to activate the *Sox10*-MCS4 enhancer, an enhancer critical for *Sox10* expression in mouse melanocytes (Antonellis et al., 2008) will be analyzed via luciferase reporter assay in the next chapter.

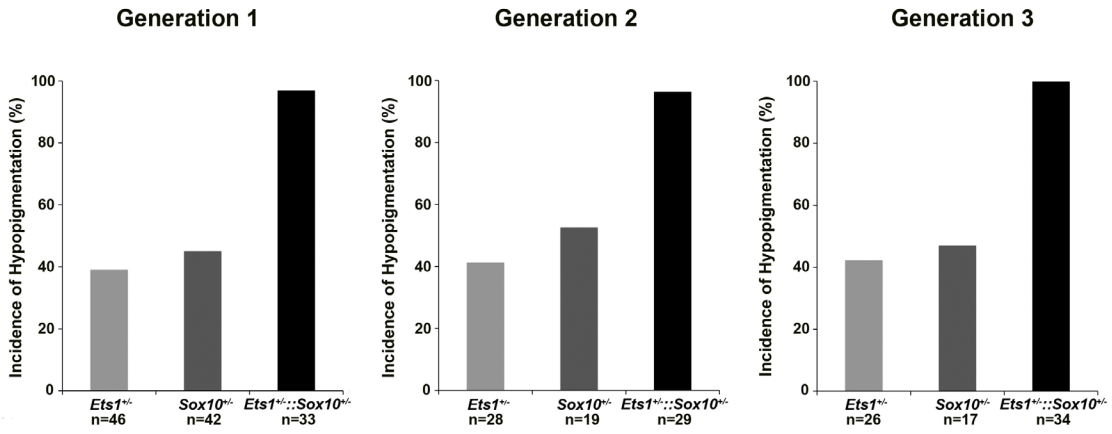

Figure 3.1. *Ets1* and *Sox10* double heterozygosity increases hypopigmentation frequency. The incidence of hypopigmentation in *Ets1*$^{+/-}$*::Sox10*$^{LacZ/+}$ mice was significantly greater than the incidence of hypopigmentation in *Ets1*$^{+/-}$ and *Sox10*$^{LacZ/+}$ mice ($p<0.001$) for all three generations analyzed.

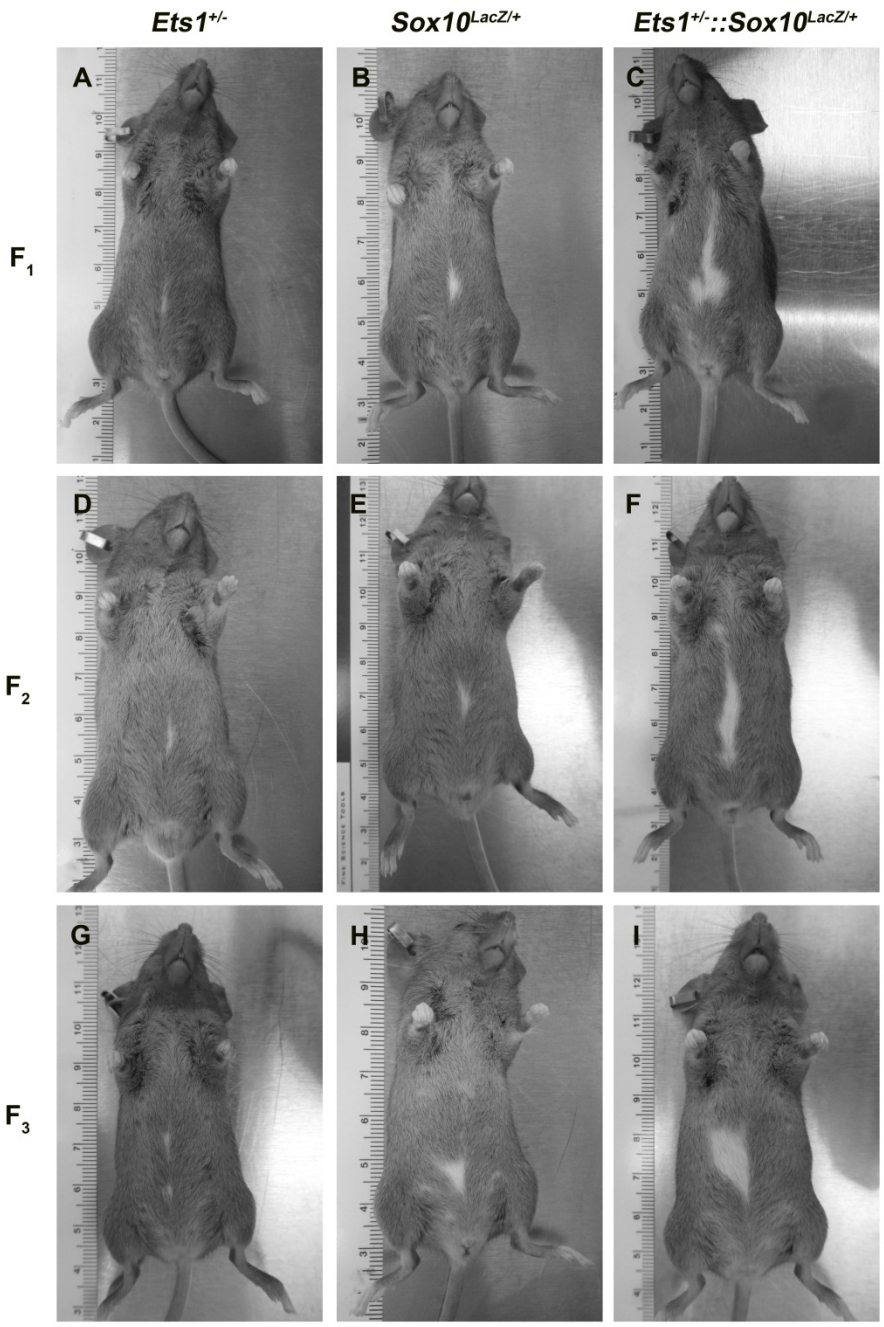

Figure 3.2. *Ets1* and *Sox10* double heterozygotes display increased ventral hypopigmentation compared to single heterozygotes. Representative pictures of ventral hypopigmentation for each genotype show that double heterozygous mice had larger areas of hypopigmentation compared to *Ets1* and *Sox10* single heterozygotes (F_1 = 1st generation, F_2 = 2nd generation, F_3 = 3rd generation).

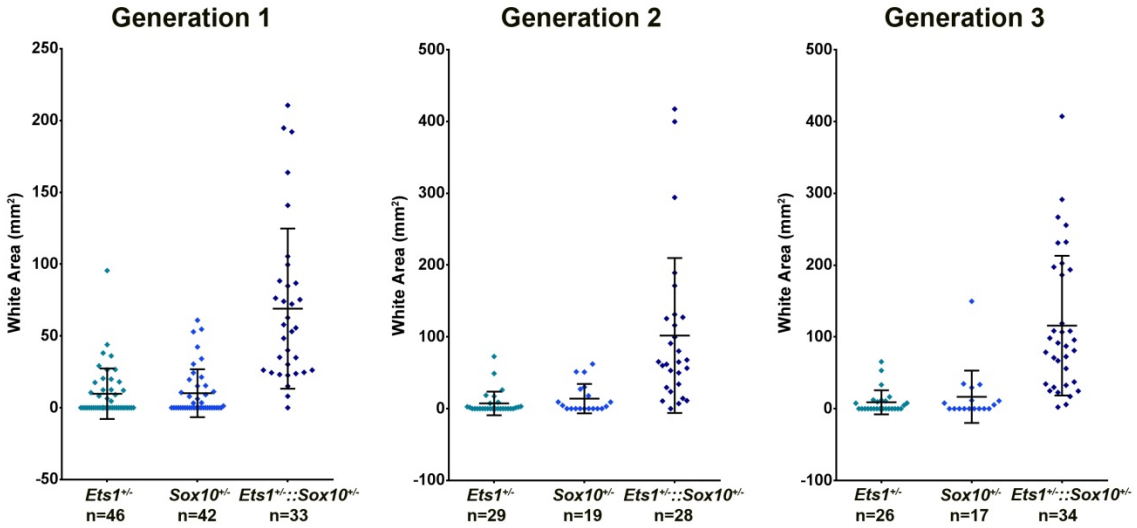

Figure 3.3. *Ets1* and *Sox10* double heterozygosity results in an aggravated hypopigmentation phenotype. The areas of hypopigmentation of $Ets1^{+/-}::Sox10^{LacZ/+}$ mice were significantly greater than the sum of the areas of hypopigmentation of $Ets1^{+/-}$ and $Sox10^{LacZ/+}$ mice ($p<0.001$) in all three generations analyzed (Appendix III).

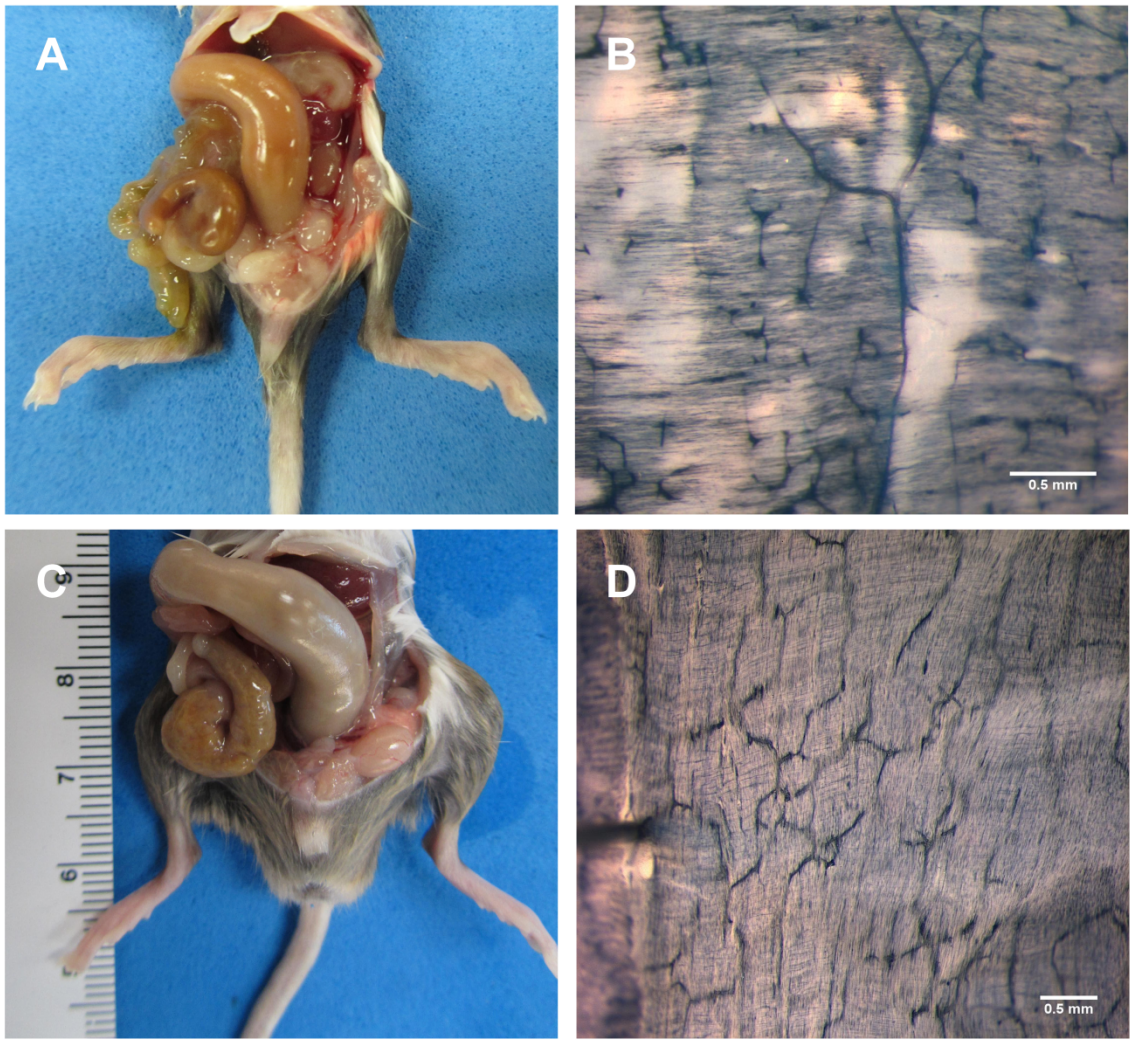

Figure 3.4. Aganglionic megacolon in *Ets1*$^{-/-}$*::Sox10*$^{LacZ/+}$ mice. (A) 3.5-week-old and (C) 3 month old *Ets1*$^{-/-}$*::Sox10*$^{LacZ/+}$ mice exhibiting megacolon as a result of impaired innervation of the distal colon (B & D, respectively) (Magnifications B=35x, D=25x).

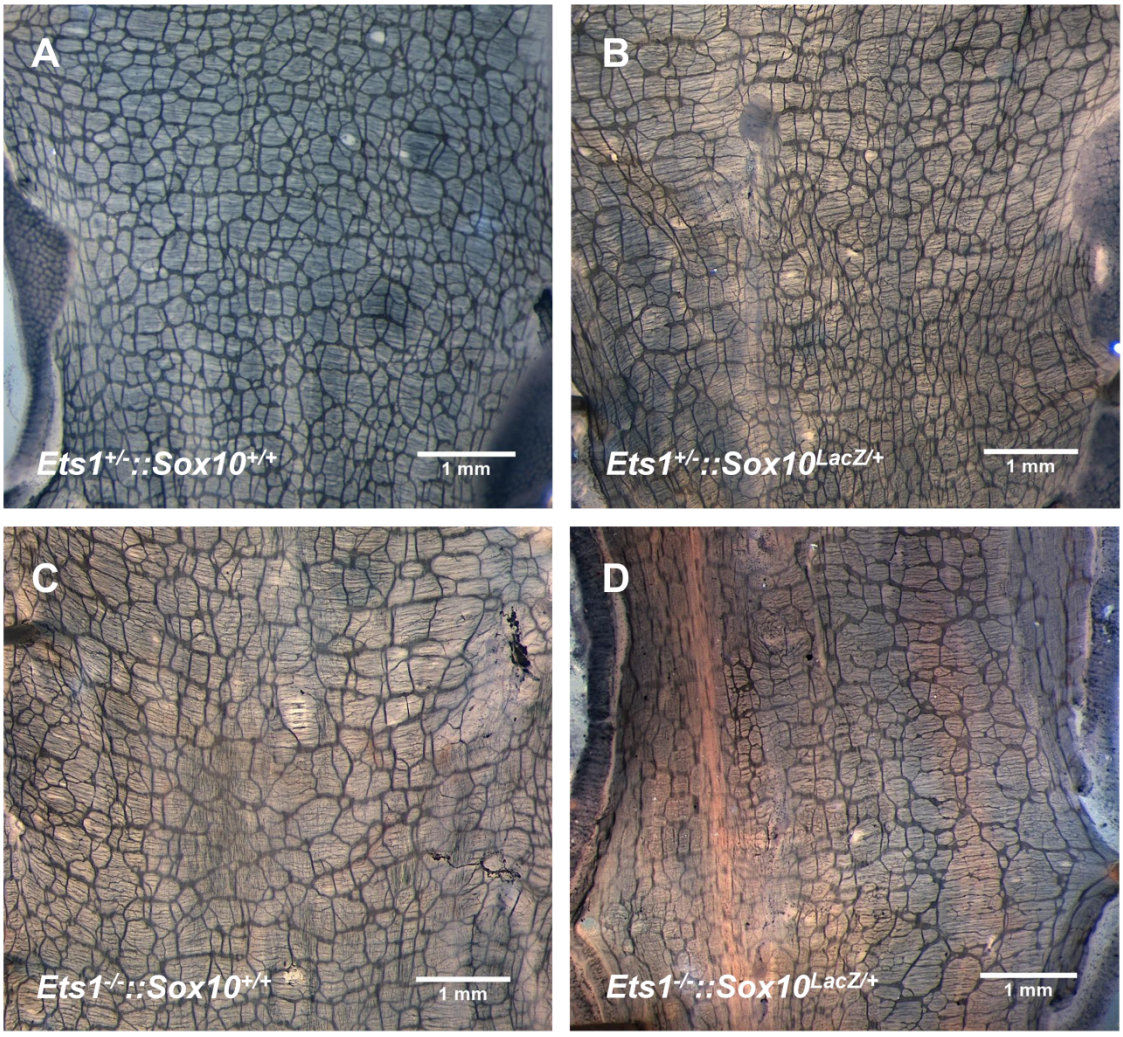

Figure 3.5. *Ets1* null mutants show decreased gut innervation. Representative images of colon innervation labeled via Acetylcholinesterase staining in colons from (A) *Ets1*$^{+/-}$*::Sox10*$^{+/+}$, (B) *Ets1*$^{+/-}$*::Sox10*$^{LacZ/+}$, (C) *Ets1*$^{-/-}$*::Sox10*$^{+/+}$, and (D) *Ets1*$^{-/-}$*::Sox10*$^{LacZ/+}$ mice. (Magnifications = 16x). Colons from *Ets1* null mutants (C & D) appear less innervated compared to colons from *Ets1* heterozygotes (A & B). (D) *Sox10* heterozygosity further exacerbates the hypoganglionic phenotype observed in *Ets1* null mutants.

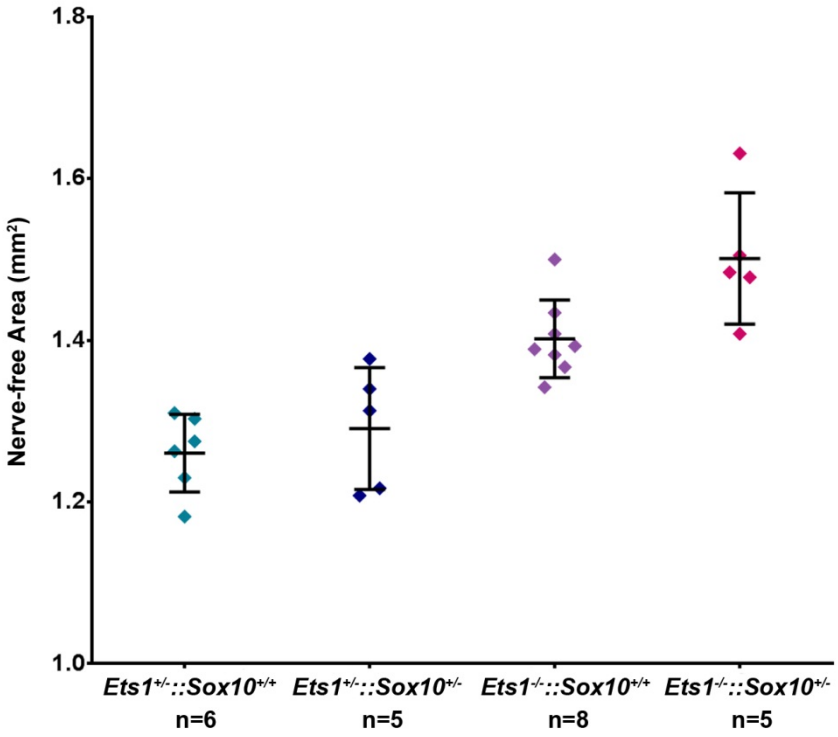

Figure 3.6. *Ets1* deficiency results in decreased gut innervation. Scatterplots showing the nerve-free areas (including means and standard deviations) in 2mm^2 regions of colons from *Ets1*$^{+/-}$*::Sox10*$^{+/+}$, *Ets1*$^{+/-}$*::Sox10*$^{LacZ/+}$, *Ets1*$^{-/-}$*::Sox10*$^{+/+}$, and *Ets1*$^{-/-}$*::Sox10*$^{LacZ/+}$ mice. The mean nerve-free area in colons from *Ets1*$^{+/-}$*::Sox10*$^{+/+}$ mice did not differ significantly from that of *Ets1*$^{+/-}$*::Sox10*$^{LacZ/+}$ (p=1.000). The mean nerve-free area of colons from *Ets1*$^{-/-}$*::Sox10*$^{+/+}$ mice was significantly larger than the mean nerve-free areas of colons from *Ets1*$^{+/-}$*::Sox10*$^{+/+}$ (p=0.001) and *Ets1*$^{+/-}$*::Sox10*$^{LacZ/+}$ (p=0.010) mice. The mean nerve-free area of the colons from *Ets1*$^{-/-}$*::Sox10*$^{LacZ/+}$mice was significantly greater compared to that of *Ets1*$^{-/-}$*::Sox10*$^{+/+}$ mice (p=0.017).

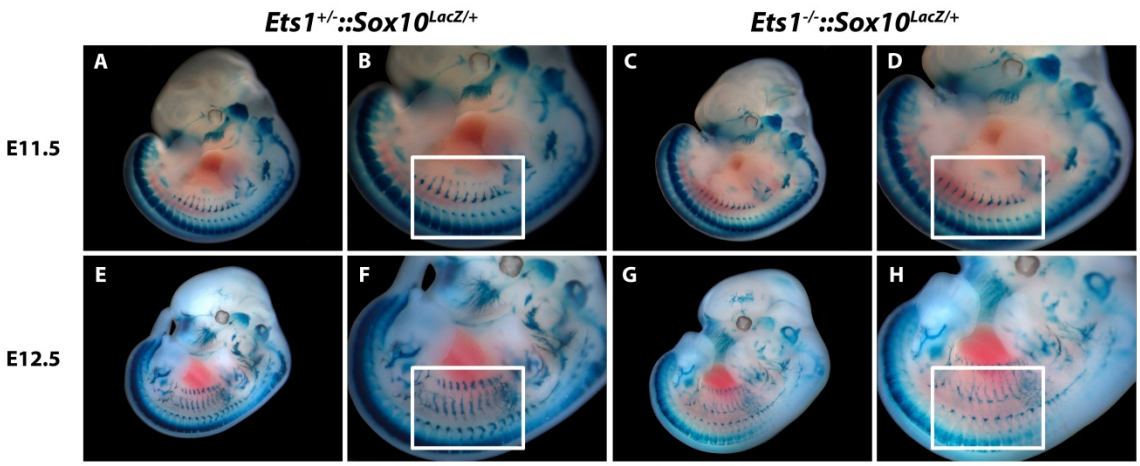

Figure 3.7. *Sox10* expression in *Ets1* mutant embryos. *Sox10* expression was visualized via LacZ staining in E11.5 (A-D) and E12.5 (E-H) embryos from intercrosses between *Ets1*$^{+/-}$*::Sox10*$^{LacZ/+}$ mice. At E11.5, *Sox10* expression appears to be reduced in 75% of *Ets1*$^{-/-}$ embryos (n=4) (C & D), compared to *Ets1*$^{+/-}$ (n=3) (A & B) and *Ets1*$^{+/+}$ (n=3) (not shown) littermates. At E12.5, *Sox10* expression appears to be reduced in 50% of *Ets1*$^{-/-}$ embryos (n=6) (G & H) compared to *Ets1*$^{+/-}$ (n=9) (E & F), and *Ets1*$^{+/+}$ (n=3) (not shown) littermates. (Magnifications: A & C= 16x, B & D= 25x, E & G= 12.5x, F & H= 21x).

3.6 References

Antonellis, A., Huynh, J., Lee-Lin, S.-Q., Vinton, R., Renaud, G., Loftus, S., Elliot, G., Wolfsberg, T., Green, E., McCallion, A., and Pavan, W.J. (2008). Identification of neural crest and glial enhancers at the mouse Sox10 locus through transgenesis in zebrafish. *PLoS genetics* 4, e1000174.

Beechey, C. V. and Harrison, M. A. (1994). A new spontaneous W allele, *W36H*. *Mouse Genome* 92, 502-502.

Betancur, P., Bronner-Fraser, M. and Sauka-Spengler, T. (2010). Genomic code for Sox10 activation reveals a key regulatory enhancer for cranial neural crest. *Proc. Natl. Acad Sci U.S.A.* 107, 3570–3575.

Britsch, S., Goerich, D., Riethmacher, D., Peirano, R., Rossner, M., Nave, K., Birchmeier, C. and Wegner, M. (2001). The transcription factor Sox10 is a key regulator of peripheral glial development. *Genes & development* 15, 66–78.

Cantrell, V., Owens, S., Chandler, R., Airey, D., Bradley, K., Smith, J. and Southard-Smith, E. (2004). Interactions between Sox10 and EdnrB modulate penetrance and severity of aganglionosis in the Sox10Dom mouse model of Hirschsprung disease. *Human molecular genetics* 13, 2289–2301.

Drees, B., Thorsson, V., Carter, G., Rives, A., Raymond, M., Avila-Campillo, I., Shannon, P. and Galitski, T. (2004). Derivation of genetic interaction networks from quantitative phenotype data. *Genome Biology* 6, R38.

Diwakar, G., Zhang, D., Jiang, S. and Hornyak, T. J. (2008). Neurofibromin as a regulator of melanocyte development and differentiation. *Journal of Cell Science* 121, 167-177.

Gariepy, C., Williams, S., Richardson, J.A., Hammer R.E., and Yanagisawa, M. (1998). Transgenic expression of the endothelin-B receptor prevents congenital intestinal aganglionosis in a rat model of Hirschsprung disease. *J. Clin. Invest* 102, 1092-1101.

Guo, X.-L., Ruan, H.-B., Li, Y., Gao, X. and Li, W. (2010). Identification of a novel nonsense mutation on the Pax3 gene in ENU-derived white belly spotting mice and its genetic interaction with c-Kit. *Pigment cell & melanoma research* 23, 252–262.

Hakami, R., Hou, L., Baxter, L. and Loftus, S., Southard-Smith, M.E., Incao, A., Cheng, J., and Pavan, W.J. (2006). Genetic evidence does not support direct regulation of EDNRB by SOX10 in migratory neural crest and the melanocyte lineage. *Mech Dev* 123, 124–134.

Hekimi, S., Bénard, C., Branicky, R. and Burgess, J., Hihi A.K. and Rea, S. (2001). Why only time will tell. *Mech Ageing Dev* 122, 571-594.

Herbarth, B., Pingault, V., Bondurand, N., Kuhlbrodt, K., Hermans-Borgmeyer, I., Puliti, A., Lemort, N., Goossens, M. and Wegner, M. (1998). Mutation of the Sry-related Sox10 gene in Dominant megacolon, a mouse model for human Hirschsprung disease. *Proc. Natl. Acad Sci U.S.A.* 95, 5161–5165.

Hodgkinson, C., Moore, K., Nakayama, A., Steingrímsson, E., Copeland, N., Jenkins, N. and Arnheiter, H. (1993). Mutations at the mouse microphthalmia locus are associated with defects in a gene encoding a novel basic-helix-loop-helix-zipper protein. *Cell* 74, 395–404.

Hou, L., Panthier, J. and Arnheiter, H. (2000). Signaling and transcriptional regulation in the neural crest-derived melanocyte lineage: interactions between KIT and MITF. *Development* 127, 5379–5389.

Kapur, R. P. (1999). Early death of neural crest cells is responsible for total enteric aganglionosis in Sox10(Dom)/Sox10(Dom) mouse embryos. *Pediatric and developmental pathology* 2, 559–569.

Lang, D., Chen, F., Milewski, R., Li, J., Lu, M. and Epstein, J.(2000). Pax3 is required for enteric ganglia formation and functions with Sox10 to modulate expression of c-ret. *The Journal of clinical investigation* 106, 963–971.

Lowenstein, M. (2009). Interactions between Endothelin Receptor B and Transcription Factors Sox10 and Pax3 in the Melanocyte Lineage. FIU Electronic Theses and Dissertations. Paper 117. http://digitalcommons.fiu.edu/etd/117

Mani, R., Onge, R., Hart, J.L., Giaever, G. and Roth, F.P. (2008). Defining genetic interaction. *Proc. Natl. Acad Sci U.S.A.* 105, 3461–3466.

McGill, G. G., Horstmann, M., Widlund, H. R., Du, J., Motyckova, G., Nishimura, E. K., Lin, Y.-L., Ramaswamy, S., Avery, W. and Ding, H.-F. (2002). Bcl2 Regulation by the Melanocyte Master Regulator Mitf Modulates Lineage Survival and Melanoma Cell Viability. *Cell* 109, 707-718.

Pérez-Pérez, J., Candela, H. and Micol, J. (2009). Understanding synergy in genetic interactions. *Trends in genetics* 25, 368–376.

Pingault, V., Bondurand, N., Kuhlbrodt, K., Goerich, D., Préhu, M., Puliti, A., Herbarth, B., Hermans-Borgmeyer, I., Legius, E., Matthijs, G., et al. (1998). SOX10 mutations in patients with Waardenburg-Hirschsprung disease. *Nature genetics* 18, 171–173.

Potterf, S., Mollaaghababa, R., Hou, L., Southard-Smith, E., Hornyak, T., Arnheiter, H. and Pavan, W. (2001). Analysis of SOX10 function in neural crest-derived melanocyte development: SOX10-dependent transcriptional control of dopachrome tautomerase. *Developmental Biology* 237, 245–257.

Sánchez-Mejías, A., Watanabe, Y., Fernández, R. M., López-Alonso, M., Antiñolo, G., Bondurand, N. and Borrego, S. (2010). Involvement of SOX10 in the pathogenesis of Hirschsprung disease: report of a truncating mutation in an isolated patient. *Journal of Molecular Medicine* 88, 507-514.

Silver, D., Hou, L. and Pavan, W. (2006). The genetic regulation of pigment cell development. Georgetown: Landes Biosciences, 155-169.

Southard-Smith, E., Kos, L. and Pavan, W. (1998). Sox10 mutation disrupts neural crest development in Dom Hirschsprung mouse model. *Nature Genetics* 18, 60–64.

Stanchina, L., Baral, V., Robert, F., Pingault, V., Lemort, N., Pachnis, V., Goossens, M. and Bondurand, N. (2006). Interactions between Sox10, Edn3 and Ednrb during enteric nervous system and melanocyte development. *Developmental biology* 295, 232–249.

Wen, B., Chen, Y., Li, H., Wang, J., Shen, J., Ma, A., Qu, J., Bismuth, K., Debbache, J., Arnheiter, H., and Hou, L. (2010). Allele-specific genetic interactions between Mitf and Kit affect melanocyte development. *Pigment cell & melanoma research* 23, 441–447.

CHAPTER IV

THE TRANSCRIPTION FACTOR Ets1 ACTIVATES THE MELANOCYTE LINEAGE-SPECIFIC *Sox10*-MCS4 ENHANCER

IV. THE TRANSCRIPTION FACTOR Ets1 ACTIVATES THE MELANOCYTE LINEAGE-SPECIFIC *Sox10*-MCS4 ENHANCER

4.1. Abstract

Phenotypic analysis of double heterozygous mutants for the transcription factors *Ets1* and *Sox10* revealed a synergistic genetic interaction between these genes in melanocyte development. The presence of this synergistic genetic interaction hinted to a potential functional interaction between *Ets1* and *Sox10*. To characterize the nature of this interaction, the ability of Ets1 to activate the *Sox10*-MCS4 enhancer, which was previously shown to direct *Sox10* expression in melanoblasts and melanocytes, was analyzed via luciferase reporter assay. In the mouse melanoma cell line B16, Ets1 was able to activate the *Sox10*-MCS4 enhancer, suggesting a possible role for *Ets1* in the regulation of *Sox10* expression. Consistent with *Ets1* function in melanocyte development, whole exome sequence analysis of the spontaneous mouse mutant *variable spotting* at the NIH Sequencing Center identified a G-to-A nucleotide transition in exon 3 of the *Ets1* gene, which results in a missense Glycine to Glutamate mutation at amino acid 102 (G102E) of the Ets1 protein. We determined that this results in a hypomorphic mutation as in vitro luciferase reporter assay demonstrated a 2-fold decrease in the activation of the *Sox10*-MCS4 enhancer compared to wild type Ets1 protein. The ability of Ets1 to activate the *Sox10*-MCS4 enhancer and the effect of the *variable spotting* mutation on *Sox10*-MCS4 activation suggest that Ets1 may act as a regulator of *Sox10* expression during melanocyte development in the mouse embryo.

4.2. Introduction

The transcription factor *Sox10* is essential for the development of various neural crest (NC) cell-derived structures during vertebrate embryogenesis. During development, *Sox10* is expressed in migrating NC cell derivatives, which include the cranial, dorsal root, sympathetic, and enteric ganglia, as well as the melanocyte precursors, or melanoblasts (Southard-Smith et al., 1998). The importance of *Sox10* in the development of NC-derived cell lineages was first recognized in the spontaneous *Dominant megacolon* (*Dom*) mouse mutant. $Sox10^{Dom}$ mutants harbor a frameshift mutation in *Sox10* that results in a truncated protein (Herbarth et al., 1998, Southard-Smith et al., 1998). $Sox10^{Dom}$ heterozygotes display ventral hypopigmentation and aganglionic megacolon (Herbarth et al., 1998, Southard-Smith et al., 1998; Kapur, 1999). Similarly, in humans, *Sox10* mutations have been associated with Waardenburg Syndrome type IV (WS4), which is characterized by pigmentation defects, congenital deafness, and aganglionosis of the distal colon, or Hirschsprung's disease (Tachibana et al., 2003).

Neural-crest derived structures can be found in $Sox10^{Dom/Dom}$ and in the genetically engineered $Sox10^{LacZ/LacZ}$ mouse mutants, indicating that *Sox10* is not required for the initial specification of NC cells (Southard-Smith et al., 1998; Britsch et al., 2001). In the absence of *Sox10*, early NC-derived structures, such as the cranial ganglia, are able to form; however, severe morphological alterations in these structures become apparent by E10.5 (Herbarth et al., 1998; Southard-Smith et al., 1998). The loss of certain NC-derived structures in $Sox10^{Dom/Dom}$ and $Sox10^{LacZ/LacZ}$ embryos has been attributed to increased apoptosis, because significantly larger numbers of dying migrating NC and dorsal root ganglia cells are observed in $Sox10^{Dom/Dom}$ mice (Southard-Smith et al., 1998). The

absence of enteric ganglia in the guts of *Sox10*$^{Dom/Dom}$ mice has also been attributed to increased apoptosis because a large number of apoptotic cells can be detected in areas containing NC cells prior to the time when they colonize the gut (Kapur, 1999). The increased apoptosis observed in migratory NC cells in *Dom* homozygous mutants suggests that *Sox10* is essential for NC cell survival (Mollaaghababa et al., 2003).

In addition to being required for NC cell survival, Sox10 is also required for the final specification of melanocytes and glia. Working in cooperation with the transcription factor Paired Box 3 (Pax3), Sox10 has been shown to bind to and activate the expression of the Microphthalmia- associated transcription factor (*Mitf*), which is required for the terminal differentiation of melanoblasts and for the activation of genes required for melanin synthesis (Bondurand et al., 2000, Potterf et al., 2000). In in vitro studies, Sox10 has also been shown to regulate the transcription of genes required for melanin synthesis, including Dopachrome tautomerase (*Dct*), and Tyrosinase (*Tyr*) (reviewed in Harris et al., 2010).

Although many transcriptional targets of *Sox10* have been identified, the various aspects of *Sox10* regulation are only now beginning to be understood. The *Sox10* promoter, which has not been well characterized, does not direct the expression of *Sox10* to most of its typical expression sites (Deal et al., 2006). However, a total of 14 multiple conserved sequences (MCS) that can drive *Sox10* expression to various cell lineages have been identified (Antonellis et al., 2006, Deal et al., 2007, Antonellis et al., 2008). A subset of these sequences was first identified by mutation analysis of the transgene-insertion *Sox10*^{Hry} mutant, a mouse model of WS4. In this mutant a 16kb area located 47kb upstream of *Sox10* is deleted (Antonellis et al., 2008). This deletion severely

impairs but does not completely abrogate *Sox10* expression, suggesting that this 16kb region contains cis-regulatory elements necessary for *Sox10* expression. Of these elements, *Sox10*-MCS1c, *Sox10*-MCS4, *Sox10*-MCS5, *Sox10*-MCS7, and *Sox10*-MCS9 can drive reporter gene expression in cultured melanocytes. Furthermore, both *Sox10*-MCS4 and *Sox10*-MCS7 are able to recapitulate *Sox10* expression *in vivo*, in almost all NC-derived structures. These enhancers contain binding sites for the SoxE family of transcription factors, which bind as dimers and include Sox8, Sox9 and Sox10 (Antonellis et al., 2008). Recent studies have shown that both Sox9 and Sox10 are able to bind to mouse *Sox10* enhancers. Other transcription factors that have been shown to bind to *Sox10* enhancers include Pax3, Activating protein 2 (AP2) and Lymphoid enhancer binding factor 1 (Lef1). Nevertheless, the ability of Sox9, Sox10, Pax3, AP2 and Lef1 to transcriptionally activate *Sox10* has not been evaluated (reviewed in Harris et al., 2010).

In the avian system, two *Sox10* enhancers have been identified approximately 1kb downstream of the *Sox10* coding region. Together, these enhancers, termed Sox10E1 and Sox10E2, are able to recapitulate *Sox10* expression in the chick embryo. Sox10E1 is active in migrating vagal and trunk NC cells, while Sox10E2 acts earlier in cranial NC cells. The regulatory activity of Sox10E2 is dependent on binding by the transcription factors Ets1, Sox9, and c-Myb; however, these factors do not appear to be required for Sox10E1 activity. In vivo, Ets1, Sox9, and c-Myb were also found to be required for endogenous *Sox10* expression in delaminating and migrating NC cells in the cranial neural tube region. In the chick embryo, *Ets1* is not normally expressed in trunk NC cells; however, ectopic *Ets1* expression can drive reporter gene expression, via Sox10E2 activation, in trunk NC cells (Betancur et al., 2010). Although in the chick, *Ets1* is not

expressed in the trunk NC, studies in the mouse embryo have reported *Ets1* expression not only in cranial NC cells (Kola et al., 1993) but also in migrating trunk NC cells (Vandenbunder et al., 1989).

Phenotypic analysis of double heterozygous mutants for the transcription factors *Ets1* and *Sox10* revealed that a synergistic genetic interaction exists between these genes. The presence of a synergistic genetic interaction between *Ets1* and *Sox10* may be the result of an underlying functional interaction. One possibility regarding the nature of this interaction, would be Ets1 acting as a regulator of *Sox10* expression. Given the findings in the chick embryo, where Ets1 regulates *Sox10* expression in the cranial NC, we sought to test whether a similar relationship exists between *Ets1* and *Sox10* in the mouse by studying the ability of wild type and mutated Ets1 protein to activate a *Sox10* regulatory region. The *Sox10*-MCS4 enhancer was chosen as a possible target for Ets1, because this enhancer is critical for *Sox10* expression in melanocytes.

4.3. Materials and methods

4.3.1. Mapping of Ets1 binding sites in the Sox10-MCS4 and Sox10-MCS7enhancers

The coordinates of the *Sox10*-MCS4 and *Sox10*-MCS7 enhancers were obtained from Antonellis et al., 2008. The coordinates given in this study are from the February 2006 University of California at Santa Cruz (UCSC) Genome Browser Mouse assembly. In order to obtain the appropriate *Sox10*-MCS4 and *Sox10*-MCS7 sequences, the coordinates were converted using BLAST analysis and the UCSC Mouse BLAT Genome search, which allows alignment to previous genome assemblies. The coordinates for *Sox10*-MCS4 and *Sox10*-MCS7 from the February 2006 UCSC Genome Browser Mouse assembly were chr15:79,020,080–79,020,899 and chr15:79,040,107–79,040,404,

respectively. These coordinates were found to correspond to chr15:79,023,255-79,024,074 and chr15:79,043,282-79,043,579 of NCBI sequence NC_000081.5, for *Sox10*-MCS4 and *Sox10*-MCS7, respectively.

Once the correct coordinates were identified, the 820bp sequence of *Sox10*-MCS4 and the 298bp sequence of *Sox10*-MCS7 were analyzed for potential Ets1 binding sites using the MatInspector program (Genomatix, Inc), which locates transcription factor binding sites within a sequence by using a library of matrix descriptions for these binding sites.

4.3.2 Cell culture

The B16-F10 (B16 hereafter) mouse melanoma cell line was purchased from ATCC (CRL-6322, ATCC). Cells were maintained in Dubelcco's Modified Eagle's Medium (DMEM) (Cellgro), supplemented with 10% Fetal Bovine Serum (FBS), 100 U/ml penicillin, and 100 U/ml streptomycin (all from Thermo Scientific), at 37˚C in 5% CO_2.

4.3.3 Plasmid constructs

The *Ets1* overexpression vector (pCMV-HA-Ets1) and the pCMV-HA empty vector (Clontech) were gifts from Dr. Satrajit Sinha (State University of New York (SUNY) at Buffalo, Buffalo, NY). The pCMV-HA-Ets1 vector contains a Hyaluronic acid (HA)-tagged version of the full length mouse *Ets1* coding sequence (Nagarajan et al., 2009). The *Sox10*-MCS4 luciferase vector (*Sox10*-MCS4 fragment in pLGF-E1b vector) was a gift from Dr. William J. Pavan (National Institutes of Health (NIH), Bethesda, MD). This vector contains the *Sox10*-MCS4 enhancer, which was shown to drive expression to melanocytes, upstream of a minimal promoter (p1EB) which directs

basal luciferase expression (Antonellis et al., 2008). The pRL-TK wild type Renilla luciferase control vector (Promega) was a gift from Dr. Erasmo Perera (Florida International University (FIU), Miami, FL). All plasmids were transformed into *Escherichia coli* Dh5α competent cells (Life Technologies) and glycerol stocks were prepared (Appendix I). Plasmids were purified from overnight culture using the QIAprep Spin Miniprep Kit (Qiagen). Ethanol precipitation was carried out to purify and concentrate plasmids to be used for transfections (Appendix V).

4.3.4 Sequencing the variable spotting mutation

DNA samples from 4 *variable spotting* mutant mice (2 homozygous and 2 heterozygous) were purchased from The Jackson Laboratory (Bar Harbor, Maine) by our collaborator (Dr. William J. Pavan, NIH, Bethesda, MD) and sent to us for further analysis. Sequencing of DNA from all 4 *variable spotting* mutant mice was carried out using the forward primer 5'- AAGGTGTAGAGTAACTAGCATCGTCAG, or the reverse primer 5'- AACTCCTAAGGCAGAGAAGAAAATAAG. Sequencing was carried out at the Florida International University DNA Core Facility (Florida International University, Miami, FL). Sequences were analyzed using the Applied Biosystems Sequence Scanner v1.0 software (Applied Biosystems) and sequence alignments against the *Mus musculus* genomic database were carried out using the megablast algorithm (for highly similar sequences) via the Nucleotide BLAST server (NCBI, NIH).

4.3.5 Site-directed mutagenesis

The mutant *Ets1* overexpression vector (pCMV-HA-Ets1Mut) was prepared from the PCMV-HA-Ets1 vector, using the Phusion Site-Directed Mutagenesis Kit (Thermo

Scientific), following the manufacturer's instructions. The High Performance Liquid Chromatography (HPLC)-purified primers 5'-TCTGTATGAGTGAAGCAGCACTGTG and 5'-CACAGTGCTGCTTCACTCATACAGA, which contain the desired G647A mutation (corresponding to G305A in the open reading frame (ORF) of *Ets1*, Ref Seq NM_011808.2) flanked by 11 non-mutated nucleotides were used to insert the mutation into the *Ets1* ORF via Polymerase Chain Reaction (PCR) (25 cycles of, 98˚C for 10s, 64˚C for 30s, 72˚C for 120s). The primers were designed to anneal back to back to the plasmid and were phosphorylated at the 5' end in order to eliminate the need of a separate phosphorylation step prior to ligation. A total of 500pg of plasmid were used for the PCR reaction and the amount of PCR product was evaluated via gel electrophoresis with DNA standards of various concentrations. The resulting PCR product was ligated for 5 minutes at room temperature and transformed into *Escherichia coli* Dh5α competent cells (Life Technologies) (Appendix I). Overnight cultures were prepared from selected colonies and the plasmid was purified from these cultures using the QIAprep Spin Miniprep Kit (Qiagen). The purified plasmid was sequenced to confirm the presence of the mutation using the primers: 5'-CAGACACCTTGCAGACAGACTACT, 5'-CACAGTGCTGCTTCACTCATACAGA, and 5'-GGTGAGGCGGTCACAACTAT. Ethanol precipitation was carried out to purify and concentrate the plasmid to be used for transfections (Appendix V).

4.3.6 Plasmid DNA transfections and luciferase assay

Approximately 1.5 x 10^5 B16 cells were seeded in antibiotic-free cell culture media, into each well of a 12 well plate (CytoOne), roughly 24 hours prior to transfection. Once cells had reached 70-90% confluency they were co-transfected with

0.5µg/well *Sox10*-MCS4 luciferase reporter vector, 0.5µg/well pCMV-HA-Ets1, or pCMV-HA-Ets1Mut or pCMV-HA empty vector, and 0.1µg/well pRL-TK Renilla luciferase control vector. For each well, plasmid DNA was diluted in 50µl of Opti-MEM I (Invitrogen). For each well, 4 µl of the lipid transfection reagent Lipofectamine 2000 (Invitrogen) were diluted in 50µl of Opti-MEM I. The diluted DNA and diluted Lipofectamine reagent were incubated 5 minutes at room temperature. After 5 minutes, the diluted DNA was combined with the diluted Lipofectamine and incubated 30 minutes at room temperature. 100µl of lipid-DNA complexes were added to each well in a drop-wise manner, evenly distributing drops throughout the well. Plates were gently rocked by hand for 20 seconds. Cells were incubated at 37˚C, 5% CO_2 for 48 hours. After 48 hours, the cells were gently washed with PBS (Thermo Scientific) and lysed with 1x Passive Lysis Buffer (Promega), for 15 minutes at room temperature with light rocking. For each well, 20µl of cell lysate were used to measure firefly and Renilla luciferase activities with the Dual Luciferase Reporter Assay System (Promega). Firefly and Renilla luciferase activities were measured using a TD-20/20 Luminometer (Turner Designs). For each experiment the ratio of firefly to Renilla luciferase activity was calculated. Three independent transfections were carried out, each one in triplicates.

4.3.7 Statistical analysis

The non-parametric Mann-Whitney U test was used to compare the mean luciferase activity in cells transfected with the *Ets1* overexpression vector to that of cells transfected with the empty PCMV-HA vector (data from 3 independent experiments carried out in triplicates). This test was also used to compare the mean relative luciferase activity in cells transfected with the *Ets1* overexpression vector to that of cells transfected

with the *Ets1* overexpression vector carrying the *variable spotting* mutation (data from 3 independent experiments carried out in triplicates).

4.4 Results

4.4.1 The Sox10-MCS4 and Sox10-MCS7 enhancers contain putative Ets1 binding sites.

Analysis of the 820bp sequence of the *Sox10*-MCS4 enhancer using the MatInspector software (Genomatix, Inc.) revealed the presence of 4 potential Ets1 binding sites (Table 4.1). One potential Ets1 binding site was identified within the 298bp *Sox10*-MSC7 sequence (ccgggagaGGAAcaaaaggtc, from 167 to 187 in the antisense strand, relative to the 5' end of the sense strand in *Sox10*-MCS7). The *Sox10*-MCS4 enhancer was chosen for further analysis because of the higher number of potential Ets1 binding sites present within this regulatory region.

4.4.2 Transactivation of the Sox10-MCS4 enhancer by Ets1

The ability of Ets1 to activate the *Sox10*-MCS4 enhancer was tested via luciferase reporter assay. Compared to cells transfected with the empty PCMV-HA vector, cells transfected with the *Ets1* overexpression vector (PCMV-HA-Ets1) showed significantly higher luciferase reporter activity ($p<0.001$) (Figure 4.1). The mean relative luciferase activity in cells transfected with the *Ets1* overexpression vector was 9.51, while in cells transfected with the empty vector this value was 1.41. This increase in the relative luciferase activity of the cells transfected with the *Ets1* overexpression vector corresponds to a 6.8 fold increase over the cells transfected with the empty vector.

4.4.3 Ets1 is the mutated gene in the spontaneous variable spotting mouse mutant

Spontaneous *variable spotting* mutant mice exhibit a similar phenotype to that of the *Ets1* mutant mice used in this study. Head blaze, white spotting of the tail and feet,

and ventral spotting, which may be large, occur sporadically in homozygous *variable spotting* (*vs/vs*) mice (Jackson Laboratories). On the other hand, the *Ets1* null mutant mice used in this study always have large belly spots and occasionally head blaze. As part of an exome sequencing project at the National Institutes of Health (NIH), a possible mutation within the ORF of *Ets1* was identified. The existence of this mouse mutant was brought to our attention by Dr. William J. Pavan (NIH, Bethesda, MD). Via direct sequencing of 4 *variable spotting* mutants, we confirmed a nucleotide G-to-A transition in exon 3 of the *Ets1* gene (Figure 4.2), which results in a missense Glycine to Glutamate mutation at amino acid 102 (G102E) of the Ets1 protein.

4.4.4 The variable spotting mutation results in decreased Sox10-MCS4 activation

In order to test whether the *variable spotting* mutation affects the ability of Ets1 to activate the *Sox10*-MCS4 enhancer, the mutation was inserted into the *Ets1* ORF via site-directed mutagenesis. A significant decrease in relative luciferase activity was observed in cells transfected with the *Ets1* overexpression vector carrying the *variable spotting* mutation compared to those transfected with the wild type *Ets1* overexpression vector ($p<0.001$) (Figure 4.3). This decrease corresponds to approximately a 50% reduction in *Sox10*-MCS4 enhancer activation and indicates that this mutation reduces but does not completely abrogate the ability of Ets1 to transactivate the *Sox10*-MCS4 enhancer.

4.5 Discussion

The proximal promoter region of *Sox10* dos not direct *Sox10* expression to cells where *Sox10* is typically expressed (Deal et al., 2006). A distant upstream region located approximately 47kb upstream of *Sox10* is able to recapitulate *Sox10* expression in vivo to most sites where *Sox10* is expressed during development (Antonellis et al., 2008).

Analysis of *Sox10*-MCS4, one of the enhancers located in this region and which drives expression to melanocytes, revealed the presence of four potential binding sites for Ets1 suggesting the possibility that Ets1 could regulate *Sox10* expression via this enhancer. Through luciferase reporter assays we showed that Ets1 is able to drive reporter gene expression through *Sox10*-MCS4. Additional experiments are needed to determine whether Ets1 activates this enhancer by directly binding to it. Mutation or deletion of the putative Ets1 binding sites within *Sox10*-MCS4, along with Chromatin Immunoprecipitation (ChIP) assays may provide some insight into whether the effect of Ets1 is mediated by direct binding to the *Sox10*-MCS4 enhancer. Nevertheless, regardless of whether or not Ets1 binds directly to *Sox10*-MCS4, its ability to drive expression through this enhancer implies that, as in the avian system, *Ets1* may regulate *Sox10* expression.

The presence of a spontaneous mutation in *Ets1* which results in a pigmentation phenotype provided the opportunity to validate the finding that Ets1 can drive expression through *Sox10*-MCS4. Although the G102E Ets1 mutant protein is able to activate the *Sox10*-MCS4 enhancer, reporter gene expression is reduced by approximately 50% compared to the wild type Ets1 protein (Figure 4.3). These results suggest that the *variable spotting* mutation is a hypomorphic mutation, which reduces but does not completely abrogate Ets1 protein function. The G102E mutation is present within the Pointed (PNT) domain of the Ets1 protein. This domain enhances the transactivation activity of Ets1 and contains a docking site for the mitogen-activated protein kinase (MAPK) ERK2 (extracellular signal regulated kinase) (Seidel and Graves, 2002). Docking of ERK2 at this site is critical for the phosphorylation of a threonine residue

(T38) that is required for enhanced transcriptional activation by Ets1 via recruitment of the transcription factor CREB-binding protein (CBP) (reviewed in Garrett-Sinha, 2013). Mutating this ERK2 docking site was found to abrogate Ras/MAPK-mediated enhancement of Ets1 transactivation activity to the same degree as mutating the phosphoacceptor T38 residue (Seidel and Graves, 2002). Three residues within the PNT domain of Ets1, Leucine 114 (L114), L116 and Phenylalanine 120 (F120) have been shown to play a role in ERK2 binding (Seidel and Graves, 2002). Given the reduced Ets1 transactivation activity of the *variable spotting* mutant protein, it is possible that the G102 residue may be important for docking of ERK2 and T38 phosphorylation; nonetheless, the hypomorphic nature of the G102E mutation suggests this residue although important, is likely not essential.

It is also possible that the effect of this mutation on *Sox10*-MCS4 activation is not related to ERK2 docking and subsequent T38 phosphorylation. Phosphorylation of T38 is important for Ets1 activation of Ras-responsive genes (Seidel and Graves, 2002). To date, no evidence exists to support a direct role for the MAPK pathway in *Sox10* activation in the melanocyte lineage. Additionally the G102E mutation is located outside of the (114) LXLXXXF(120) domain, which is crucial for ERK docking (Dittmer, 2003). Additional experiments are needed to dissect the specific mechanism via which the *variable spotting* mutation results in decreased *Sox10*-MCS4 activation.

From	To	Anchor	Strand	Matrix Sim	Sequence
111	131	121	+	0.969	cggccccaGGATgctccagga
121	141	131	+	0.994	atgctccaGGAAgtgctgtgc
206	226	216	+	0.925	ggatgcaaGGAAggggccctt
388	408	398	-	0.908	aaacaagaGGAAccagataaa

Table 4.1. Putative Ets1 binding sites in the *Sox10*-MCS4 enhancer sequence. Using the MatInspector program, 4 potential Ets1 binding sites where identified within *Sox10*-MCS4. The matrix similarity value refers to the conservation of the individual nucleotide positions within in the sequence for the transcription factor in question. A matrix similarity value greater than 0.80 usually indicates a good match to the matrix. The positions of the potential Ets1 binding sites are indicated from the 5' end of the sense strand of the *Sox10*-MCS4 sequence. The core sequences are indicated in capital letters.

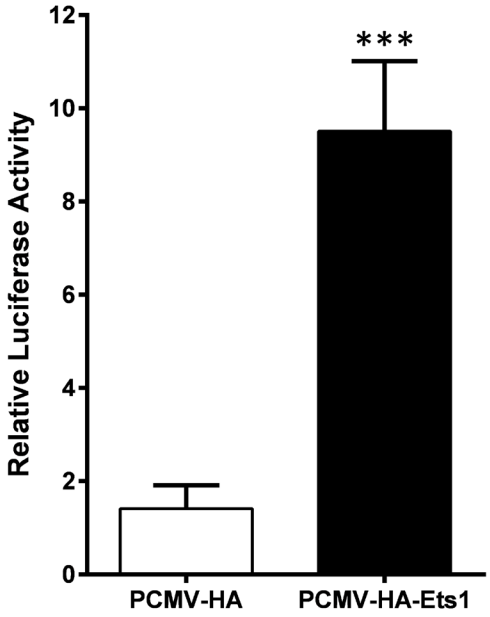

Figure 4.1. Activation of the *Sox10*-MCS4 enhancer by Ets1. B16 mouse melanoma cells were co-transfected with the *Sox10*-MCS4 luciferase reporter vector, the pRL-TK Renilla luciferase control vector, and an expression vector encoding an HA-tagged version of the full length mouse *Ets1* coding sequence (PCMV-HA-Ets1) or the PCMV-HA empty vector. *Sox10*-MCS4 enhancer activation, as measured by relative luciferase activity, was significantly higher in cells transfected with the *Ets1* overexpression vector (PCMV-HA-Ets1), compared to cells transfected with the empty PCMV-HA vector (Mann Whitney U, ***$p<0.001$). Firefly luciferase activity was normalized by Renilla luciferase activity. Data represent the mean (bar height) and standard deviation (error bars) of 3 independent experiments carried out in triplicates.

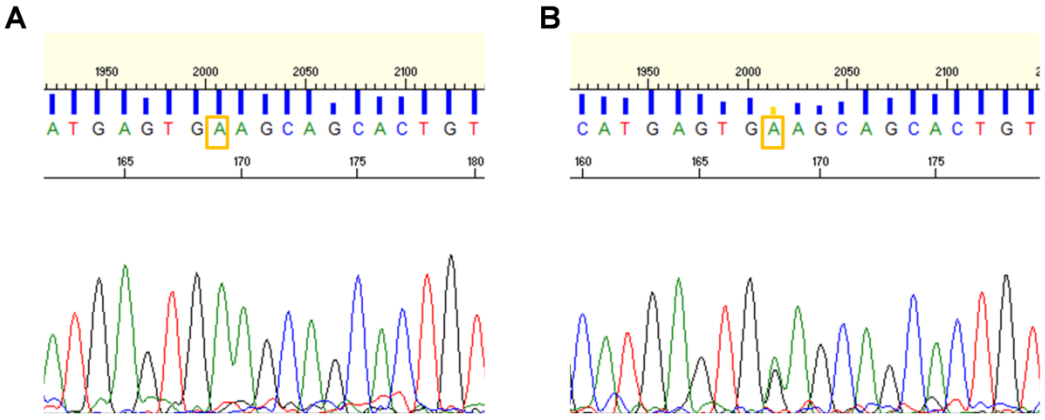

Figure 4.2. Mutation analysis of *variable spotting* mice. Sequencing of (A) homozygous and (B) heterozygous *variable spotting* mutant mice revealed a G-to-A transition (yellow boxes) in exon 3 of the *Ets1* gene at nucleotide position 647 (RefSeq NM_011808.2). This mutation results in a Glycine to Glutamate change at amino acid 102 (G102E) of the Ets1 protein.

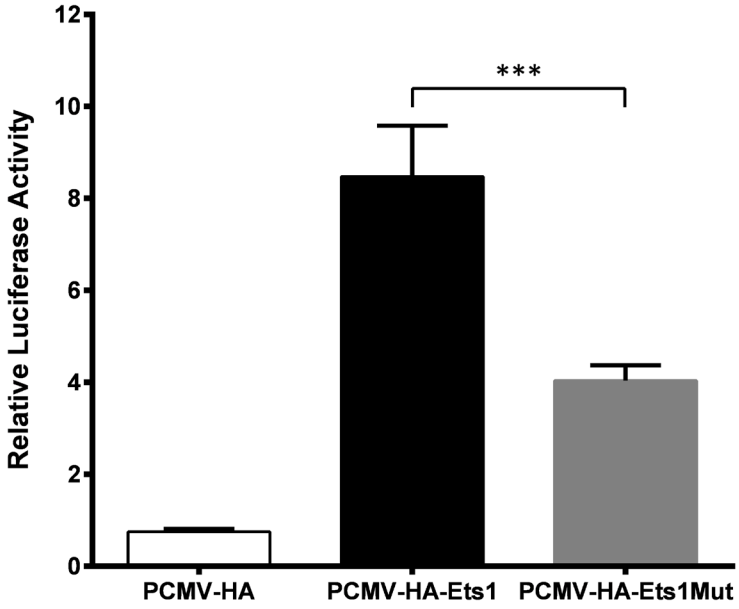

Figure 4.3. The *variable spotting* mutation inhibits Ets1-induced *Sox10*-MCS4 enhancer activation. B16 mouse melanoma cells were co-transfected with the *Sox10*-MCS4 luciferase reporter vector, the pRL-TK Renilla luciferase control vector, and either an expression vector encoding an HA-tagged version of the full length mouse *Ets1* coding sequence (PCMV-HA-Ets1), an expression vector encoding an HA-tagged version of the full length mouse *Ets1* coding sequence harboring the *variable spotting* mutation (PCMV-HA-Ets1Mut), or the PCMV-HA empty vector. Relative luciferase activity was significantly lower in cells transfected with the with the *Ets1* overexpression vector carrying the *variable spotting* mutation compared to the wild type *Ets1* overexpression vector (Mann Whitney U, ***$p<0.001$). The firefly luciferase activity was normalized by Renilla luciferase activity. Data represent mean (bar height) and standard deviation (error bars) of 3 independent experiments carried out in triplicates.

4.6. References

Antonellis, A., Bennett, W., Menheniott, T., Prasad, A., Lee-Lin, S.-Q., Green, E., Paisley, D., Kelsh, R., Pavan, W. and Ward, A. (2006). Deletion of long-range sequences at Sox10 compromises developmental expression in a mouse model of Waardenburg-Shah (WS4) syndrome. *Human molecular genetics* 15, 259–271.

Antonellis, A., Huynh, J., Lee-Lin, S.-Q., Vinton, R., Renaud, G., Loftus, S., Elliot, G., Wolfsberg, T., Green, E., McCallion, A.S. abd Pavan, W.J. (2008). Identification of neural crest and glial enhancers at the mouse Sox10 locus through transgenesis in zebrafish. *PLoS genetics* 4, e1000174.

Betancur, P., Bronner-Fraser, M. and Sauka-Spengler, T. (2010). Genomic code for Sox10 activation reveals a key regulatory enhancer for cranial neural crest. *Proc. Natl. Acad Sci U.S.A.* 107, 3570–3575.

Bondurand, N., Pingault, V., Goerich, D., Lemort, N., Sock, E., Le Caignec, C., Wegner, M. and Goossens, M. (2000). Interaction among SOX10, PAX3 and MITF, three genes altered in Waardenburg syndrome. *Human molecular genetics* 9, 1907–1917.

Britsch, S., Goerich, D., Riethmacher, D., Peirano, R., Rossner, M., Nave, K., Birchmeier, C. and Wegner, M. (2001). The transcription factor Sox10 is a key regulator of peripheral glial development. *Genes & development* 15, 66–78.

Deal, K., Cantrell, V., Chandler, R., Saunders, T., Mortlock, D. and Southard-Smith, E. (2006). Distant regulatory elements in a Sox10-beta GEO BAC transgene are required for expression of Sox10 in the enteric nervous system and other neural crest-derived tissues. *Developmental dynamics* 235, 1413–1432.

Dittmer, J. (2003). The biology of the Ets1 proto-oncogene. *Molecular cancer* 2, 29.

Garrett-Sinha, L. A. (2013). Review of Ets1 structure, function, and roles in immunity. *Cellular and Molecular Life Sciences* 70, 3375-3390.

Harris, M., Buac, K., Shakhova, O., Hakami, R., Wegner, M., Sommer, L. and Pavan, W. (2012). A dual role for SOX10 in the maintenance of the postnatal melanocyte lineage and the differentiation of melanocyte stem cell progenitors. *PLoS genetics* 9, e1003644.

Herbarth, B., Pingault, V., Bondurand, N., Kuhlbrodt, K., Hermans-Borgmeyer, I., Puliti, A., Lemort, N., Goossens, M. and Wegner, M. (1998). Mutation of the Sry-related Sox10 gene in Dominant megacolon, a mouse model for human Hirschsprung disease. *Proc. Natl. Acad Sci U.S.A.* 95, 5161–5165.

Kapur, R. P. (1999). Early death of neural crest cells is responsible for total enteric aganglionosis in Sox10(Dom)/Sox10(Dom) mouse embryos. *Pediatric and developmental pathology* 2, 559–569.

Kola, I., Brookes, S., Green, A.R., Garber, R., Tymms, M., Papas, T.S. and Seth, A. (1993). The Ets1 transcription factor is widely expressed during murine embryo development and is associated with mesodermal cells involved in morphogenetic processes such as organ formation. *Proc. Natl. Acad Sci U.S.A.* 90, 7588-7592.

Mollaaghababa, R. and Pavan, W. (2003). The importance of having your SOX on: role of SOX10 in the development of neural crest-derived melanocytes and glia. *Oncogene* 22, 3024–3034.

Nagarajan, P., Parikh, N., Garrett-Sinha, L. and Sinha, S. (2008). Ets1 induces dysplastic changes when expressed in terminally-differentiating squamous epidermal cells. *PloS one* 4, e4179.

Potterf, S., Furumura, M., Dunn, K., Arnheiter, H. and Pavan, W.(2000). Transcription factor hierarchy in Waardenburg syndrome: regulation of MITF expression by SOX10 and PAX3. *Human genetics* 107, 1–6.

Seidel, J. J. and Graves, B.J. (2002). An ERK2 docking site in the Pointed domain distinguishes a subset of ETS transcription factors. *Genes & Development* 16, 127-137.

Southard-Smith, E., Kos, L. and Pavan, W. (1998). Sox10 mutation disrupts neural crest development in Dom Hirschsprung mouse model. *Nature Genetics* 18, 60–64.

Tachibana, M., Kobayashi, Y. and Matsushima, Y. (2003). Mouse models for four types of Waardenburg syndrome. *Pigment cell research* 16, 448–454.

Vandenbunder, B., Pardanaud, L. and Jaffredo, T., Mirabel M.A., Stehelin D. (1989). Complementary patterns of expression of c-ets 1, c-myb and c-myc in the blood-forming system of the chick embryo. *Development* 106, 265-274.

CHAPTER V

Ets1 KNOCKDOWN INDUCES THE UPREGULATION OF THE TRANSCRIPTION FACTOR *Sox9* IN MOUSE MELANOMA CELLS

V. *Ets1* KNOCKDOWN INDUCES THE UPREGULATION OF THE TRANSCRIPTION FACTOR *Sox9* IN MOUSE MELANOMA CELLS

5.1. Abstract

The development of melanocytes from the neural crest (NC) is dependent upon the activation of several signaling pathways and transcription factors. These transcription factors, which include, Mitf, Sox10, and Pax3, work together in the modulation of melanocyte development. In addition to these transcription factors, signaling through the G-protein coupled Endothelin receptor b (Ednrb) and the tyrosine kinase receptor c-Kit is required for melanoblast survival, proliferation, migration, and differentiation. Much of what is known about the factors that regulate normal and pathological processes in melanocytes has been elucidated through the study of mouse pigmentation mutants. Mutations or deletions in the transcription factor *Ets1* result in ventral hypopigmentation in the mouse. We previously showed that this hypopigmentation phenotype is, at least in part, the result of decreased survival of NC cells and melanocyte precursors (melanoblasts). We also characterized a synergistic genetic interaction between *Ets1* and *Sox10*, and the ability of Ets1 to transactivate a *Sox10* enhancer known to drive *Sox10* expression to melanocytes and melanoblasts. In order to characterize the molecular basis for the hypopigmentation phenotype observed in *Ets1* mutant mice, we analyzed the effect of *Ets1* overexpression and knockdown on the expression of various genes required for melanocyte development. Gene expression analysis in mouse melanocyte and melanoma cells did not reveal changes in the expression levels of *Sox10*, *Pax3*, *Mitf*, *Kit*, and *Ednrb*. Nevertheless, knockdown of *Ets1* in a mouse melanoma cell line resulted in a 6-fold increase in the expression levels of the transcription factor *Sox9*. Although *Sox9*

has been implicated in melanocyte development, specifically in the activation of *Sox10* in the chick embryo and in the survival of trunk NC cells in the mouse, it is also required for the final specification of NC cells as chondrocytes. Our data suggest that *Ets1* may act as a negative regulator of *Sox9* and consequently a repressor of cartilage cell fate. These results point to an additional role for *Ets1* in the specification of NC cell fate.

5.2 Introduction

During development melanoblasts migrate dorsolaterally below the surface ectoderm, eventually colonizing the epidermis and hair follicles where they proliferate and differentiate into pigment-producing melanocytes (Le Douarin and Kalcheim, 1999). Large numbers of melanocytes were also shown to derive from Schwann cell precursors (SCPs), which arise from ventrally migrating NC cells (Adameyko et al., 2009). The development of melanocytes from the NC is dependent on the activation of several signaling pathways and transcription factors (Figure 5.1). These transcription factors, which include, Mitf, Sox10 and Pax3, work together in the modulation of melanocyte development. Additionally, the transcription factors Lef1, acting downstream of the canonical Wnt/β-catenin signaling pathway, and β-catenin itself, which can translocate to the nucleus and act as a transcription factor, have been shown to be important modulators of melanocyte development (reviewed in Lin and Fisher, 2007; Hou and Pavan, 2008). In addition to these transcription factors, signaling through the G-protein coupled Endothelin receptor b (Ednrb) and the tyrosine kinase receptor c-Kit is required for melanoblast survival, proliferation, migration, and differentiation (reviewed in Hou and Pavan, 2008; Saldana-Caboverde and Kos, 2010).

The transcription factor Mitf has been described as the master regulator of melanocyte development. It has been implicated in melanocyte survival, proliferation and differentiation through the study of several *Mitf* allelic mouse pigmentation mutants (Hou and Pavan, 2008). Mitf is required for melanocyte survival by acting as a transcriptional regulator of the anti-apoptotic protein *Bcl2* (McGill et al., 2002) and of cyclin-dependent kinase 2 (*Cdk2*), a cell cycle regulator essential for maintenance of melanoma cell viability and cell cycle (Du et al., 2004). Another transcriptional target of Mitf, is the hepatocyte growth factor (HGF) receptor *c-Met*, which has been shown to be involved in melanocyte survival in vitro (McGill et al., 2006). Mitf regulates melanocyte proliferation via transcriptional regulation of *Cdk2* and the T-Box transcription factor 2 (*TBX2*) (Hou and Pavan, 2008). It also promotes early melanocyte fate specification and melanocyte differentiation through direct transcriptional regulation of the pigment enzymes Tyrosinase (*TYR*), Tyrosinase related protein-1 (*TRP1*), and Dopachrome tautomerase (*Dct*). Other genes that have been implicated in melanocyte differentiation and are transcriptionally regulated by Mitf include absent in melanoma-1 (*AIM-1*), melanoma antigen recognized by T-cells 1 (*MART1*), and silver homolog (*SILV or Pmel17*) (reviewed in Levy et al., 2006).

The transcription factor Sox10, a member of the SoxE family of transcription factors, is also required for melanocyte development. The importance of *Sox10* for melanocyte survival is evidenced by the hypopigmentation phenotype that results when it is mutated or deleted**.** Its targeted deletion in the mouse results in almost a complete absence of trunk melanoblasts (Hou et al., 2006). Sox10 regulates genes important for melanocyte development via *Mitf* transcriptional activation. In cooperation with Pax3,

Sox10 binds to and transcriptionally activates *Mitf* (Bondurand et al., 2000, Potterf et al., 2000). It also activates the transcription of the melanogenic proteins *Dct* and *TYR,* which are essential for melanocyte differentiation (reviewed in Harris et al., 2010). Another SoxE-family transcription factor that has been recently implicated in melanocyte development is *Sox9*. The transcription factor *Sox9* is expressed in pre- and post-migratory NC cells and has been found to be important for the survival of trunk NC cells (Cheung et al., 2005). Studies in the mouse, chick and *Xenopus* suggest that *Sox9* acts upstream of *Sox10* (Silver et al., 2006). In the chick Sox9 was recently shown to directly bind to and activate *Sox10* regulatory regions, and to be required, along with Ets1, for *Sox10* expression in cranial NC cells (Betancur et al., 2010).

The transcription factor *Pax3* is another important regulator of melanocyte development; however, its specific roles in melanocyte development are not fully understood. Pax3 has been shown to directly bind to and activate the *Mitf* promoter (Watanabe et al., 1998), and to act synergistically with Sox10 to activate *Mitf* transcription (Bondurand et al., 2000; Potterf et al., 2000). Recently, Pax3 was found to indirectly activate the *Kit* promoter in various cell lines, including melanocytes (Guo et al., 2010). Pax3 has also been shown to inhibit Sox10- and Mitf-dependent transcriptional activation of *Dct*. By promoting the transcription of *Mitf* while inhibiting that of *Dct*, Pax3 may be involved in the initial fate decision of melanoblasts as well as in preventing the terminal differentiation of precursors in order to allow the sufficient expansion of melanocyte precursors before they become terminally differentiated (Lang et al., 2005).

Signaling via Ednrb is required for melanoblast survival, proliferation, migration, and differentiation. Binding of Endothelin 3 (Edn3) to Ednrb leads to the activation of the

G proteins Gq/G11. Hypermorphic alleles of these G proteins lead to hyperpigmentation in mice, however, their deletion does not result in hypopigmentation suggesting that other G proteins may act downstream of Ednrb during melanocyte development. The activation of G-proteins by Ednrb results in transcriptional and translational regulation of *Mitf* and mediates many of the Ednrb-induced effects in melanoblast development; however, other downstream targets of Ednrb, which may also be important for melanocyte development, and particularly in melanoblast migration, are not currently known. Endothelin signaling has been shown to interact with Kit signaling to promote melanoblast survival, proliferation, and differentiation, with Ednrb being required in the final steps of melanocyte differentiation rather than in the initial commitment to the melanocytic fate (reviewed in Saldana-Caboverde and Kos, 2010). In the mouse, c-*Kit* and Kit ligand *(Kitl)* mutations result in a phenotype characterized by a belly spot in heterozygous animals, and by anemia, lack of coat pigmentation, and sterility in the few homozygotes that survive. c-*KIT* and *KITL* mutations are responsible for human piebaldism, which is characterized by, among other things, hair and skin hypopigmentation (reviewed in Hou and Pavan, 2008). Signaling via c-Kit has been found to modulate *Mitf* and to be required for the induction of *Tyr* expression (Hou et al., 2000).

The hypopigmentation phenotype of *Ets1* mutant mice implies that this transcription factor is important in melanocyte development. We previously showed that this pigmentation phenotype appears to be the result, at least to some extent, of decreased NC cell and melanoblast survival. In an attempt to characterize the molecular mechanism via which *Ets1* regulates melanocyte development, we examined the expression levels of several melanoblast-specific genes in cells with higher and lower than normal levels of

Ets1 protein. Understanding the molecular targets of Ets1 will provide more insight into the specific function of this transcription factor in melanocyte development.

5.3. Materials and methods

5.3.1 Cell culture

The B16-F10 (B16 hereafter) mouse melanoma cell line was purchased from ATCC (CRL-6322, ATCC). Cells were maintained in Dubelcco's Modified Eagle's Medium (DMEM) (10-013-CV, Cellgro) supplemented with 10% Fetal Bovine Serum (FBS), 100 U/ml penicillin, and 100 U/ml streptomycin (all from Thermo Scientific), at 37˚C in 5% CO_2. The immortalized mouse melanocyte cell line melan-a (Sviderskaya et al., 2002), was a kind gift from Dr. William J. Pavan (NIH, Bethesda, MD). Melan-a cells were maintained in cell culture media consisting of RPMI 1640 (10-041-CV, Cellgro), 10% FBS, 100 U/ml penicillin, 100 U/ml streptomycin, 2mM L-glutamine (all from Thermo Scientific), 200 nM 12-O-tetradecanoyl phorbol 13-acetate (TPA), and 200pM Cholera Toxin (both from Sigma-Aldrich), at 37 ˚C, 10% CO_2.

5.3.2 Plasmid constructs

The *Ets1* overexpression vector (pCMV-HA-Ets1) and the pCMV-HA empty vector (Clontech) were gifts from Dr. Satrajit Sinha (SUNY at Buffalo, Buffalo, NY). The pCMV-HA-Ets1 vector contains a Hyaluronic acid (HA)-tagged version of the full length mouse *Ets1* coding sequence (Nagarajan et al., 2009). Both plasmids were transformed into *Escherichia coli* Dh5α competent cells (Life Technologies) and glycerol stocks were prepared (Appendix I). Plasmids were purified from overnight cultures using the QIAprep Spin Miniprep Kit (Qiagen). Ethanol precipitation was carried out to purify and concentrate plasmids to be used for transfections (Appendix V).

5.3.3 Plasmid DNA transfections

For plasmid DNA transfection, approximately, 3.5 x 10^5 melan-a or B16 cells were seeded in antibiotic-free cell culture media, into each well of a 6 well plate (CytoOne) roughly 24 hours before transfection. Once cells had reached 70-90% confluency they were transfected with 2µg/well of plasmid DNA. For each well, 2µg of DNA (PCMV-HA-Ets1 or PCMV_HA empty vector) were diluted in 125µl of Opti-MEM I (Invitrogen). For each well, 10µl of the lipid transfection reagent Lipofectamine 2000 (Invitrogen) were diluted in 125µl of Opti-MEM I. The diluted DNA and diluted Lipofectamine reagent were incubated 5 minutes at room temperature. After 5 minutes, the diluted DNA and diluted Lipofectamine were combined and incubated 30 minutes at room temperature. 250µl of these lipid-DNA complexes were added to each well in a drop-wise manner, evenly distributing drops throughout the well. Plates were gently rocked by hand for 20 seconds. Cells were then incubated at 37˚C, 5% CO_2 (B16) or 10% CO_2 (melan-a) for 48 hours. After 48 hours, cells were harvested for total RNA and protein to assay *Ets1* expression by semi-quantitative real time PCR (See *5.3.5*) and Ets1 protein by Western blot (See *5.3.6*). For each cell line, three independent transfections were carried out, each one in triplicates.

5.3.4 siRNA transfections

For siRNA transfections, approximately 1.5 x 10^5 melan-a or 2 x 10^5 B16 cells were seeded in antibiotic-free cell culture media, into each well of a 6 well plate (CytoOne) roughly 24 hours prior to transfecting. Once cells had reached 40–50% confluency they were transfected with mouse Ets1 siRNAs or Non-targeting siRNA controls. For one set of experiments, cells were transfected with 75pmol of the

siGENOME SMARTpool Mouse Ets1 siRNA (Thermo Scientific) or 75pmol of the siGENOME Non-Targeting siRNA Pool (Thermo Scientific). Each of these siRNA pools was composed of 4 siRNAs. For each cell line, three independent transfections were carried out, each one in triplicates.

In order to validate the results of the first set of experiments and to evaluate possible off-target effects, cells were transfected with individual Ets1 and non-targeting control siRNAs. Melan-a cells were transfected with 50pmol of each of 2 ON-TARGETplus Mouse Ets1 siRNAs (Thermo Scientific, designated as siRNAs 1 and 2) or 100pmol of the siGENOME Non-targeting siRNA (Thermo Scientific). Three independent transfections were carried out, each one in triplicates. B16 cells were transfected with two sets of 2 Ets1 siRNAs from the ON-TARGETplus Mouse Ets1 siRNA set of 4 (Thermo Scientific). Cells were transfected with 50pmol of each of 2 ON-TARGETplus Mouse Ets1 siRNAs (designated siRNAs 1 and 2 and siRNAs 3 and 4, Thermo Scientific) or 100pmol of the siGENOME Non-targeting siRNA (Thermo Scientific). For each set of Ets1 siRNAs, three independent transfections were carried out, each one in triplicates.

All transfections were carried out using the Lipofectamine 2000 (Invitrogen) lipid transfection reagent following the manufacturer's instructions. For each well, a total of 75-100pmol of siRNA (Ets1 or non-targeting control, as described above) were diluted in 100µl of Opti-MEM I. For each well, 7.5µl of Lipofectamine 2000 were diluted in 100 µl of Opti-MEM I. The diluted siRNA and diluted Lipofectamine were incubated for 5 minutes at room temperature. After 5 minutes, the diluted siRNA and diluted Lipofectamine were combined and incubated for 30 minutes at room temperature. 200µl

of these lipid-siRNA complexes were added to each well, in a drop-wise manner, evenly distributing drops throughout the well. Plates were gently rocked by hand for approximately 20 seconds. Cells were then incubated at 37˚C, 5% CO_2 (B16) or 10% CO_2 (melan-a) for 48 hours. After 48 hours, cells were harvested for total RNA and protein to assay *Ets1* expression by semi-quantitative real time PCR (See *5.3.5*) and Ets1 protein by Western blot (See *5.3.6*).

5.3.5 RNA extraction, cDNA synthesis, and semi-quantitative real-time PCR

Approximately 48 hours after transfection, B16 and melan-a cells were washed twice with ice cold filter-sterilized Phosphate Buffered Saline (PBS) (Thermo Scientific). Total RNA from B16 or melan-a cells was isolated using the RNeasy Mini Kit (Qiagen). RNA was treated with the RNase-free DNase Set (Qiagen) to remove genomic DNA contamination. RNA quantification was carried out with the Nanodrop 3000 System (Thermo Scientific). The RNA samples were then subjected to reverse transcription using Maxima Reverse Transcriptase (Thermo Scientific) following the manufacturer's instructions. PCR using the primers 5'-CAAGCTTGCTGGTGAAAAGGA and 5'-TGCGCTCATCTTAGGCTTTGT (Colombo et al., 2012), which flank an intronic region of the housekeeping gene hypoxanthine–guanine phosphoribosyltransferase (*HPRT*), was carried out to test cDNAs for the presence of genomic DNA contamination. PCR products were visualized in a 2% agarose gel. A single band at 186bp confirmed the absence of genomic DNA contamination, while the presence of an extra band at 1024bp indicated the presence of genomic DNA. Mouse genomic DNA was used as a positive control. All cDNAs synthesized were found to be free of genomic DNA contamination.

The levels of expression of *Ets1*, *Sox10*, *Mitf*, *Pax3*, *Ednrb*, *Kit*, *Sox9*, and Glyceraldehyde 3-phosphate dehydrogenase (*Gapdh*) were examined via semi-quantitative real-time PCR. Real-time PCR was performed using the Maxima® SYBR Green/ROX qPCR Master Mix (Thermo Scientific) on a 7300 Real-Time System (Applied Biosystems). The following primers were used to assay the levels of expression of each gene: *Ets1*: 5'-AGCGCTACGTATACCGCTTT, and 5'-ACTAGTCAGCATCCGGCTTT, *Sox10*: 5'-GGACTACAAGTACCAACCTCGG and 5'-GGACTGCAGCTCTGTCTTTGG (Seong et al., 2012), *Mitf*: 5'-TGAAACCTTGCTATGCTGGA and 5'-TACCTGGTGCCTCTGAGCTT (Colombo et al., 2012), *Pax3*: 5'-TCCATCCGACCTGGTGCCAT and 5'-TTCTCCACGTCAGGCGTTG, *Ednrb*: 5'-TTTGCGCATTCTTGTCTAGG and 5'-CTCTTGGGCATTCTTTCACA, *Kit*: 5'-TCCTCTGGGAGCTCTTCTCCTT and 5'-GTTGGACAACCTGCTTGAATGTT, *Sox9*: 5'-CGGAGGAAGTCGGTGAAGA, and 5'-GTCGGTTTTGGGAGTGGTG and *Gapdh*: 5'-GTCTCCTGCGACTTCAGC, and 5'-TCATTGTCATACCAGGAAATGAGC. The thermal profile of the PCR reaction was 95˚C for 10 minutes and 40 cycles of 95˚C for 15 seconds and 58˚C for 1 minute. Samples were analyzed in triplicates and the $2^{-\Delta\Delta C}{}_{T}$ method was used to determine relative levels of expression of the target genes, which were normalized to *Gapdh* expression levels (Livak and Schmittgen, 2001). The reduction in *Ets1* mRNA levels in cells transfected with Ets1 siRNA relative to those transfected with non-targeting siRNA was estimated from the fold change in *Ets1* expression calculated via the $2^{-\Delta\Delta C}{}_{T}$ method.

5.3.6 Protein extraction and Western Blot

Overexpression and knockdown efficiency were also assayed via Western blot. Approximately 48 hours after transfection, B16 and melan-a cells were washed twice with ice cold filter-sterilized PBS (Thermo Scientific) and lysed using ice cold RIPA Lysis Buffer (20mM Tris-HCl (pH7.5), 150mM NaCl, 1% Nonidet P40, 0.05% Sodium Deoxycholate, 0.1% SDS, 2mM EDTA (pH8.0)) containing 1mM phenylmethylsulfonyl fluoride (PMSF) (Sigma-Aldrich) and 1X Pierce Protease Inhibitor (Thermo Scientific) to prevent protein degradation. Cell lysates were centrifuged at 16,000 RPM, 20 minutes at 4˚C. 4X NuPAGE LDS Sample Buffer (Invitrogen) containing 5% β-mercaptoethanol (Sigma-Aldrich) was added to the supernatants to a final concentration of 1X. Samples were boiled for 5 minutes and allowed to cool to room temperature prior to loading onto Any kD™ Mini-PROTEAN® TGX™ Precast Gels (Bio-Rad) for SDS-PAGE protein separation. Proteins were then transferred to 0.2µm PVDF membranes. After protein transfer, the membranes were blocked with 5% Carnation non-fat instant dry milk in TBST (Tris Buffered Saline + 0.2% Tween 20), 1 hour at room temperature, rocking at 75 RPM. The membranes were then incubated with a rabbit polyclonal anti-Ets1 antibody (C-20) (sc-350, Santa Cruz Biotechnology) (1:400 in blocking solution), overnight at 4˚C, rocking at 75 RPM. On the next day, the membranes were washed with TBST and incubated with a goat anti-rabbit Horseradish Peroxidase (HRP)-conjugated antibody (611-1324, Rockland Immunochemicals) (1:3,000 in blocking solution). Membranes were incubated with Peroxide/Lumiglo Substrate (Cell Signaling), 15 seconds at room temperature. Proteins were visualized by exposure to classic blue X-ray films (MidScientific).

Normalization was carried out by re-probing the membrane used for Ets1 Western blot with a mouse monoclonal anti-β-actin antibody. After visualizing the results of the Ets1 Western blot, membranes were rinsed extensively with 1X TBS. The membranes were then stripped of bound antibody by incubating in stripping buffer (7M Guanidine Hydrochloride (MP Biomedicals), 50mM Glycine (Fisher Scientific), 100mM KCl (Fisher Scientific), 0.05mM EDTA (Fisher Scientific), 1.39% β-mercaptoethanol (Sigma-Aldrich)), 10 minutes at room temperature rocking at 80 RPM. Subsequently, membranes were washed extensively with distilled water and blocked with 5% Carnation non-fat instant dry milk in TBST, for 1 hour at room temperature, rocking at 75 RPM. The membranes were then incubated with a mouse monoclonal anti-β-actin antibody (A5316, Sigma-Aldrich) (1:15,000 in blocking solution), overnight at 4˚C, rocking at 75 RPM. The next day, the membranes were washed with TBST and incubated with a goat anti-mouse Horseradish Peroxidase (HRP)-conjugated antibody (31430, Thermo Scientific/Pierce) (1:40,000 in blocking solution). Membranes were then incubated with Peroxide/Lumiglo Substrate, 15 seconds at room temperature. Proteins were visualized by exposure to classic blue X-ray films (MidScientific).

5.4 Results

5.4.1 Ets1 overexpression does not affect the expression of melanoblast-specific genes in mouse melanocytes and mouse melanoma cells.

In order to characterize the molecular mechanism via which *Ets1* regulates melanocyte development, mouse melanocytes (melan-a) and melanoma cells (B16) were transfected with an *Ets1* overexpression vector (PCMV-HA-Ets1) or an empty vector (PCMV-HA). *Ets1* was confirmed to be overexpressed in the cells transfected with

PCMV-HA-Ets1 via semi-quantitative real-time PCR and Western Blot, in both melan-a and B16 cells (Figures 5.2 and 5.3, respectively). Transfection with PCMV-HA-Ets1 resulted in approximately a 100 fold increase in *Ets1* expression in melan-a cells, and a 1,300 fold increase in *Ets1* expression in B16 melanoma cells. For melan-a cells, the expression levels of *Kit*, *Ednrb*, *Pax3*, *Mitf*, *Sox10* and *Sox9* were analyzed and no substantial changes in expression were detected (Figure 5.2). Similarly, no considerable changes in the expression levels of *Kit*, *Pax3*, *Mitf*, *Sox10* and *Sox9* were detected in B16 cells overexpressing *Ets1*. *Ednrb* expression was not assayed in B16 cells because endogenous *Ednrb* expression in this cell line is very low, making it impossible to accurately detect changes in expression levels via real-time PCR.

5.4.2 Knockdown of Ets1 leads to Sox9 upregulation in mouse melanoma cells.

Given the lack of substantial changes in the expression of melanoblast-specific genes as a result of *Ets1* overexpression, the effect of *Ets1* knockdown on the expression of these genes was assessed. The reduction in *Ets1* mRNA levels in melan-a cells transfected with Ets1 siRNAs relative to those transfected with non-targeting siRNAs ranged from approximately 68% for cells transfected with 2 individual siRNAs to 80% for cells transfected with the Ets1 siRNA pool (4 siRNAs). For B16 cells, the reduction in *Ets1* mRNA levels relative to the control ranged from approximately 65% for cells transfected with 2 individual siRNAs to 72% for those transfected with the Ets1 siRNA pool.

For both melan-a and B16 cells, an off-target effect on *Kit* expression was detected in cells treated with the siGENOME Non-targeting siRNA pool (Thermo Scientific); for this reason, *Kit* expression was not reported for these sets of experiments

(Figures 5.4 B and 5.5 B). Nonetheless, no significant changes in Kit expression levels were detected in melan-a and B16 cells transfected with sets of 2 individual Ets1 siRNAs compared to those transfected with control siRNA (Figures 5.4 C and 5.5 C, D). Similarly, for both cell lines, no substantial changes on the expression levels of *Pax3*, *Mitf*, and *Sox10* were detected (Figures 5.4 and 5.5). We observed a slight upregulation in *Ednrb* expression (fold change = 2.006±0.087), in melan-a cells transfected with 2 individual Ets1 siRNAs (Figure 5.4 C). This upregulation was not observed in cells transfected with the Ets1 siRNA pool (Figure 5.4 B). *Ednrb* expression was not assayed for B16 cells because *Ednrb* expression in this cell line is very low, making it impossible to accurately detect changes in expression levels via real-time PCR. A 6 fold increase in *Sox9* expression was observed in B16 cells transfected with Ets1 siRNA, regardless of the siRNA or non-targeting control used (Figure 5.5 B, C & D). This change was not observed in melan-a cells for which *Sox9* expression was only evaluated in cells transfected with individual Ets1 and control siRNAs (Figure 5.4 C).

5.5 Discussion

Deletion or mutation of the transcription factor *Ets1* results in ventral hypopigmentation in the mouse. The increased apoptosis observed in NC cells and melanoblasts in *Ets1* null embryos suggests that *Ets1* is required for the survival of these cells. We previously characterized a synergistic genetic interaction between *Ets1* and *Sox10*, a transcription factor required for the development of several NC cell derivatives, including melanocytes. Additionally, we described the ability of Ets1 to activate the *Sox10*-MCS4 enhancer, which drives *Sox10* expression to melanoblasts and melanocytes, and the impact of the spontaneous *variable spotting* mutation on the transactivation

ability of Ets1. To further characterize the role of *Ets1* in melanocyte development, we sought to determine the molecular targets of Ets1 regulation via gene expression analysis of melanocyte and melanoma cells with higher and lower than normal *Ets1* expression levels.

In mouse melanocytes and melanoma cells, the expression levels of the transcription factors *Pax3*, *Mitf*, and *Sox10* were not visibly affected by overexpression or knockdown of *Ets1*. It is possible that neither *Pax3* nor *Mitf* are direct targets of Ets1; however, the lack of an effect in *Sox10* expression was surprising given the ability of Ets1 to activate the *Sox10*-MCS4 enhancer and the synergistic genetic interaction between *Ets1* and *Sox10*. One reasonable explanation for the absence of an effect on *Sox10* expression as a result of *Ets1* knockdown is that in the mouse melanocyte and melanoma cell lines used for this experiment other factors might be able to compensate for Ets1 deficiency. In the case of *Ets1* overexpression, the absence of a significant change in the expression of *Sox10* or other potential downstream targets could result if endogenous Ets1 protein is sufficient to drive the expression of said targets, so that in essence, the regulatory regions of these genes are already saturated by the endogenous protein.

We also failed to detect substantial changes in the expression levels of *Kit* in mouse melanocytes and melanoma cells as a result of *Ets1* overexpression or knockdown. A slight upregulation was observed in *Ednrb* (fold change = 2.006±0.087) in melan-a cells transfected with 2 individual Ets1 siRNAs (Figure 5.4 C); however, this effect was not observed in this cell line when transfected with an Ets1 siRNA pool (Figure 5.4 B). It is possible that off-target effects caused by the Ets1 or non-targeting control siRNAs

might be responsible for this discrepancy. This is a plausible explanation because an off-target effect on *Kit* expression was detected and found to be caused by one of the siRNAs in the control siRNA pool used for the first set of siRNA transfections. Additional experiments are needed to determine whether the slight upregulation of *Ednrb* expression observed in mouse melanocytes as a result of *Ets1* knockdown is biologically relevant.

Knockdown of *Ets1* led to a 6-fold increase in *Sox9* expression in B16 melanoma cells (Figure 5.5). This upregulation was not observed in melan-a cells (Figure 5.4). The difference in *Sox9* expression levels in B16 and melan-a cells emphasizes the impact that the use of different cell lines can have on the expression levels of downstream target genes in knockdown, as well as overexpression, studies. *Ets1* overexpression did not affect *Sox9* expression in melanocytes (Figure 5.2) or melanoma cells (Figure 5.3), which suggests that endogenous Ets1 protein might be sufficient to suppress *Sox9* expression in these cells.

The transcription factor Sox9 is a member of the SoxE family of transcription factors, which includes Sox8, Sox9, and Sox10 (reviewed in Lee and Saint-Jeannet, 2011). *Sox9* is expressed in pre-migratory NC cells and its expression precedes that of migratory NC cell markers. Forced expression of *Sox9* in the neural tube induces neural crest-like properties at the expense of neuronal progenitors; however, other factors are required to induce NC cell delamination (Cheung and Briscoe, 2003). In *Xenopus* embryos, morpholino-induced *Sox9* depletion results in the loss of NC cell progenitors (Spokony et al., 2002). In the mouse embryo, *Sox9* is first expressed around E8.5, in the hindbrain region at the dorsal tip of the closing neural tube and in the dorsal folds of the neural tube in the trunk. *Sox9* remains expressed in migrating cranial NC cells (reviewed

in Lee and Saint-Jeannet, 2011) but it is downregulated in trunk NC cells soon after they become migratory (Cheung et al., 2005). *Sox9* later becomes expressed in NC-derived chondrocyte precursor cells, where it drives the expression of alpha-1 type-II Collagen (*Col2A1*) (Bell et al., 1997). In the mouse, homozygous deletion of *Sox9* is embryonic lethal. *Sox9* heterozygotes, on the other hand, die shortly after birth with severe skeletal defects, including malformations of endochondral bones, a shortened jaw, and cleft palate (Hong and Saint-Jeannet, 2005). In humans *SOX9* mutations are responsible for Campomelic Dysplasia, a disease characterized by skeletal and craniofacial malformations as well as sex reversal resulting from abnormal testis development (Wagner et al., 1994).

The transcription factor Sox9 has been implicated in early melanocyte development because it is required for *Sox10* expression (reviewed in Silver et al., 2006). In the chick embryo, Sox9, together with Ets1, and c-Myb, are required for endogenous *Sox10* expression in the cranial NC (Betancur et al., 2010). *Sox9* expression has also been shown to be required for the formation of trunk NC cell derivatives. In mouse embryos carrying a conditional *Sox9* null allele, the numbers of neurons and glia in the trunk region were severely reduced. In these mutants, *Sox10* expression was maintained in pre-migratory NC cells, but reduced along the NC cell migration route. The large decrease in the number of NC cell derivatives in *Sox9* mutant mice was found to be the result of increased apoptosis of pre-migratory and early migrating NC cells at E9.5 and E10.5. In pre-migratory NC cells, *Sox9* was also found to be required for the expression of *Snail* (Cheung et al., 2005), a transcription factor that has been implicated in early pigment cell development and differentiation (Silver et al., 2006). Although *Sox9* seems to be required

for melanocyte development early on, its prolonged expression has been shown to negatively affect melanocyte development. Ectopic expression of *Sox9* under the melanocyte-specific Dopachrome tautomerase (*Dct*) promoter, which drives expression to melanoblasts beginning at E10 and thereafter (Steel et al., 1992), results in pigmentation defects in the mouse (Qin et al., 2004). The effect of prolonged *Sox9* expression on pigmentation implies that failure to downregulate *Sox9* in melanocyte precursors can negatively affect melanocyte development (Qin et al., 2004). For this reason, it has been suggested that the importance of *Sox9* for melanocyte development is centered on its ability to induce *Sox10* expression (Harris et al., 2013).

Although *Sox9* becomes downregulated early on during melanocyte development, it has been found to be expressed in melanocytes (Cook et al., 2005; Passeron et al., 2007), nevi, primary melanoma, and melanoma metastases (Passeron et al., 2007; Passeron et al., 2009; Bakos et al., 2010; Rao et al., 2010). The relationship between *Sox9* expression and melanoma progression is not well understood. A small but statistically significant correlation between *Sox9* expression, measured via immunohistochemistry, and melanoma progression has been reported (Bakos et al., 2010). Conversely, a moderate decrease in the levels of *Sox9* expression with melanoma progression has also been reported (Passeron et al., 2009). In addition, *Sox9* overexpression in various melanoma cell lines was found to inhibit the proliferation of these cells and their tumorigenic potential in mice and in a human ex vivo model of melanoma, suggesting that a negative relationship exists between *Sox9* expression and melanoma progression (Passeron et al., 2009).

In the present study, knockdown of *Ets1* led to a significant increase in *Sox9* expression in mouse melanoma cells. At first glance, this result appears to contradict a positive role for *Ets1* in melanocyte development, since it suggests that *Ets1* acts as a negative regulator of *Sox9*, which is required for the development of trunk NC cell derivatives. However, given the survival defect observed in NC cells and melanoblasts in *Ets1* null mutants, it is likely that *Ets1* plays a dual role in melanocyte development, initially, in the maintenance of NC cells and early melanocyte precursors, and later in cell lineage specification by modulating the expression of other NC genes, including *Sox9*. A role for *Ets1* in cell lineage specification has been previously proposed. The upregulation of *Sox9* in the hearts of *Ets1* mutant mice and the presence of ectopic NC cell-derived cartilage nodules in these hearts suggests that *Ets1* may act as a negative regulator of *Sox9*, and thus cartilage fate, in NC cells (Gao et al., 2010). Additionally, because prolonged *Sox9* expression appears to negatively impact melanocyte development (Qin et al., 2004), Ets1-induced *Sox9* repression may be important for melanocyte differentiation. It is possible that in trunk NC cells destined to become melanocytes, as in cardiac NC cells, Ets1 serves as a repressor of chondrocyte fate. Future experiments comparing *Sox9* expression and the numbers of chondrocyte precursors in the trunk region of *Ets1* wild type and mutant embryos will help to address whether the effects of *Ets1* deficiency on melanocyte development are also the result of improper NC or melanoblast differentiation.

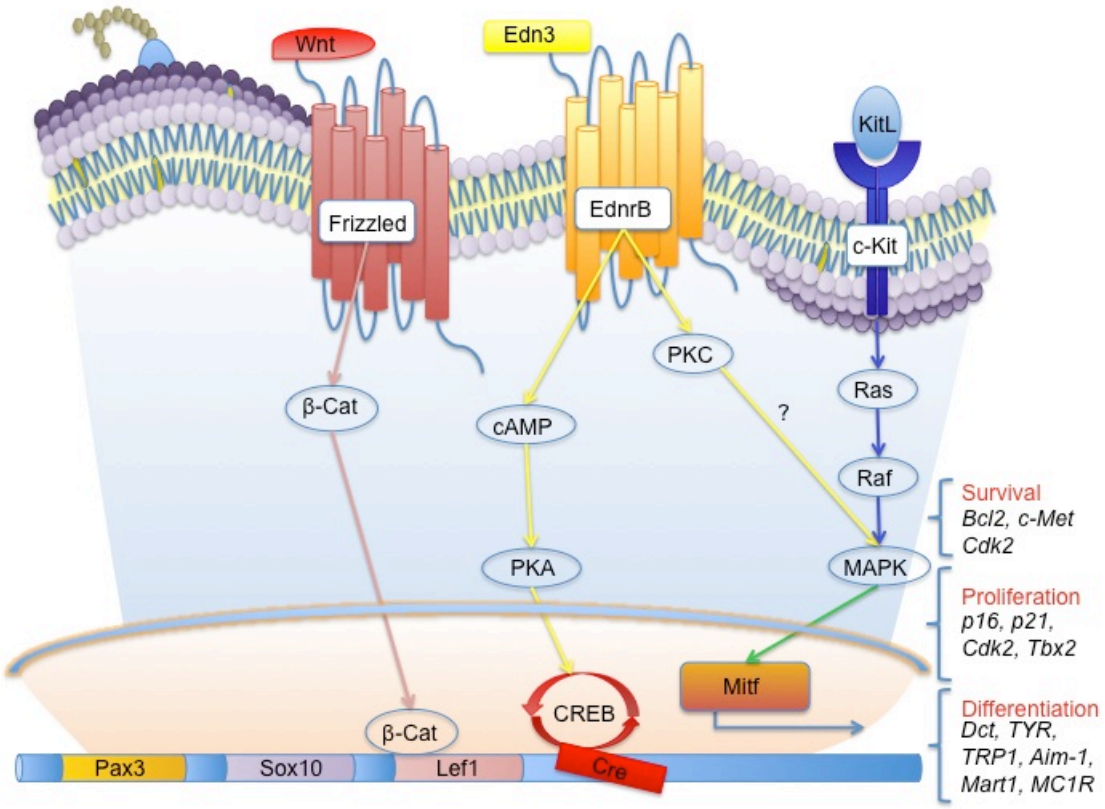

Figure 5.1. The molecular basis for melanocyte development. The development of melanocytes from the NC is dependent on the activation of several signaling pathways and transcription factors. These transcription factors, which include, Mitf, Sox10 and Pax3, work together in the modulation of melanocyte development. Additionally, the transcription factors Lef1, acting downstream of the canonical Wnt/β-catenin signaling pathway, and β-catenin itself, have been shown to be important modulators of melanocyte development. In addition to these transcription factors, the G-protein coupled Endothelin receptor b (Ednrb) and the tyrosine kinase receptor c-Kit are required for melanoblast survival, proliferation, migration, and differentiation.

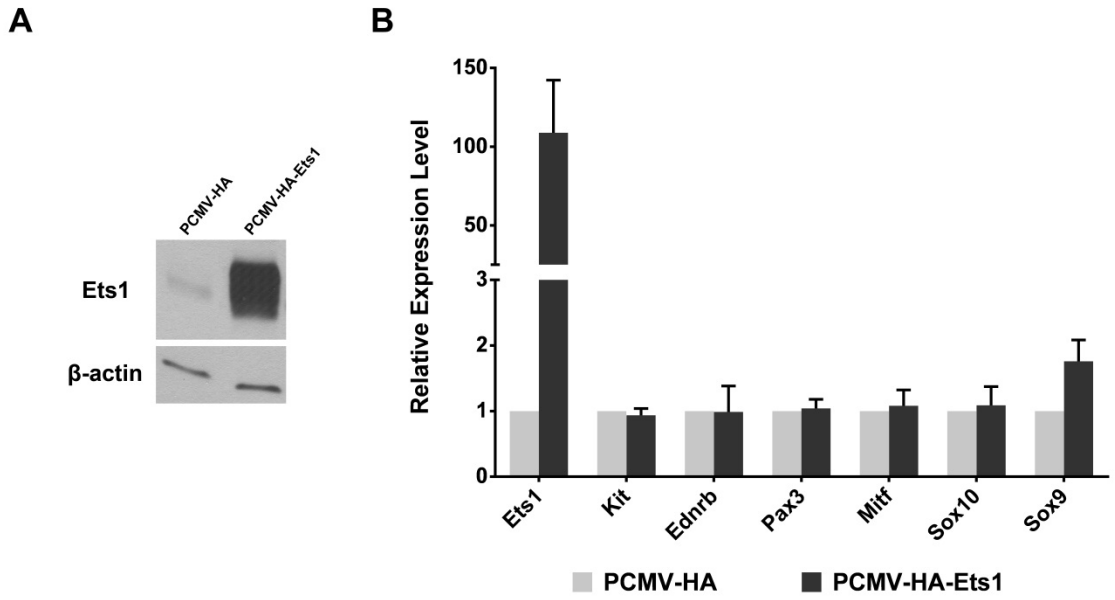

Figure 5.2. *Ets1* overexpression in melan-a cells does not substantially affect the expression of melanoblast-specific genes. Melan-a cells were transfected with an *Ets1* overexpression vector (PCMV-HA-Ets1) or an empty vector (PCMV-HA). *Ets1* mRNA and Ets1 protein overexpression were confirmed via semi-quantitative real-time PCR (B) and Western blot (A), respectively. The expression of the genes *Kit*, *Ednrb*, *Pax3*, *Mitf*, *Sox10*, and *Sox9* did not differ substantially between cells transfected with the *Ets1* overexpression vector and those transfected with empty vector. Data represent gene expression levels in cells transfected with PCMV-HA-Ets1 relative to those transfected with PCMV-HA. The mean (bar height) and standard deviation (error bars) are shown for 3 independent experiments carried out in triplicates.

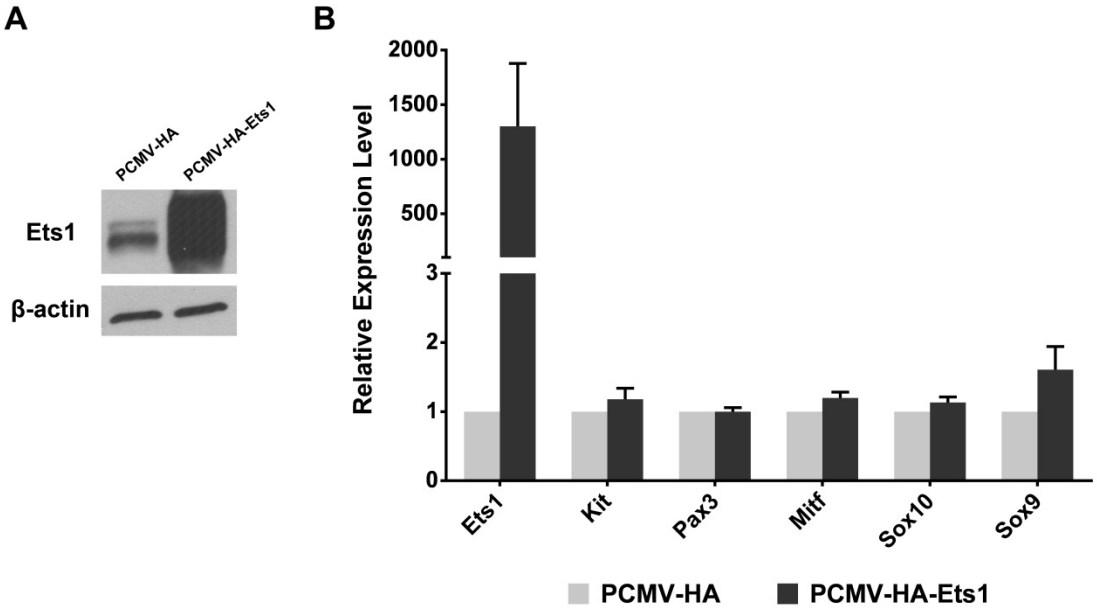

Figure 5.3. *Ets1* overexpression in B16 cells does not considerably affect the expression of melanoblast-specific genes. B16 cells were transfected with an *Ets1* overexpression vector (PCMV-HA-Ets1) or an empty vector (PCMV-HA). *Ets1* mRNA and Ets1 protein overexpression were confirmed via semi-quantitative real-time PCR (B) and Western blot (A), respectively. The expression levels of *Kit*, *Pax3*, *Mitf*, *Sox10*, and *Sox9* did not differ substantially between cells transfected with the *Ets1* overexpression vector and those transfected with empty vector. Data represent gene expression levels in cells transfected with PCMV-HA-Ets1 relative to those transfected with PCMV-HA. The mean (bar height) and standard deviation (error bars) are shown for 3 independent experiments carried out in triplicates.

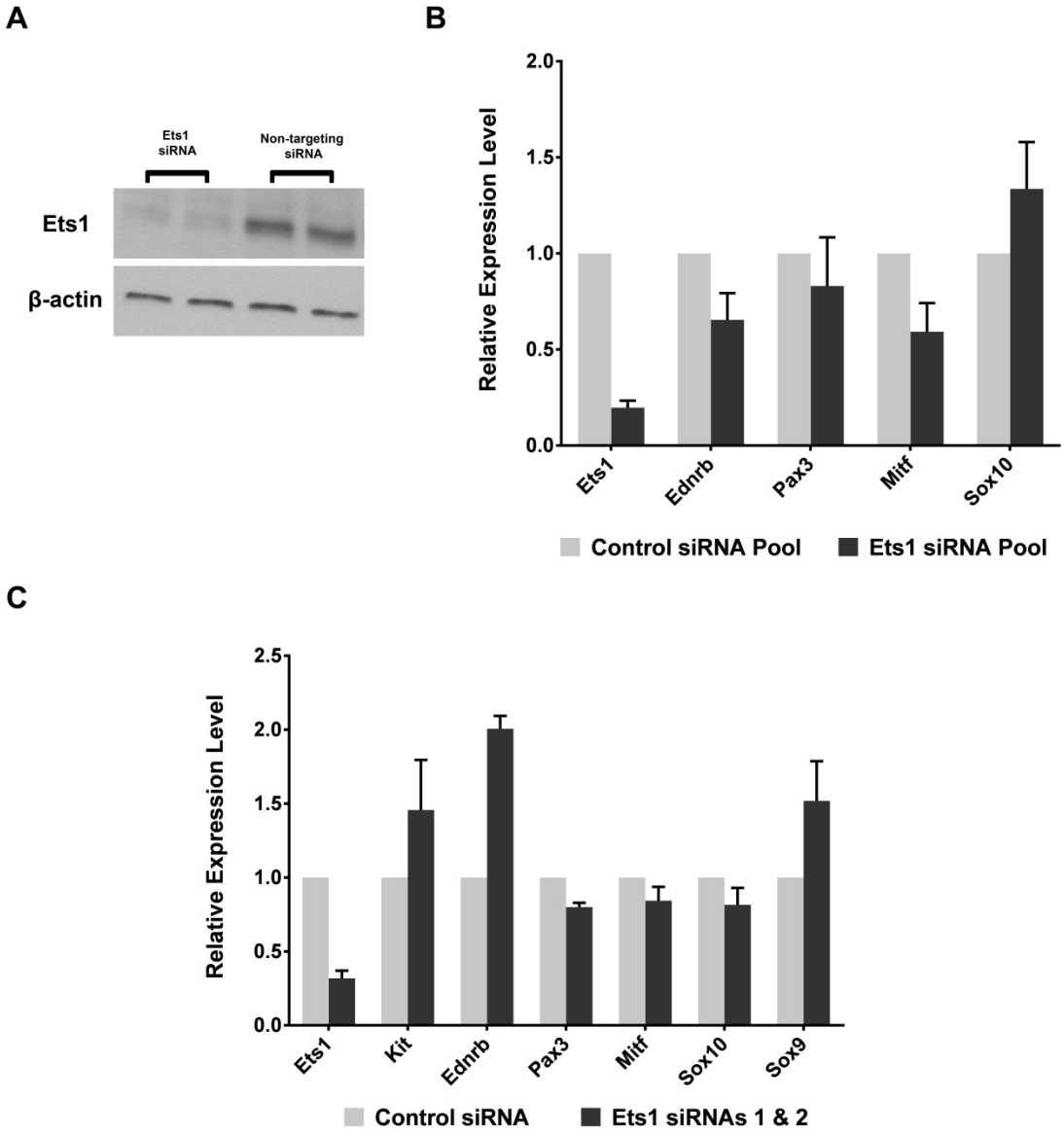

Figure 5.4. *Ets1* knockdown in melan-a cells does not substantially affect the expression of melanoblast-specific genes. Melan-a cells were transfected with an Ets1 siRNA pool or a non-targeting control siRNA pool (A & B), or with 2 individual siRNAs from the siRNA pool and a different individual control siRNA (C). Knockdown was confirmed via Western blot (A) and semi-quantitative real-time PCR (B & C). The levels of *Kit*, *Pax3*, *Mitf*, *Sox10*, and *Sox9* did not differ considerably between cells transfected with the Ets1 siRNAs and those transfected with the non-targeting control siRNAs. *Ednrb* expression appeared to be slightly upregulated in cells transfected with individual Ets1 siRNAs, but this effect on *Ednrb* was not observed in cells transfected with the Ets1 siRNA pool. Data represent gene expression levels in cells transfected with Ets1 siRNAs relative to those transfected with control siRNAs. The mean (bar height) and standard deviation (error bars) are shown for 3 independent experiments carried out in triplicates.

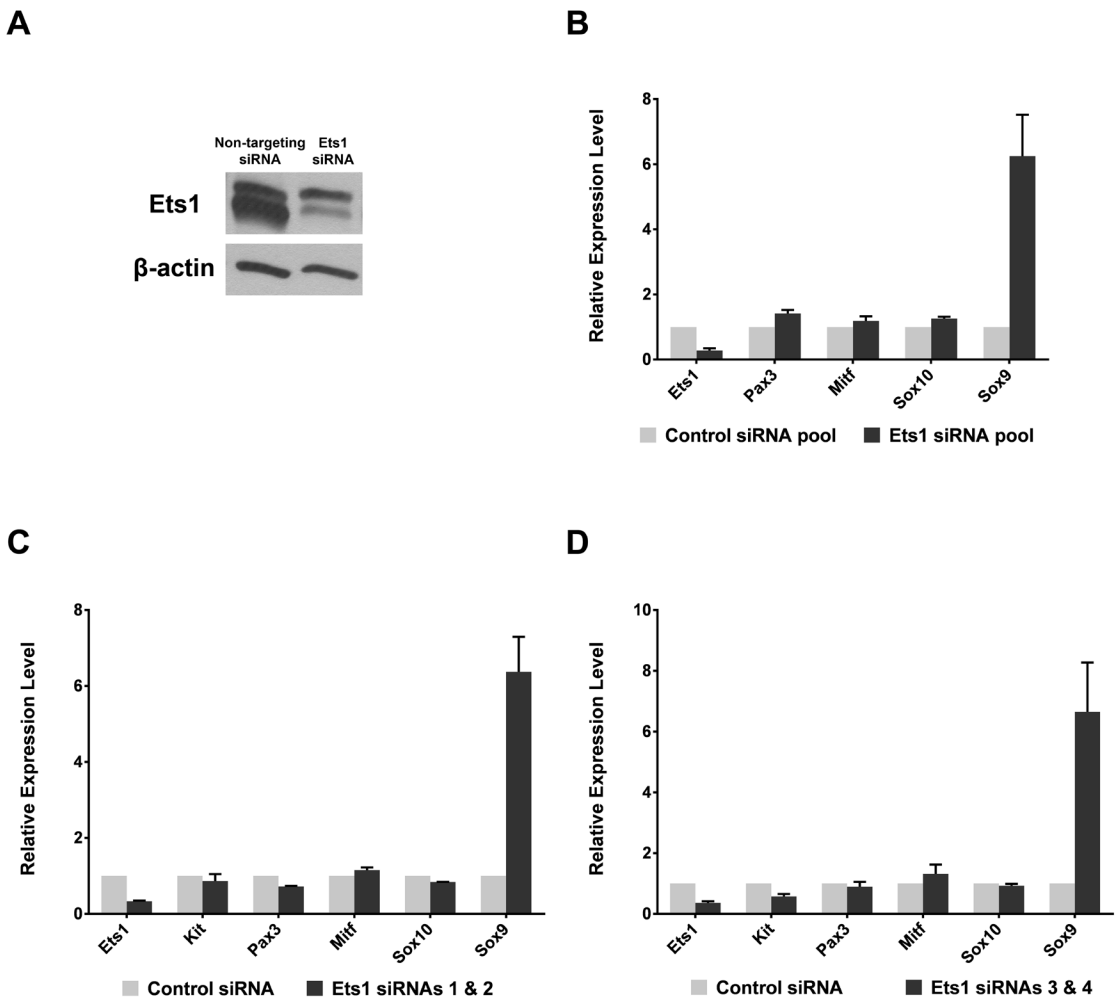

Figure 5.5. *Ets1* knockdown in B16 melanoma cells results in *Sox9* upregulation. B16 cells were transfected with an Ets1 siRNA pool or a non-targeting control siRNA pool (A & B), or with 2 individual siRNAs from the siRNA pool and a different individual control siRNA (C & D). Knockdown was confirmed via Western blot (A) and semi-quantitative real-time PCR (B, C, D). (B, C, D) The expression levels of *Kit*, *Pax3*, *Mitf*, and *Sox10* did not differ substantially between cells transfected with Ets1 siRNA and those transfected with control siRNA. *Sox9* was notably upregulated in B16 cells transfected with Ets1 siRNAs compared to those transfected with control siRNAs. Data represent gene expression levels in cells transfected with Ets1 siRNAs relative to those transfected with control siRNAs. The mean (bar heights) and standard deviation (error bars) are shown for 3 independent experiments carried out in triplicates.

5.6. References

Adameyko, I., Lallemend, F., Aquino, J., Pereira, J., Topilko, P., Müller, T., Fritz, N., Beljajeva, A., Mochii, M., Liste, I., Usoskin, D., Suter, U., Birchmeier, C. and Ernfors, P. (2009). Schwann cell precursors from nerve innervation are a cellular origin of melanocytes in skin. *Cell* 139, 366–379.

Bakos, R., Maier, T., Besch, R., Mestel, D., Ruzicka, T., Sturm, R. and Berking, C. (2010). Nestin and SOX9 and SOX10 transcription factors are coexpressed in melanoma. *Experimental dermatology* 19, e89–94.

Bell, D., Leung, K., Wheatley, S., Ng, L., Zhou, S., Ling, K., Sham, M., Koopman, P., Tam, P. and Cheah, K. (1997). SOX9 directly regulates the type-II collagen gene. *Nature genetics* 16, 174–178.

Betancur, P., Bronner-Fraser, M. and Sauka-Spengler, T. (2010). Genomic code for Sox10 activation reveals a key regulatory enhancer for cranial neural crest. *Proc. Natl. Acad Sci U.S.A.* 107, 3570–3575.

Bondurand, N., Pingault, V., Goerich, D., Lemort, N., Sock, E., Le Caignec, C., Wegner, M. and Goossens, M. (2000). Interaction among SOX10, PAX3 and MITF, three genes altered in Waardenburg syndrome. *Human molecular genetics* 9, 1907–1917.

Cheung, M. and Briscoe, J. (2003). Neural crest development is regulated by the transcription factor Sox9. *Development* 130, 5681-5693.

Cheung, M., Chaboissier, M.-C., Mynett, A., Hirst, E., Schedl, A. and Briscoe, J. (2005). The transcriptional control of trunk neural crest induction, survival, and delamination. *Developmental cell* 8, 179–192.

Colombo, S., Champeval, D., Rambow, F. and Larue, L.(2011). Transcriptomic analysis of mouse embryonic skin cells reveals previously unreported genes expressed in melanoblasts. *The Journal of investigative dermatology* 132, 170–178.

Cook, A., Smith, A., Smit, D., Leonard, J. and Sturm, R. (2005). Co-expression of SOX9 and SOX10 during melanocytic differentiation in vitro. *Experimental cell research* 308, 222–235.

Du, J., Widlund, H., Horstmann, M., Ramaswamy, S., Ross, K., Huber, W., Nishimura, E., Golub, T. and Fisher, D. (2004). Critical role of CDK2 for melanoma growth linked to its melanocyte-specific transcriptional regulation by MITF. *Cancer cell* 6, 565–576.

Gao, Z., Kim, G., Mackinnon, A., Flagg, A., Bassett, B., Earley, J. and Svensson, E. (2010). Ets1 is required for proper migration and differentiation of the cardiac neural crest. *Development* 137, 1543–1551.

Guo, X.-L., Ruan, H.-B., Li, Y., Gao, X. and Li, W. (2010). Identification of a novel nonsense mutation on the Pax3 gene in ENU-derived white belly spotting mice and its genetic interaction with c-Kit. *Pigment cell & melanoma research* 23, 252–262.

Harris, M. L., Baxter, L. L., Loftus, S. K. and Pavan, W. J. (2010). Sox proteins in melanocyte development and melanoma. *Pigment Cell & Melanoma Research* 23, 456-513.

Hong, C.-S. and Saint-Jeannet, J.-P. (2005). Sox proteins and neural crest development. *Seminars in Cell & Developmental Biology* 16, 694-703.

Hou, L., Panthier, J. and Arnheiter, H. (2000). Signaling and transcriptional regulation in the neural crest-derived melanocyte lineage: interactions between KIT and MITF. *Development* 127, 5379–5389.

Hou, L., Arnheiter, H. and Pavan, W. (2006). Interspecies difference in the regulation of melanocyte development by SOX10 and MITF. *Proc. Natl. Acad Sci U.S.A.* 103, 9081–9085.

Hou, L. and Pavan, W. (2008). Transcriptional and signaling regulation in neural crest stem cell-derived melanocyte development: do all roads lead to Mitf? *Cell research* 18, 1163–1176.

Lang, D., Lu, M., Huang, L., Engleka, K., Zhang, M., Chu, E., Lipner, S., Skoultchi, A., Millar, S. and Epstein, J.(2005). Pax3 functions at a nodal point in melanocyte stem cell differentiation. *Nature* 433, 884–887.

Le Douarin, N. and Kalcheim, C. (1999). The neural crest. Cambridge: Cambridge University Press.

Lee, Y.-H. and Saint-Jeannet, J.-P. (2011). Sox9 function in craniofacial development and disease. *Genesis* 49, 200-208.

Levy, C., Khaled, M. and Fisher, D. (2006). MITF: master regulator of melanocyte development and melanoma oncogene. *Trends in molecular medicine* 12, 406–414.

Lin, J. and Fisher, D. (2007). Melanocyte biology and skin pigmentation. *Nature* 445, 843–850.

Livak, K. and Schmittgen, T. (2001). Analysis of relative gene expression data using real-time quantitative PCR and the 2(-Delta Delta C(T)) Method. *Methods* 25, 402–408.

McGill, G. G., Horstmann, M., Widlund, H. R., Du, J., Motyckova, G., Nishimura, E. K., Lin, Y.-L., Ramaswamy, S., Avery, W. and Ding, H.-F. (2002). Bcl2 regulation by the melanocyte master regulator Mitf modulates lineage survival and melanoma cell viability. *Cell* 109, 707-718.

McGill, G., Haq, R., Nishimura, E. and Fisher, D. (2006). c-Met expression is regulated by Mitf in the melanocyte lineage. *The Journal of biological chemistry* 281, 10365–10373.

Nagarajan, P., Parikh, N., Garrett-Sinha, L. and Sinha, S. (2008). Ets1 induces dysplastic changes when expressed in terminally-differentiating squamous epidermal cells. *PloS one* 4, e4179.

Passeron, T., Valencia, J., Bertolotto, C., Hoashi, T., Le Pape, E., Takahashi, K., Ballotti, R. and Hearing, V. (2007). SOX9 is a key player in ultraviolet B-induced melanocyte differentiation and pigmentation. *Proceedings of the National Academy of Sciences of the United States of America* 104, 13984–13989.

Passeron, T., Valencia, J. C., Namiki, T., Vieira, W. D., Passeron, H., Miyamura, Y. and Hearing, V. J. (2009). Upregulation of SOX9 inhibits the growth of human and mouse melanomas and restores their sensitivity to retinoic acid. *Journal of Clinical Investigation* 119, 954-963.

Potterf, S., Furumura, M., Dunn, K., Arnheiter, H. and Pavan, W. (2000). Transcription factor hierarchy in Waardenburg syndrome: regulation of MITF expression by SOX10 and PAX3. *Human genetics* 107, 1–6.

Qin, Y., Kong, L., Poirier, C., Truong, C., Overbeek, P. and Bishop, C. (2004). Long-range activation of Sox9 in Odd Sex (Ods) mice. *Human molecular genetics* 13, 1213–1218.

Rao, P., Fuller, G. and Prieto, V. (2010). Expression of Sox-9 in metastatic melanoma--a potential diagnostic pitfall. *The American Journal of dermatopathology* 32, 262–266.

Saldana-Caboverde, A. and Kos, L. (2010). Roles of endothelin signaling in melanocyte development and melanoma. *Pigment cell & melanoma research* 23, 160–170.

Seong, I., Min, H., Lee, J.-H., Yeo, C.-Y., Kang, D., Oh, E.-S., Hwang, E. and Kim, J. (2011). Sox10 controls migration of B16F10 melanoma cells through multiple regulatory target genes. *PloS one* 7, e31477.

Silver, D., Hou, L. and Pavan, W. (2006). The genetic regulation of pigment cell development. Georgetown: Landes Biosciences, 155-169.

Sommer, L. (2005). Checkpoints of melanocyte stem cell development. *Science Signaling* 2005, pe42.

Spokony, R., Aoki, Y., Saint-Germain, N., Magner-Fink, E., and Saint-Jeannet, J.-P. (2002). The transcription factor Sox9 is required for cranial neural crest development in Xenopus. *Development* 129, 421-432

Steel, K., Davidson, D. and Jackson, I. (1992). TRP-2/DT, a new early melanoblast marker, shows that steel growth factor (c-kit ligand) is a survival factor. *Development* 115, 1111-1119.

Sviderskaya, E., Wakeling, W. and Bennett, D. (1995). A cloned, immortal line of murine melanoblasts inducible to differentiate to melanocytes. *Development* 121, 1547–1557.

Wagner, T., Wirth, J., Meyer, J., Zabel, B., Held, M., Zimmer, J., Pasantes, J., Bricarelli, F., Keutel, J., Hustert, E., Wolf, U., Tommerup, N., Schempp, W. and Scherer, G. (1994). Autosomal sex reversal and campomelic dysplasia are caused by mutations in and around the SRY-related gene SOX9. *Cell* 79, 1111–1120.

Watanabe, A., Takeda, K., Ploplis, B. and Tachibana, M. (1998). Epistatic relationship between Waardenburg syndrome genes MITF and PAX3. *Nature genetics* 18, 283–286.

CHAPTER VI

CONCLUSIONS AND FUTURE DIRECTIONS

VI. CONCLUSIONS AND FUTURE DIRECTIONS

6.1 Conclusions

Melanocytes, the pigment producing cells, are responsible for hair and skin pigmentation, which serves to protect organisms from damaging ultraviolet (UV) radiation (Lin and Fisher, 2007). The skin is the most common site of cancer in humans. Of all the types of skin cancers, melanoma, the cancer resulting from the malignant transformation of melanocytes, is the least common but is responsible for the highest number of skin cancer-related deaths in the United States (American Cancer Society, 2014). Melanocytes are derived from neural crest (NC) cells, a population of pluripotent cells that arise from the dorsal aspect of the neural tube during vertebrate development (Le Douarin and Kalcheim, 1999). Melanocyte development is guided by the activation of transcription factors and by signaling molecules encountered by melanocyte precursors (melanoblasts) during their migration. Pigmentation mutants of various species have provided insight into the molecular pathways at work in melanocyte development and pigment production. These mutants have also served as models of human pigmentation disorders, including piebaldism, the four known types of Waardenburg Syndrome, and albinism (reviewed in Baxter et al., 2004).

The deletion of the transcription factor *Ets1* was recently found to result in hypopigmentation in mice (Gao et al., 2010). The aim of this study was to establish the temporal requirement and role of *Ets1* during melanocyte development and to characterize genetic and molecular interactions between *Ets1* and other genes required for melanocyte development. To this end, a combination of in vivo assays, genetic crosses, and in vitro molecular assays were employed.

In Chapter 2, the effect of *Ets1* deletion on melanoblast and NC cell survival were described. To establish the temporal requirement and mechanism of action of *Ets1* during melanocyte development, *Dct-LacZ* transgenic mice in which *LacZ* expression is driven to melanoblasts under the control of the Dopachrome tautomerase (*Dct*) promoter, were used to label melanoblasts via β-galactosidase staining in *Ets1* null ($Ets1^{-/-}$), heterozygous ($Ets1^{+/-}$) , and wild type ($Ets1^{+/+}$) embryos. *Ets1* null embryos were found to have fewer melanoblasts, compared to heterozygous and wild type littermates, at all stages examined (Embryonic day (E) 10.75-E15.5). Melanoblast proliferation was not affected at E10.75, but a significant increase in melanoblast cell death was observed at this stage in *Ets1* null embryos compared to heterozygous littermates. At E10.25, NC cell survival was found to be negatively affected in *Ets1* null mutant embryos; however, the numbers of NC cells, labeled via Sox10 immunofluorescence, did not differ significantly between *Ets1* null and *Ets1* heterozygous embryos at this stage. Similarly, the amount and pattern of *Sox10* expression was found to be unaffected in *Ets1* null embryos at E9.5. These results suggest that *Ets1* is required between E10 and E11 in melanocyte development and that it regulates the melanoblast and NC cell survival at this stage.

Given the early melanoblast and NC cell survival defect observed in *Ets1* null mutant mice, it seemed likely that Ets1 would play a role in the regulation of one or more genes essential for the development of melanocytes and other NC cell derivatives. In Chapter 3, a genetic interactions approach was chosen to determine whether a synergistic genetic interaction exists between *Ets1* and the transcription factor *Sox10*. *Sox10* was chosen for this study because experiments in the avian system have shown that *Ets1* regulates *Sox10* expression in cranial NC cells (Betancur et al., 2010). By comparing the

frequency and area of hypopigmentation in single (*Ets1*$^{+/-}$ and *Sox10*$^{LacZ/+}$) and double heterozygous (*Ets1*$^{-/-}$*::Sox10*$^{LacZ/+}$) progeny from crosses between *Ets1* heterozygous and *Sox10* heterozygous mice, *Ets1* and *Sox10* were found to interact synergistically during melanocyte development.

In addition to its role in melanocyte development, the transcription factor *Sox10* is also required for proper gut innervation (Southard-Smith et al., 1998; Kapur, 1999). For this reason, the effect of *Ets1* deficiency on gut innervation was also examined. The nerve free area in the distal colon of *Ets1* null mice was found to be significantly greater than in *Ets1* heterozygous mice, indicating that *Ets1* is also important for the development of enteric ganglia, which are also derived from NC cells. Furthermore, *Sox10* heterozygosity was found to further exacerbate the decreased innervation observed in *Ets1* null mice. In fact, severe hypoganglionosis of the distal colon, which led to megacolon, was detected in two *Ets1*$^{-/-}$*::Sox10*$^{LacZ/+}$ mice.

In order to further characterize the nature of the synergistic genetic interaction between *Ets1* and *Sox10*, the amount and pattern of *Sox10* expression was compared in *Ets1* null, heterozygous, and wild type littermates. At E11.5 and E12.5 an apparent decrease in *Sox10* expression was observed in at least 50% of *Ets1* null embryos compared to *Ets1* heterozygous and wild type littermates. These results suggest that *Ets1* may regulate embryonic *Sox10* expression; however, they could also be indicative of a reduction in the number of Sox10 positive cells.

Synergistic genetic interactions may or may not indicate the presence of a functional interaction between the genes in question. In order to gain a better understanding of the underlying functional interaction that may exist between *Ets1* and

Sox10, the ability of Ets1 to activate the *Sox10*-MCS4 enhancer, an enhancer critical for *Sox10* expression in mouse melanocytes and melanoblasts (Antonellis et al., 2008) was analyzed in Chapter 4 via in vitro luciferase reporter assay. In the mouse melanoma cell line B16, Ets1 was able to activate this enhancer, suggesting a possible role for *Ets1* in the regulation of *Sox10* expression. In this chapter, the spontaneous *variable spotting* mutation, which causes hypopigmentation in mice and was suspected to be a mutation in *Ets1*, was confirmed to be a G-to-A nucleotide transition in exon 3 of the *Ets1* gene, which predicts in a Glycine to Glutamate amino acid change at position 102 of the Ets1 protein (G102E missense mutation). Given that *variable spotting* mutants exhibit a hypopigmentation phenotype, this mutation likely impairs Ets1 protein function, particularly as it relates to potential roles in the regulation of genes critical for melanocyte development. Consequently, this mutation provided a means to confirm the effect of Ets1 in *Sox10*-MCS4 enhancer activity. The *variable spotting* mutation led to a 2-fold decrease in the activation of the *Sox10*-MCS4 enhancer, which suggests that this mutation is hypomorphic, since it inhibits but does not completely abrogate Ets1 protein function. The ability of Ets1 to activate the *Sox10*-MCS4 enhancer and the effect of the *variable spotting* mutation on *Sox10*-MCS4 activation suggest that Ets1 may act as a regulator of *Sox10* expression during melanocyte development.

To assess the potential role of Ets1 in regulating *Sox10* expression, the effect of *Ets1* overexpression and knockdown on *Sox10* expression was investigated via semi-quantitative real-time PCR in Chapter 5. The expression of other genes critical for melanocyte development, including *Pax3*, *Mitf*, *Kit*, *Sox9*, and *Ednrb* was also examined. *Ets1* overexpression and knockdown were carried out in mouse melanocyte and

melanoma cell lines because mouse melanoblast survival is severely impaired by traditional transfection protocols. The expression levels of *Sox10*, *Pax3*, *Mitf*, *Kit*, and *Ednrb* were not significantly affected by *Ets1* overexpression or knockdown. Nonetheless, in mouse melanoma cells, *Ets1* knockdown led to approximately a 6-fold increase in the expression levels of the transcription factor *Sox9*. The lack of a change in the expression level of *Sox10* in cells where *Ets1* was knocked down, suggests that the interaction between *Ets1* and *Sox10* may be indirect. Alternatively, it is possible that in the cell lines used for this experiment other factors may be able to compensate for *Ets1* deficiency. In the case of *Ets1* overexpression, the absence of a significant change in the expression of *Sox10* or other potential downstream targets could result if the endogenous Ets1 protein is sufficient to drive the expression of said targets.

The expression of the transcription factor *Sox9* was significantly upregulated as a result of *Ets1* knockdown in mouse melanoma cells. *Sox9* has been implicated in the development of melanocytes and other NC cell derivatives (reviewed in Hong and Saint-Jeannet, 2005; Silver et al., 2006; Lee and Saint-Jeannet, 2011). Sox9, along with Ets1, is required for *Sox10* expression in cranial NC cells in the chick embryo (Betancur et al., 2010). In the mouse, *Sox9* has been shown to be required for the survival of trunk NC cells (Cheung et al., 2005) and for the formation of NC-derived chondrocytes (Bell et al., 1997). The apparent role of *Ets1* as a negative regulator of *Sox9* appears to be in contradiction with the essential functions of *Sox9* in early NC development; however, ectopic and prolonged *Sox9* expression has been shown to negatively affect melanocyte development (Qin et al., 2004), possibly because *Sox9* is involved in chondrocyte fate specification. For this reason, Ets1-induced *Sox9* repression may be important for

melanocyte differentiation by preventing the activation of genes critical for chondrocyte differentiation. It is possible that in trunk NC cells destined to become melanocytes, *Ets1* serves as a repressor of chondrocyte fate.

Together, the results of this study suggest that *Ets1* plays a dual role in melanocyte development. The transcription factor Ets1 acts early during melanocyte development by regulating the survival of NC cells and melanoblasts. The early role of *Ets1* in NC and melanoblast survival may be mediated through an interaction with the transcription factor *Sox10*. The synergistic genetic interaction between *Ets1* and *Sox10*, and the ability of Ets1 to activate *Sox10* regulatory regions required for embryonic *Sox10* expression support this possibility. In addition to being required early for NC and melanoblast survival, *Ets1* may also be indirectly involved in melanocyte fate specification by acting as a repressor of cartilage fate.

6.2. Future Directions

This study provided insights into the role of the transcription factor *Ets*1 in melanocyte development and its interaction with the transcription factor *Sox10* in this process. Future research will focus on characterizing the molecular interaction between Ets1 and Sox10 and Ets1 and Sox9, and on in vivo experiments aimed at understanding whether the regulatory role of Ets1 on *Sox9* expression impacts melanocyte development.

Although an apparent decrease in *Sox10* expression was observed in *Ets1* null mutant embryos compared to heterozygous and wild type littermates, additional experiments, involving the labeling and quantification of Sox10 positive cells, are needed to determine whether *Ets1* does in fact regulate embryonic *Sox10* expression, or whether this apparent decrease in *Sox10* expression is the result of a decrease in the number of

Sox10 positive cells. *Sox10* expression was found to be unaffected by *Ets1* knockdown and overexpression in mouse melanocyte and melanoma cell lines; however, these cell lines do not accurately represent the conditions present in melanoblasts. Given the difficulties involved with the transfection of melanoblasts, experiments involving viral infection as a means of overexpressing and knocking down *Ets1* will be useful in addressing a potential role for Ets1 in regulating *Sox10* expression during melanocyte development. Mouse NC cultures from *Ets1* null, heterozygous and wild type embryos may also be able to provide some insight regarding the timing during which *Ets1* is critical for melanocyte development and the regulation of other genes critical in this process. Neural crest cultures can also be used as a tool to assay the effect of *Ets1* deficiency on migration and fate specification.

Using in vitro luciferase reporter assay Ets1 was shown to activate the *Sox10*-MCS4 enhancer. Bioinformatic analysis revealed the presence of 4 putative Ets1 binding sites in this enhancer, which suggests that Ets1 may act by directly binding this *Sox10* regulatory region. Mutation or deletion of the putative Ets1 binding sites within *Sox10*-MCS4, along with Chromatin Immunoprecipitation (ChIP) assays may provide some insight into whether the effect of Ets1 is mediated by direct binding to the *Sox10*-MCS4 enhancer. It will also be important to characterize the effects of the *variable spotting* mutation on Ets1 protein function in order to understand how this mutation affects the activation of downstream targets.

Gene expression analysis revealed a negative relationship between Ets1 and the transcription factor Sox9 in mouse melanoma cells; however, it is unclear whether this relationship exists in melanoblasts, and whether it is relevant in vivo. Future experiments

should be aimed at characterizing *Sox9* expression in *Ets1* mutant embryos in vivo, and in mouse melanoblasts and NC cells in vitro, using similar methods as aforementioned. If *Sox9* is found to be upregulated in *Ets1* mutant mice, a detailed characterization of chondrocyte precursor numbers and location could provide insight into a putative role for Ets1 in NC lineage specification. The effect of *Ets1* overexpression on *Sox9* promoter activation, in cells known to express *Sox9*, and direct binding of Ets1 to the *Sox9* promoter, should also be assayed to determine whether Ets1 inhibits *Sox9* expression directly or indirectly.

In this study we also characterized the effect of *Ets1* deficiency on the development of enteric ganglia, which also derive from the NC. This study provided evidence to support a role for *Ets1* in gut innervation and a potential interaction with *Sox10* in this process. Additional cell survival and proliferation assays to compare the numbers of dying and proliferating enteric ganglia precursor cells in $Ets1^{-/-}::Sox10^{+/+}$ and $Ets1^{-/-}::Sox10^{LacZ/+}$ embryos are needed to determine whether *Ets1* and *Sox10* work together to promote the survival and/or proliferation of these cells.

The results of this study in combination with the future work proposed will provide a better understanding of the gene regulatory network directing melanocyte development. A detailed characterization of this network is critical because alterations in genes required for the development of melanocytes and other NC cell derivatives have been recognized in human pathological conditions, including cancer. Many of the genes required for melanocyte survival, proliferation, migration, and/or differentiation during embryogenesis, have also been linked to melanoma development and progression. Some transcription factors, such as *Mitf*, *Pax3*, *Sox10* and *Lef1*, which are required for

melanocyte development, have also been found to be either amplified or up-regulated in melanoma tumors compared to normal melanocytes (Larue and Delmas, 2006; Levi et al., 2006; Kubic et al., 2008; Plummer et al., 2008; Flamminger et al., 2009; Bakos et al., 2010). Several studies have also reported increased *Ets1* expression in melanoma lesions, compared to benign melanocytic lesions and primary melanocytes (Keehn et al., 2003; Rothhammer et al., 2004; Rothhamer et al., 2005). A better understanding of the signaling molecules and transcription factors involved in melanocyte development will be instrumental for the creation of more effective therapies against melanoma and other pathological conditions of melanocytes.

6.3. References

American Cancer Society (2014) Cancer Facts and Figures 2014. Atlanta, GA: American Cancer Society.

Antonellis, A., Bennett, W., Menheniott, T., Prasad, A., Lee-Lin, S.-Q., Green, E., Paisley, D., Kelsh, R., Pavan, W. and Ward, A. (2006). Deletion of long-range sequences at Sox10 compromises developmental expression in a mouse model of Waardenburg-Shah (WS4) syndrome. *Human molecular genetics* 15, 259–271.

Bakos, R., Maier, T., Besch, R., Mestel, D., Ruzicka, T., Sturm, R. and Berking, C. (2010). Nestin and SOX9 and SOX10 transcription factors are coexpressed in melanoma. *Experimental dermatology* 19, e89–94.

Baxter, L., Hou, L., Loftus, S. and Pavan, W. J. (2004). Spotlight on spotted mice: a review of white spotting mouse mutants and associated human pigmentation disorders. *Pigment cell research* 17, 215–224.

Bell, D., Leung, K., Wheatley, S., Ng, L., Zhou, S., Ling, K., Sham, M., Koopman, P., Tam, P. and Cheah, K. (1997). SOX9 directly regulates the type-II collagen gene. *Nature genetics* 16, 174–178.

Betancur, P., Bronner-Fraser, M. and Sauka-Spengler, T. (2010). Genomic code for Sox10 activation reveals a key regulatory enhancer for cranial neural crest. *Proc. Natl. Acad Sci U.S.A.* 107, 3570–3575.

Cheung, M., Chaboissier, M.-C., Mynett, A., Hirst, E., Schedl, A. and Briscoe, J. (2005). The transcriptional control of trunk neural crest induction, survival, and delamination. *Developmental cell* 8, 179–192.

Flammiger, A., Besch, R., Cook, A., Maier, T., Sturm, R. and Berking, C. (2009). SOX9 and SOX10 but not BRN2 are required for nestin expression in human melanoma cells. *The Journal of investigative dermatology* 129, 945–953.

Gao, Z., Kim, G., Mackinnon, A., Flagg, A., Bassett, B., Earley, J. and Svensson, E. (2010). Ets1 is required for proper migration and differentiation of the cardiac neural crest. *Development* 137, 1543–1551.

Hong, C.-S. and Saint-Jeannet, J.-P. (2005). Sox proteins and neural crest development. *Seminars in Cell & Developmental Biology* 16, 694-703.

Kapur, R. P. (1999). Early death of neural crest cells is responsible for total enteric aganglionosis in Sox10(Dom)/Sox10(Dom) mouse embryos. *Pediatric and developmental pathology* 2, 559–569.

Keehn, C., Smoller, B. and Morgan, M. (2003). Expression of the ets-1 proto-oncogene in melanocytic lesions. *Modern Pathology* 16, 772–777.

Kubic, J., Young, K., Plummer, R., Ludvik, A. and Lang, D.(2008). Pigmentation PAX-ways: the role of Pax3 in melanogenesis, melanocyte stem cell maintenance, and disease. *Pigment cell & melanoma research* 21, 627–645.

Larue, L. and Delmas, V. (2006). The WNT/Beta-catenin pathway in melanoma. *Frontiers in Bioscience* 11, 733-742.

Le Douarin, N. and Kalcheim, C. (1999). The neural crest, 2nd ed. Cambridge: Cambridge University Press.

Lee, Y.-H. and Saint-Jeannet, J.-P. (2011). Sox9 function in craniofacial development and disease. *Genesis* 49, 200-208.

Levy C., Khaled M. and Fisher D.E. (2006). MITF: master regulator of melanocyte development and melanoma oncogene. *Trends in Molecular Medicine* 2, 408-414.

Lin, J. and Fisher, D. (2007). Melanocyte biology and skin pigmentation. *Nature* 445, 843–850.

Plummer R. S., Shea C. R., Nelson M., Powell S. K., Freeman D. M., Dan C. P. and Lang, D. (2008). PAX3 expression in primary melanomas and nevi. *Modern pathology* 21, 525-530.

Qin, Y., Kong, L., Poirier, C., Truong, C., Overbeek, P. and Bishop, C. (2004). Long-range activation of Sox9 in Odd Sex (Ods) mice. *Human molecular genetics* 13, 1213–1218.

Rothhammer, T., Hahne, J., Florin, A., Poser, I., Soncin, F., Wernert, N. and Bosserhoff, A.-K. (2003). The Ets-1 transcription factor is involved in the development and invasion of malignant melanoma. *Cellular and molecular life sciences : CMLS* 61, 118–128.

Rothhammer, T., Poser, I., Soncin, F., Bataille, F., Moser, M. and Bosserhoff, A.-K. (2005). Bone morphogenic proteins are overexpressed in malignant melanoma and promote cell invasion and migration. *Cancer research* 65, 448–456.

Silver, D., Hou, L. and Pavan, W. (2006). The genetic regulation of pigment cell development. Georgetown: Landes Biosciences, 155-169.

Southard-Smith, E., Kos, L. and Pavan, W. (1998). Sox10 mutation disrupts neural crest development in Dom Hirschsprung mouse model. *Nature Genetics* 18, 60–64.

APPENDICES

APPENDIX I

A. Transformation

For each plasmid used, transformation into *Escherichia coli* Dh5α^{TM}-T1^{R} chemically competent cells (Life Technologies) was carried out as follows. A vial of *E. coli* Dh5α competent cells (Life Technologies) containing 50µl of cell suspension was removed from -80˚C and thawed on ice. Working near a flame, 1µl of 100-200ng/µl plasmid DNA was added to the vial of chemically competent cells. The tube was closed tightly and the cells gently mixed by tapping the tube 2 times. Cells were incubated on ice for 30 minutes. Cells were then heat shocked at 42˚C (in a water bath) for 30 seconds and incubated on ice for 5 minutes. After 5 minutes, working near a flame, 250µl of room temperature S.O.C medium (Life Technologies) was added to the vial of cells. Cells were then incubated at 37˚C for 1 hour, rocking at 250 RPM. Working near a flame, cells were spread on pre-warmed Luria Broth (LB) agar plates (1% Bacto-Tryptone (BD Biosciences), 0.5% yeast extract (Fisher Scientific), 1% NaCl (Fisher Scientific), 1.5% agarose (Fisher Scientific)), containing 100µg/ml Ampicillin (Fisher Scientific). The following dilutions were plated: 20µl of cell suspension + 80µl of LB, 50µl of cell suspension + 50µl of LB, or 100µl of undiluted cell suspension. Sterile, flamed Pasteur pipets were used to spread cell suspensions on the LB agar plates. Plates were allowed to dry at room temperature, near a flame for 15 minutes and then incubated overnight, upside down at 37˚C.

B. Pre-culture and Overnight Culture Preparation

Plates containing transformed cells were removed from the 37˚C incubator after overnight incubation following transformation. Working near a flame, individual colonies from each plate were carefully selected, using a different sterile pipet tip for each colony, and placed in sterile 15ml conical tubes (Fisher Scientific) containing 3ml of LB media with 100µg/ml Ampicillin (Fisher Scientific). Tubes were incubated at 37˚C, for 8 hours. For colonies that produced growth, 100µl of pre-culture were added to a sterile 50ml centrifuge tube containing 10ml of LB media with 100µg/ml Ampicillin. Cultures were incubated overnight (no more than 16 hours).

C. Glycerol Stock Preparation

Plasmid purification was carried out using the Promega Wizard Plus SV Minipreps DNA Purification System (Promega) or the QIAprep Spin Miniprep Kit (Qiagen), following the manufacturer's instructions. Approximately 8ml of overnight culture were used for plasmid purification (2 minipreps of 4ml each). The remaining 2ml of culture were used to prepare glycerol stocks (between 3 and 4 stocks per construct).

Glycerol stocks were prepared from overnight cultures for cryopreservation. Working near a flame 600µl of filtered, sterile 50% Glycerol (Fisher Scientific) were added to a 2ml cryovial (Corning). Subsequently 400µl of overnight culture were added to the vial, which was then sealed tightly. Cells were mixed very gently by tapping the tube 3 times. Cryovials were then placed on ice and transferred to -80˚C for long term storage.

Note: The cultures used for glycerol stocks were confirmed to contain the desired plasmid prior to preparing the glycerol stock. For plasmids used for in situ hybridization riboprobe synthesis, purified plasmids were visualized via gel electrophoresis (1% agarose). Plasmids used for transfections into mammalian cells (luciferase and overexpression assays) were analyzed via Polymerase Chain Reaction (PCR) or DNA sequencing.

APPENDIX II

Embryo Powder

E15.5 embryos were dissected in cold PBS (pH7.4). Embryos were homogenized in PBS by passing the embryos first through a 1ml pipette and then through a syringe with 18gauge 1 ½ inch needle. The homogenized embryos were transferred to a sterile 50ml centrifuge tube (Corning). Four volumes of cold acetone were added to the homogenized embryos. The embryos were incubated in ice for 30 minutes and centrifuged at 10,000g, for 10 minutes at 4˚C. The supernatant was discarded and the pellet was washed with cold acetone, and centrifuged once again at 10,000g, for 10 minutes at 4˚C. The supernatant was discarded and the pellet was placed in a mortar and macerated into a fine powder using a pestle. The embryo powder was placed on a sheet of filter paper and air-dried overnight at room temperature. The embryo powder was transferred to sterile 2ml centrifuge tubes and stored at 4˚C.

APPENDIX III

A. Normal Q-Q plots of original and transformed hypopigmentation area data for generation 1 (F1)

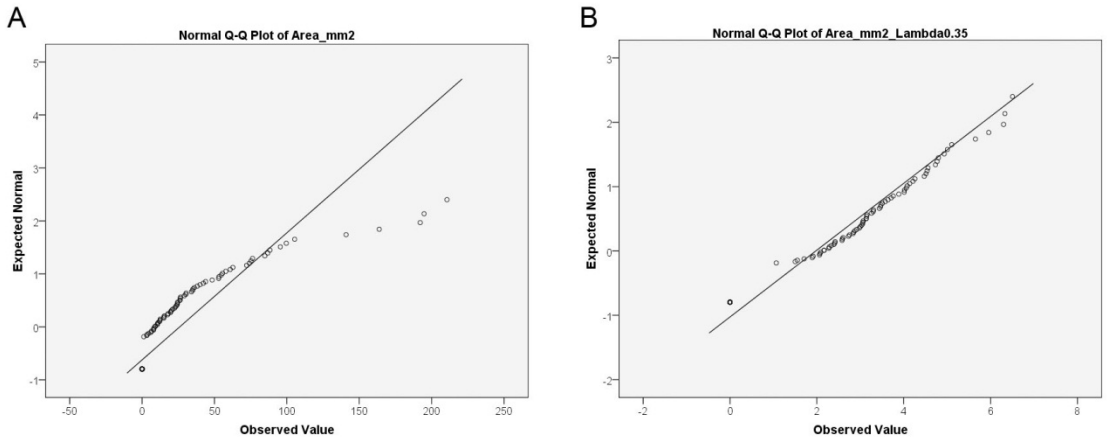

Figure A.1 Normal Q-Q plots of raw and transformed hypopigmentation area data for generation 1. Normal Q-Q plots before (A) and after (B) applying the Box-Cox transformation using a lambda value of 0.35. The transformed data have a distribution that more closely resembles the normal distribution.

B. PAWS Output for One-Way ANOVA and contrasts of hypopigmentation areas of Generation 1 (F_1)

Descriptives

Area_mm2_Lambda0.35

	N	Mean	Std. Deviation	Std. Error	95% Confidence Interval for Mean		Minimum	Maximum
					Lower Bound	Upper Bound		
Ets1+/-	46	1.1719	1.49371	.22024	.7283	1.6155	.00	4.93
Sox10+/-	42	1.2282	1.49597	.23083	.7620	1.6943	.00	4.21
Ets1+/-::Sox10+/-	33	4.0468	1.34398	.23396	3.5702	4.5233	.00	6.50
Total	121	1.9755	1.92505	.17500	1.6290	2.3220	.00	6.50

Table A.1. Descriptive statistics for Box-Cox-transformed hypopigmentation area data for generation 1.

Test of Homogeneity of Variances

Area_mm2_Lambda0.35

Levene Statistic	df1	df2	Sig.
3.200	2	118	.044

Table A.2. Levene's test of Homogeneity of Variances for the areas of hypopigmentation of *Ets1*$^{+/-}$, *Sox10*$^{LacZ/+}$, and *Ets1*$^{+/-}$*::Sox10*$^{LacZ/+}$ mice in generation 1. The population variances are significantly different ($p=0.044$, $\alpha=0.05$).

ANOVA

Area_mm2_Lambda0.35

	Sum of Squares	df	Mean Square	F	Sig.
Between Groups	194.741	2	97.370	45.967	.000
Within Groups	249.958	118	2.118		
Total	444.699	120			

Table A.3. One-Way ANOVA for the areas of hypopigmentation of *Ets1*$^{+/-}$, *Sox10*$^{LacZ/+}$, and *Ets1*$^{+/-}$*::Sox10*$^{LacZ/+}$ mice in generation 1. The population means are significantly different ($p<0.001$, $\alpha=0.05$).

Contrast Coefficients

Contrast	Genotype		
	Ets1+/-	Sox10+/-	Ets1+/-::Sox10+/-
1	1	1	-2

Table A.4. Contrast Coefficients assigned to *Ets1*$^{+/-}$, *Sox10*$^{LacZ/+}$, and *Ets1*$^{+/-}$*::Sox10*$^{LacZ/+}$ mice in generation 1. These contrast coefficients were assigned to test whether the mean area of hypopigmentation of *Ets1*$^{+/-}$*::Sox10*$^{LacZ/+}$ mice was significantly greater than the sum of the mean areas of hypopigmentation of *Ets1*$^{+/-}$ and *Sox10*$^{LacZ/+}$ mice.

Contrast Tests

		Contrast	Value of Contrast	Std. Error	t	df	Sig. (2-tailed)
Area_mm2_ Lambda0.35	Assume equal variances	1	-5.6935	.59435	-9.579	118	.000
	Does not assume equal variances	1	-5.6935	.56633	-10.053	63.517	.000

Table A.5. Contrast test comparing the sum of the mean areas of hypopigmentation in *Ets1*$^{+/-}$ and *Sox10*$^{LacZ/+}$ mice to the mean area of hypopigmentation of *Ets1*$^{+/-}$*::Sox10*$^{LacZ/+}$ mice in generation 1. The mean area of hypopigmentation of *Ets1*$^{+/-}$*::Sox10*$^{LacZ/+}$ mice is significantly greater than the sum of the mean areas of hypopigmentation of *Ets1*$^{+/-}$ and *Sox10*$^{LacZ/+}$ mice (equal variances not assumed (Table A.2), $p<0.001$, $\alpha=0.05$).

C. Normal Q-Q plots of original and transformed hypopigmentation area data for generation 2 (F_2)

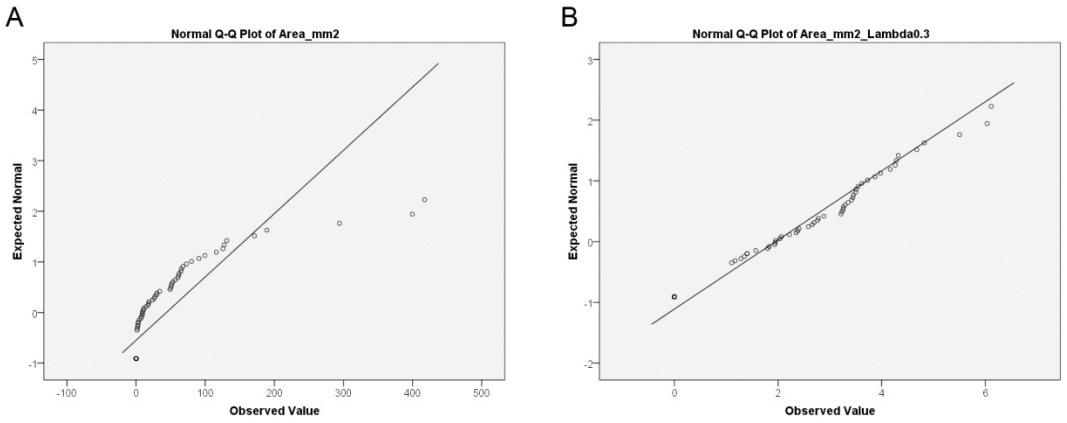

Figure A.2 Normal Q-Q plots of raw and transformed hypopigmentation area data for generation 2. Normal Q-Q plots before (A) and after (B) applying the Box-Cox transformation using a lambda value of 0.3. The transformed data have a distribution that more closely resembles the normal distribution.

D. PAWS Output for One-Way ANOVA and contrasts of hypopigmentation areas of Generation 2 (F_2)

Descriptives

Area_mm2_Lambda0.3

	N	Mean	Std. Deviation	Std. Error	95% Confidence Interval for Mean		Minimum	Maximum
					Lower Bound	Upper Bound		
Ets1+/-	29	.8388	1.14211	.21208	.4044	1.2732	.00	3.62
Sox10+/-	19	1.2997	1.36898	.31407	.6399	1.9595	.00	3.45
Ets1+/-::Sox10+/-	28	3.5491	1.30402	.24644	3.0435	4.0548	.00	6.11
Total	76	1.9526	1.75732	.20158	1.5510	2.3541	.00	6.11

Table A.6. Descriptive statistics for Box-Cox-transformed hypopigmentation area data for generation 2.

Test of Homogeneity of Variances

Area_mm2_Lambda0.3

Levene Statistic	df1	df2	Sig.
1.121	2	73	.332

Table A.7. Levene's test of Homogeneity of Variances for the areas of hypopigmentation of $Ets1^{+/-}$, $Sox10^{LacZ/+}$, and $Ets1^{+/-}::Sox10^{LacZ/+}$ mice in generation 2. The population variances are not significantly different ($p=0.332$, $\alpha=0.05$).

ANOVA

Area_mm2_Lambda0.3

	Sum of Squares	df	Mean Square	F	Sig.
Between Groups	115.443	2	57.722	36.272	.000
Within Groups	116.170	73	1.591		
Total	231.613	75			

Table A.8. One-Way ANOVA for the areas of hypopigmentation of $Ets1^{+/-}$, $Sox10^{LacZ/+}$, and $Ets1^{+/-}::Sox10^{LacZ/+}$ mice in generation 2. The population means are significantly different ($p<0.001$, $\alpha=0.05$).

Contrast Coefficients

Contrast	Genotype		
	Ets1+/-	Sox10+/-	Ets1+/-::Sox10+/-
1	1	1	-2

Table A.9. Contrast Coefficients assigned to $Ets1^{+/-}$, $Sox10^{LacZ/+}$, and $Ets1^{+/-}::Sox10^{LacZ/+}$ mice in generation 2. These contrast coefficients were assigned to test whether the mean area of hypopigmentation of $Ets1^{+/-}::Sox10^{LacZ/+}$ mice was significantly greater than the sum of the mean areas of hypopigmentation of $Ets1^{+/-}$ and $Sox10^{LacZ/+}$ mice.

Contrast Tests

		Contrast	Value of Contrast	Std. Error	t	df	Sig. (2-tailed)
Area_mm2_ Lambda0.3	Assume equal variances	1	-4.9597	.60495	-8.199	73	.000
	Does not assume equal variances	1	-4.9597	.62172	-7.977	53.392	.000

Table A.10. Contrast test comparing the sum of the mean areas of hypopigmentation in $Ets1^{+/-}$ and $Sox10^{LacZ/+}$ mice to the mean area of hypopigmentation of $Ets1^{+/-}::Sox10^{LacZ/+}$ mice in generation 2. The mean area of hypopigmentation of $Ets1^{+/-}::Sox10^{LacZ/+}$ mice is significantly greater than the sum of the mean areas of hypopigmentation of $Ets1^{+/-}$ and $Sox10^{LacZ/+}$ mice (equal variances assumed (Table A.7), $p<0.001$, $\alpha=0.05$).

E. Normal Q-Q plots of original and transformed hypopigmentation area data for generation 3 (F_3)

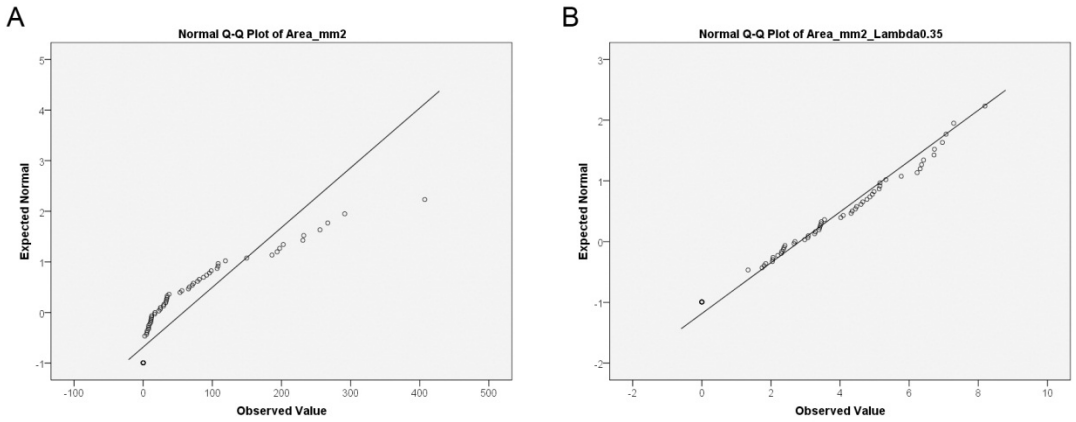

Figure A.3 Normal Q-Q plots of raw and transformed hypopigmentation area data for generation 3. Normal Q-Q plots before (A) and after (B) applying the Box-Cox transformation using a lambda value of 0.35. The transformed data have a distribution that more closely resembles the normal distribution.

F. PAWS Output for One-Way ANOVA and contrasts of hypopigmentation areas of Generation 3 (F_3)

Descriptives

Area_mm2_Lambda0.35

	N	Mean	Std. Deviation	Std. Error	95% Confidence Interval for Mean		Minimum	Maximum
					Lower Bound	Upper Bound		
Ets1+/-	26	1.1366	1.45646	.28564	.5484	1.7249	.00	4.32
Sox10+/-	17	1.4384	1.78357	.43258	.5213	2.3554	.00	5.77
Ets1+/-::Sox1o+/-	34	4.8214	1.63322	.28009	4.2516	5.3913	1.34	8.19
Total	77	2.8303	2.39041	.27241	2.2877	3.3729	.00	8.19

Table A.11. Descriptive statistics for Box-Cox-transformed hypopigmentation area data for generation 3.

Test of Homogeneity of Variances

Area_mm2_Lambda0.35

Levene Statistic	df1	df2	Sig.
.492	2	74	.613

Table A.12. Levene's test of Homogeneity of Variances for the areas of hypopigmentation of *Ets1*$^{+/-}$, *Sox10*$^{LacZ/+}$, and *Ets1*$^{+/-}$*::Sox10*$^{LacZ/+}$ mice in generation 3. The population variances are not significantly different ($p=0.613$, $\alpha=0.05$).

ANOVA

Area_mm2_Lambda0.35

	Sum of Squares	df	Mean Square	F	Sig.
Between Groups	242.313	2	121.156	46.707	.000
Within Groups	191.954	74	2.594		
Total	434.267	76			

Table A.13. One-Way ANOVA for the areas of hypopigmentation of *Ets1*$^{+/-}$, *Sox10*$^{LacZ/+}$, and *Ets1*$^{+/-}$*::Sox10*$^{LacZ/+}$ mice in generation 3. The population means are significantly different ($p<0.001$, $\alpha=0.05$).

Contrast Coefficients

Contrast	Genotype		
	Ets1+/-	Sox10+/-	Ets1+/-::Sox1o+/-
1	1	1	-2

Table A.14. Contrast Coefficients assigned to *Ets1*$^{+/-}$, *Sox10*$^{LacZ/+}$, and *Ets1*$^{+/-}$*::Sox10*$^{LacZ/+}$ mice in generation 3. These contrast coefficients were assigned to test whether the mean area of hypopigmentation of *Ets1*$^{+/-}$*::Sox10*$^{LacZ/+}$ mice was significantly greater than the sum of the mean areas of hypopigmentation of *Ets1*$^{+/-}$ and *Sox10*$^{LacZ/+}$ mice.

Contrast Tests

		Contrast	Value of Contrast	Std. Error	t	df	Sig. (2-tailed)
Area_mm2_ Lambda0.35	Assume equal variances	1	-7.0678	.74668	-9.466	74	.000
	Does not assume equal variances	1	-7.0678	.76323	-9.260	62.390	.000

Table A.15. Contrast test comparing the sum of the mean areas of hypopigmentation in *Ets1*$^{+/-}$ and *Sox10*$^{LacZ/+}$ mice to the mean area of hypopigmentation of *Ets1*$^{+/-}$*::Sox10*$^{LacZ/+}$ mice in generation 3. The mean area of hypopigmentation of *Ets1*$^{+/-}$*::Sox10*$^{LacZ/+}$ mice is significantly greater than the sum of the mean areas of hypopigmentation of *Ets1*$^{+/-}$ and *Sox10*$^{LacZ/+}$ mice (equal variances not assumed (Table A.12), $p<0.001$, $\alpha=0.05$).

APPENDIX IV

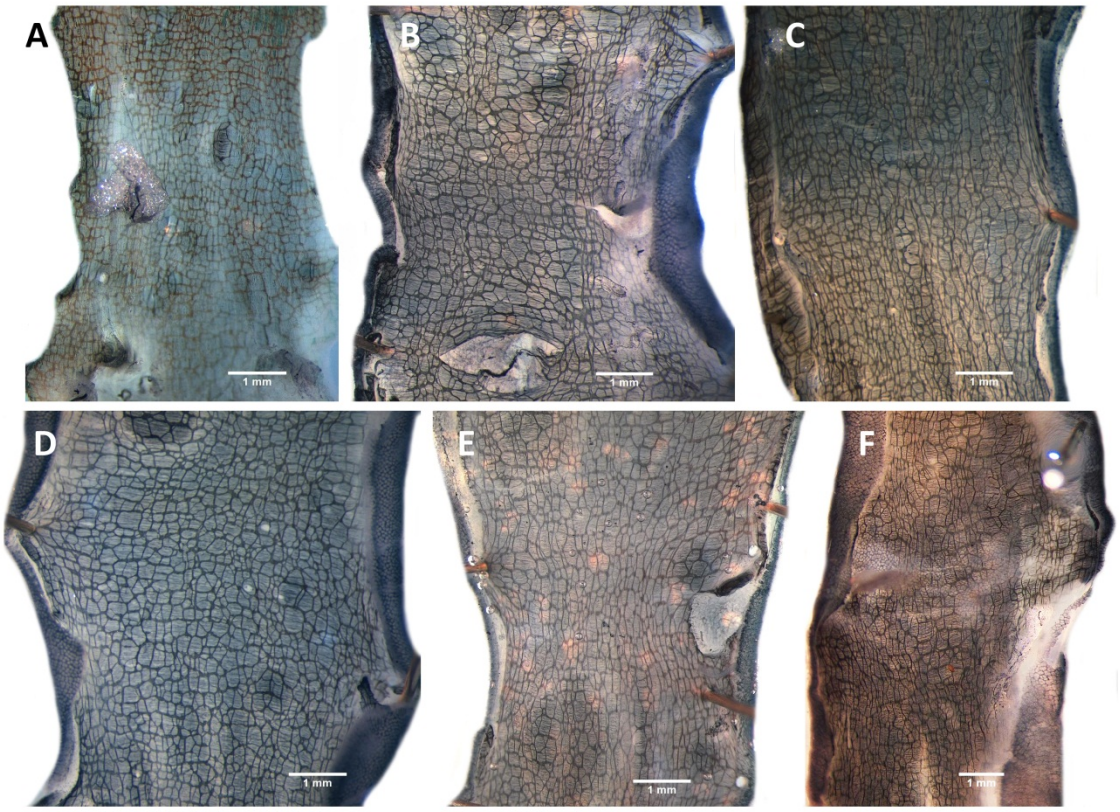

Figure A.4. Acetylcholinesterase staining on the distal portion of colons from *Ets1*$^{+/-}$*::Sox10*$^{+/+}$ mice. For each colon shown, the nerve free area in 8 randomly selected 0.25mm^2 squares was measured using the ImageJ Program (NIH) (Magnifications A-E = 16x, F=12.5x).

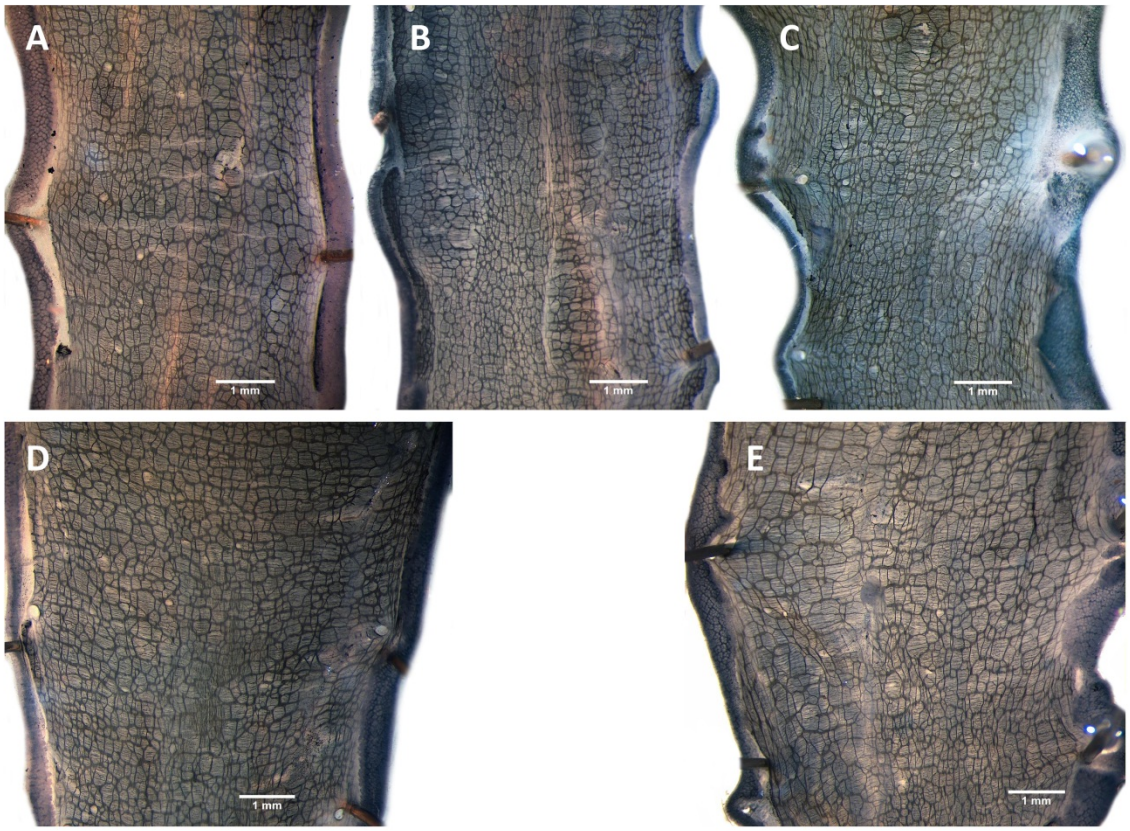

Figure A.5. Acetylcholinesterase staining on the distal portion of colons from *Ets1*$^{+/-}$*::Sox10*$^{LacZ/+}$ mice. For each colon shown, the nerve free area in 8 randomly selected 0.25mm^2 squares was measured using the ImageJ Program (NIH) (Magnifications A-E = 16x).

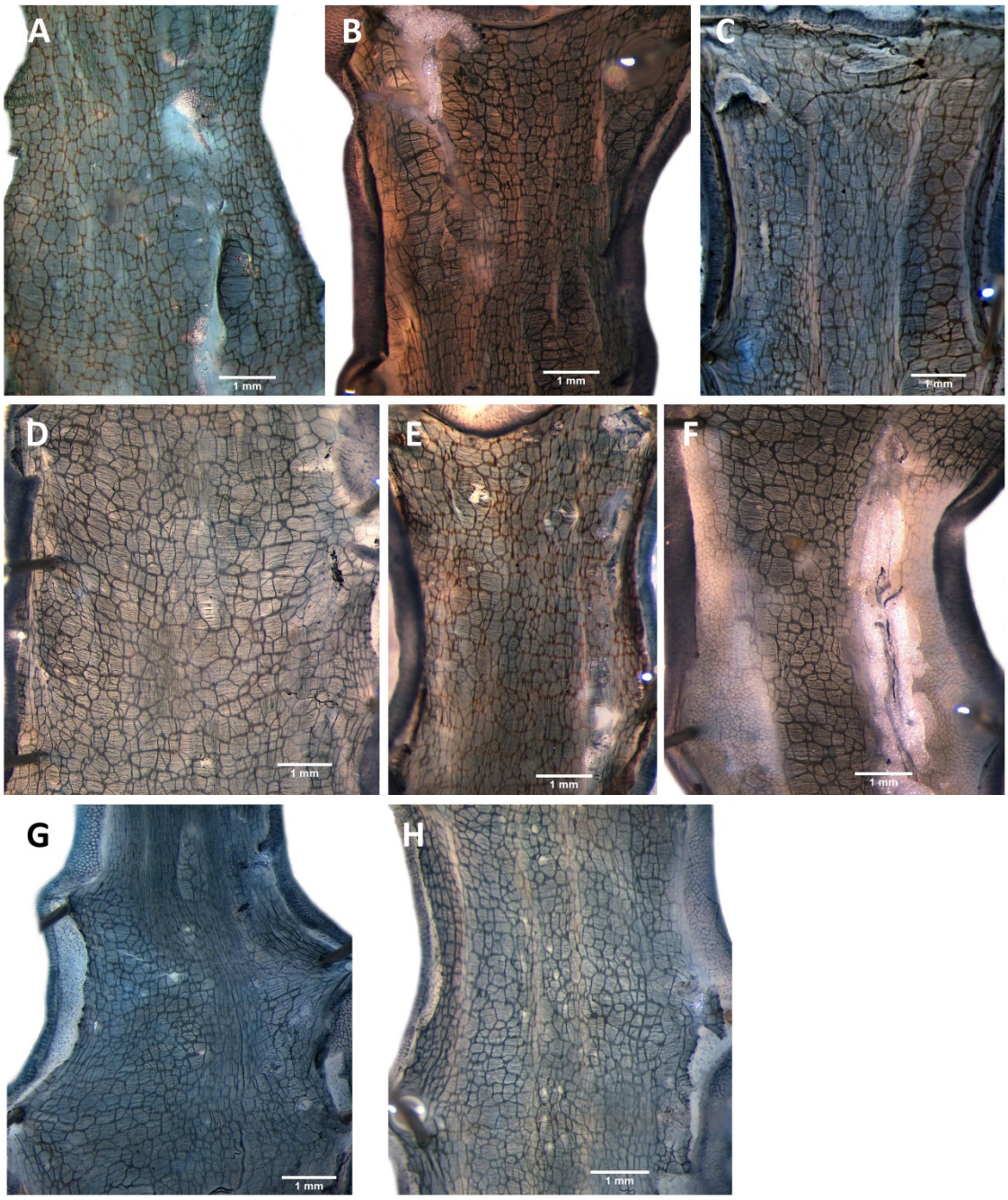

Figure A.6. Acetylcholinesterase staining on the distal portion of colons from *Ets1*$^{-/-}$ *::Sox10*$^{+/+}$ mice. For each colon shown, the nerve free area in 8 randomly selected 0.25mm^2 squares was measured using the ImageJ Program (NIH) (Magnifications A-H = 16x).

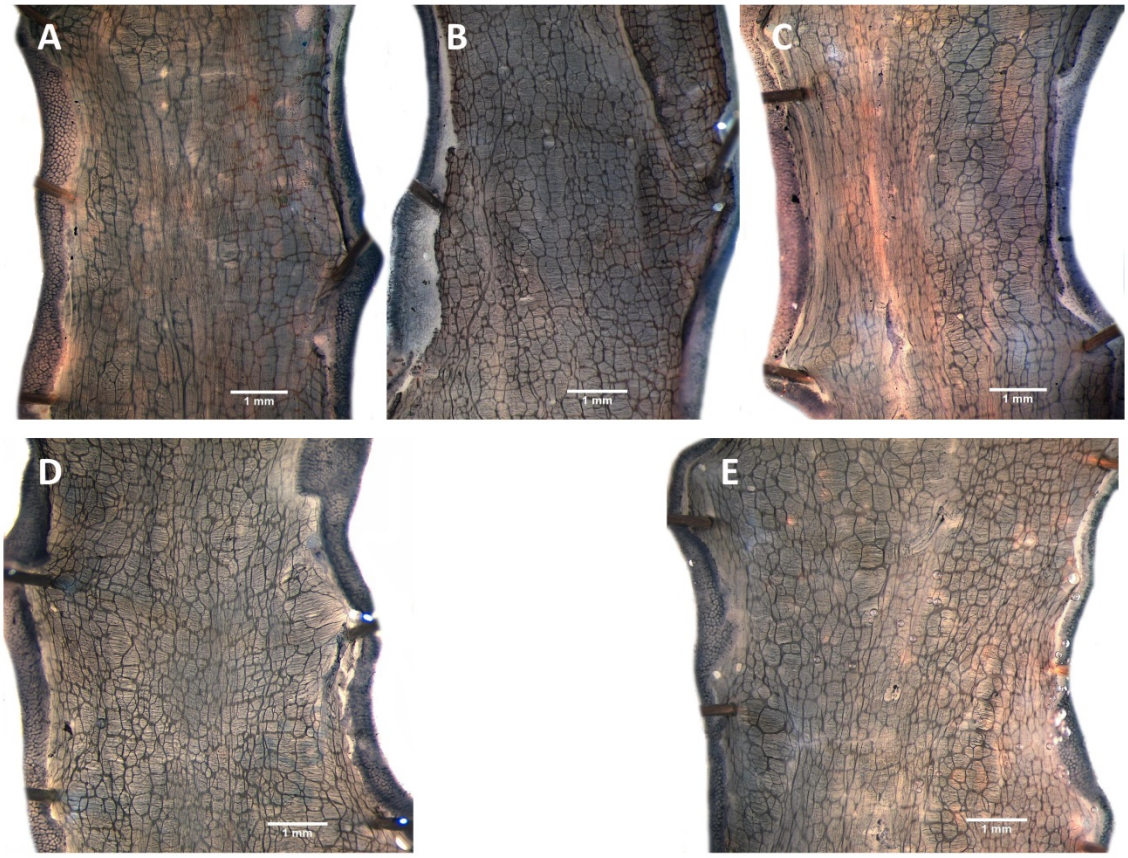

Figure A.7. Acetylcholinesterase staining on the distal portion of colons from *Ets1*$^{-/-}$*::Sox10*$^{LacZ/+}$ mice. For each colon shown, the nerve free area in 8 randomly selected 0.25mm^2 squares was measured using the ImageJ Program (NIH) (Magnifications A-E = 16x).

APPENDIX V

Ethanol Precipitation

Ethanol precipitation was carried out to purify and concentrate plasmids to be used for transfections into mammalian cells. The process was carried out in a biosafety hood to avoid contamination. To each plasmid, 2.5 volumes of 100% ethanol (Fisher Scientific) and one tenth volume of 3M Na+ Acetate (Fisher Scientific) were added and the samples mixed gently by inverting. Plasmids were incubated overnight at -20˚C. On the following day, plasmids were centrifuged at 13,000 RPM, 30 minutes at 4˚C and the supernatant discarded. Plasmids were washed with 70% Ethanol (diluted in Nuclease-free water (Thermo Scientific)), and centrifuged at 13,000 RPM, 15 minutes at 4˚C. After discarding the supernatant plasmid pellets were allowed to dry for 10 minutes at room temperature. Plasmids were then re-suspended in nuclease-free water and the concentration of each plasmid was measured using a spectrophotometer. All plasmids were diluted to the desired final concentrations using nuclease-free water.

VITA

AMY SALDANA TAVARES

2006-2007	Research Trainee, Department of Biological Sciences Florida International University, Miami, FL
2007	B.S., *magna cum laude*, Biology Florida International University, Miami, FL
2007-2014	Ph.D. Candidate, Department of Biological Sciences Florida International University, Miami, FL
2007-2009	Graduate Research Assistant, Department of Biological Sciences Florida International University, Miami, FL
2007-2012	Minority Biomedical Research Support (MBRS), Research Initiative for Scientific Enhancement (RISE) Doctoral Fellowship NIH (R25 GM 061347) Florida International University, Miami, FL
2008	Biomedical Research Initiative (BRI) Student Summer Research Award. Proposal title: "*EdnrB* expression pattern and role in the developing murine brain and spinal cord." Florida International University, Miami, FL
2009-2010	Graduate Teaching Assistant, Department of Biological Sciences Florida International University, Miami, FL
2010-2014	Graduate Research Assistant, Department of Biological Sciences Florida International University, Miami, FL
2010	BRI Student Summer Research Award Proposal title: "*Ets1* expression pattern and role in melanocyte development." Florida International University, Miami, FL
2012	BRI Student Summer Research Award Proposal title: "Multiple roles of *Ets1* in early murine melanocyte development." Florida International University, Miami, FL

SELECTED PUBLICATIONS AND PRESENTATIONS

Saldana Tavares A, Kos L (2007). UV-dependent, *Endothelin-3* transgenic mouse model of melanoma. Minority Biomedical Research Support (MBRS) Student Mini-Symposium, Florida International University, Miami, FL (Oral Presentation)

Saldana Tavares A, Kos L (2008). *Ednrb* expression pattern and role in the developing murine brain and spinal cord. The American Society for Cell Biology 48th Annual Meeting, San Francisco, CA (Poster Presentation)

Saldana-Caboverde A, Kos L. (2010). Roles of endothelin signaling in melanocyte development and melanoma. *Pigment Cell and Melanoma Res* 23(2): 160-170.

Saldana-Caboverde, A, Kos L (2010). UV-dependent *Endothelin-3* transgenic mouse model of melanoma. 2010 Biology Symposium, Florida International University, Miami, FL (Oral Presentation)

Saldana-Caboverde A, Kos L (2010). The role of *Ets1* in melanocyte development. The American Society for Cell Biology 50th Annual Meeting, Philadelphia, PA (Poster Presentation)

Saldana-Caboverde A, Kos L (2011). The transcription factor *Ets1* is required for melanocyte development. 13th Biomedical & Comparative Immunology Symposium, Florida International University, Miami, FL (Oral Presentation)

Saldana-Caboverde A, Kos L (2011). *Ets1* interacts with *Sox10* during melanocyte development. 21st International Pigment Cell Conference, Bordeaux, France (Oral Presentation)

Saldana-Caboverde A, Ortega J, Kos L (2011). UV radiation interacts with Endothelin-3 and loss of the *CDKN2A* locus to promote melanomagenesis. 2011 International Melanoma Congress, Tampa, FL (Poster Presentation)

Saldana-Caboverde A, Kos L (2012). The transcription factors Ets1 and Sox10 interact during murine melanocyte development. Mouse Molecular Genetics 2012. Pacific Grove, CA (Poster Presentation)

Saldana-Caboverde A, Kos L (2013). The transcription factors *Ets1* and *Sox10* interact during murine melanocyte development. 2013 Biology Symposium, Florida International University, Miami, FL (Poster Presentation)

Saldana-Caboverde A, Kos L (2013). The transcription factors *Ets1* and *Sox10* interact in the development of the melanocyte lineage. 15th Biomedical & Comparative Immunology Symposium, Florida International University, Miami, FL (Oral Presentation)

Saldana-Caboverde A, Kos L (2013). *Ets1* interacts with *Sox10* for proper melanocyte development. PanAmerican Society for Pigment Cells Research, Madison, WI (Oral and Poster Presentations)